

Multiscale mortar mixed finite element methods for the Biot system of poroelasticity

Manu Jayadharan* Ivan Yotov*

November 8, 2022

Abstract

We develop a mixed finite element domain decomposition method on non-matching grids for the Biot system of poroelasticity. A displacement–pressure vector mortar function is introduced on the interfaces and utilized as a Lagrange multiplier to impose weakly continuity of normal stress and normal velocity. The mortar space can be on a coarse scale, resulting in a multiscale approximation. We establish existence, uniqueness, stability, and error estimates for the semidiscrete continuous-in-time formulation under a suitable condition on the richness of the mortar space. We further consider a fully-discrete method based on the backward Euler time discretization and show that the solution of the algebraic system at each time step can be reduced to solving a positive definite interface problem for the composite mortar variable. A multiscale stress–flux basis is constructed, which makes the number of subdomain solves independent of the number of iterations required for the interface problem, as well as the number of time steps. We present numerical experiments verifying the theoretical results and illustrating the multiscale capabilities of the method for a heterogeneous benchmark problem.

1 Introduction

In this paper we develop and study a domain decomposition method for the quasistatic Biot system of poroelasticity [12] using mixed finite element subdomain discretizations with non-matching grids along the interfaces. The Biot system models flow of viscous fluids through deformable porous media. The system has a wide range of applications, including in the geosciences, such as earthquakes, landslides, groundwater cleanup, and hydraulic fracturing, as well as in biomedicine, such as arterial flows and biological tissues. The model consists of an equilibrium equation for the solid medium coupled with a mass balance equation for the fluid flow through the medium. Various numerical methods for the Biot system have been developed in the literature, considering two-field displacement–pressure formulations [24, 40, 48], three-field displacement–pressure–Darcy velocity formulations [44, 56, 31, 38, 45, 54], three-field displacement–pressure–total pressure formulations [39, 41], and four-field stress–displacement–pressure–Darcy velocity mixed formulations [55, 1]. In this work we consider the five-field weakly symmetric stress–displacement–rotation–pressure–Darcy velocity formulation [36, 5]. The four-field and five-field formulations lead to mixed finite element (MFE) approximations, which exhibit local mass and momentum conservation, accurate normal-continuous Darcy velocity and solid stress, as well as robust and locking-free behavior for a wide range of physical parameters. An additional advantage of the five-field weakly symmetric MFE method is that it can be reduced to a positive definite cell-centered scheme for the pressure and displacement only, as it is done in the multipoint stress–multipoint flux MFE method developed in [5], through the use of a vertex quadrature rule and local elimination of some of the variables. We note that our analysis for the weakly symmetric formulation can be carried over to the strongly symmetric formulation found in [55].

*Department of Mathematics, University of Pittsburgh, Pittsburgh, PA 15260, USA; {manu.jayadharan@pitt.edu, yotov@math.pitt.edu}. Partially supported by NSF grants DMS 1818775 and DMS 2111129.

Numerical methods for the Biot system of poroelasticity usually lead to large algebraic systems, due to the coupling of unknowns, as well as the size of the domain and the wide range of scales associated with practical applications. Domain decomposition methods [53, 46] are commonly used for solving large systems resulting from discretizations of partial differential equations, as they lead to parallel and efficient solution algorithms. In this work we focus on non-overlapping domain decomposition methods, where the domain is split into non-overlapping subdomains and the continuity of the solution variables at the subdomain interfaces is enforced through a suitable interface Lagrange multiplier. The global problem can be reduced to solving iteratively an interface problem, involving the solution of smaller subdomain systems at each iteration, which can be performed in parallel. Despite the extensive studies of numerical methods for the Biot system of poroelasticity, there have been relatively few results on domain decomposition methods for this problem and they have been mostly based on the two-field displacement–pressure formulation [25, 21, 20, 29]. To the best of our knowledge, the only paper on domain decomposition for Biot with a mixed formulation is [32], which is based on the five-field mixed formulation with weak stress symmetry. Two types of methods are developed in [32]. One is a monolithic domain decomposition method, which involves solving the Biot system on each subdomain. The second is a partitioned method, which splits the Biot system into solving separate elasticity and flow equations, and applies domain decomposition for each of the equations. The developments in [32] are motivated by earlier works on non-overlapping domain decomposition methods for MFE discretizations of Darcy flow [27, 18, 6] and elasticity [33].

The domain decomposition methods in [32] are limited to subdomain grids that match at the interfaces. In this paper we generalize the work in [32] to enable the use of non-matching subdomain grids through the use of mortar finite elements [6, 7, 22, 34, 42, 33]. This generality provides the flexibility to use different grid resolution in different subdomains, as well as a coarser mortar space, resulting in a multiscale approximation. We refer to the method as a multiscale mortar mixed finite element (MMMFE) method. The MMMFE method has been studied for mixed formulations of scalar elliptic equations in [6, 7, 23] and for weakly-symmetric mixed elasticity in [33]. Following the monolithic domain decomposition method from [32], we utilize a physically heterogeneous Lagrange multiplier vector consisting of interface displacement and pressure variables to impose weakly the continuity of the normal components of stress and velocity, respectively. In contrast to [32], we choose the Lagrange multiplier vector from a space of mortar finite elements defined on a separate interface grid, which allows for handling non-matching subdomain grids through projections from and onto the mortar finite element space. This also allows for the mortar space to be on a coarser scale H , see [43, 7, 23], compared to a finer subdomain grid size h . The multiscale capability adds an extra layer of flexibility over the methods from [32].

The main contributions of this paper are as follows. We first consider the semidiscrete continuous-in-time formulation and establish existence, uniqueness, and stability of the MMMFE method for the Biot system, employing the theory of degenerate evolutionary systems of partial differential equations with monotone operators. For the solvability of the associated resolvent problem we utilize, under a condition on the richness of the mortar finite element space, an inf-sup condition for the mortar space, as well as inf-sup conditions for the stress and velocity spaces with weak interface continuity of normal components. Next, we establish a priori error estimates for the stress, displacement, rotation, pressure, and Darcy velocity, as well as the displacement and pressure mortar variables in their natural norms. We then consider a fully-discrete method based on the backward Euler time discretization. We show that the solution of the algebraic system at each time step can be reduced to solving a positive definite interface problem for the composite displacement–pressure mortar variable. Motivated by the multiscale flux basis from [23] and the multiscale stress basis from [33], we propose the construction and use of a multiscale stress–flux basis, which makes the number of subdomain solves independent of the number of iterations required for the interface problem. Moreover, since the basis can be reused at each time step, the total number of subdomain solves is independent of the number of time steps. This illustrates that the multiscale basis results in a significant reduction of computational cost in the case of time-dependent problems. Finally, we present the results of several numerical tests designed to illustrate the well-posedness, stability, and accuracy of the proposed MMMFE method. We also consider a test based on data from the Society of Petroleum Engineers SPE10 benchmark, illustrating the multiscale capabilities of the method and the advantages of using a multiscale basis.

The rest of the paper is organized as follows. Section 2 introduces the model problem and its domain decomposition mixed finite element approximation. The well-posedness, stability, and error analysis for the semi-discrete formulation is presented in Section 3. In Section 4 we discuss the fully discrete method, the reduction to an interface problem, and the construction of the multiscale stress–flux basis. Numerical results are reported in Section 5.

2 Formulation of the method

In this section, we introduce the mathematical model of interest and its mixed finite element approximation. We also develop the framework for the multiscale mortar mixed finite element domain decomposition method. Projection operators critical in the analysis of the method and various bounds associated with them are introduced. Finally, we introduce the weakly continuous spaces of stress, $\mathbb{X}_{h,0}$, and velocity, $Z_{h,0}$, and reformulate the MMMFE method in terms of these spaces.

2.1 Mathematical formulation of model Problem

Let $\Omega \subset \mathbb{R}^d$, $d = 2, 3$ be a simply connected domain. We use the notation \mathbb{M} , \mathbb{S} and \mathbb{N} for the spaces of $d \times d$ matrices, symmetric matrices, and skew-symmetric matrices, respectively, all over the field of real numbers. Let $I \in \mathbb{S}$ represents the $d \times d$ identity matrix. The partial derivative operator with respect to time, $\frac{\partial}{\partial t}$, is often abbreviated to ∂_t . C denotes a generic positive constant that is independent of the discretization parameters h and H . Throughout the thesis, the divergence operator is the usual divergence for vector fields, which produces vector field when applied to matrix field by taking the divergence of each row. The divergence operator is represented by either $\nabla \cdot$ or div .

For a set $G \subset \mathbb{R}^d$, the $L^2(G)$ inner product and norm are denoted by $(\cdot, \cdot)_G$ and $\|\cdot\|_G$, respectively, for scalar, vector, or tensor valued functions. For any fraction r , $\|\cdot\|_{r,G}$ denotes the $H^r(G)$ -norm, for example $\|\cdot\|_{0,G} = \|\cdot\|_G$. We omit subscript G if $G = \Omega$. For a section of the domain or element boundary $S \subset \mathbb{R}^{d-1}$, we write $\langle \cdot, \cdot \rangle_S$ and $\|\cdot\|_S$ for the $L^2(S)$ inner product (or duality pairing) and norm, respectively. We will also use the spaces

$$\begin{aligned} H(\text{div}; \Omega) &= \{\zeta \in L^2(\Omega, \mathbb{R}^d) : \text{div } \zeta \in L^2(\Omega)\}, \\ H(\text{div}; \Omega, \mathbb{M}) &= \{\tau \in L^2(\Omega, \mathbb{M}) : \text{div } \tau \in L^2(\Omega, \mathbb{R}^d)\}, \end{aligned}$$

with the norm $\|\tau\|_{\text{div}} = (\|\tau\|^2 + \|\text{div } \tau\|^2)^{1/2}$. Let $\|\cdot\|_\star$ be the natural norm associated with the space $\star \in \{\mathbb{X}, V, \mathbb{Q}, Z, W\}$, where the set of spaces will be introduced later in this section.

Given a vector field f representing body forces and a source term g , we consider the quasi-static Biot system of poroelasticity ([12]):

$$-\text{div } \sigma(u) = f, \quad \text{in } \Omega \times (0, T], \quad (2.1)$$

$$K^{-1}z + \nabla p = 0, \quad \text{in } \Omega \times (0, T], \quad (2.2)$$

$$\frac{\partial}{\partial t}(c_0 p + \alpha \text{div } u) + \text{div } z = g, \quad \text{in } \Omega \times (0, T], \quad (2.3)$$

where u is the displacement, p is the fluid pressure, z is the Darcy velocity, and σ is the poroelastic stress, defined as

$$\sigma = \sigma_e - \alpha p I. \quad (2.4)$$

Here I is the $d \times d$ identity matrix, $0 < \alpha \leq 1$ is the Biot-Willis constant, and σ_e is the elastic stress satisfying the stress-strain relationship

$$A\sigma_e = \epsilon(u), \quad \epsilon(u) := \frac{1}{2}(\nabla u + (\nabla u)^T), \quad (2.5)$$

where A is the compliance tensor, which is a symmetric, bounded and uniformly positive definite linear operator acting from $\mathbb{S} \rightarrow \mathbb{S}$, extendible to $\mathbb{M} \rightarrow \mathbb{M}$. In the special case of homogeneous and isotropic body, A is given by,

$$A\sigma = \frac{1}{2\mu} \left(\sigma - \frac{\lambda}{2\mu + d\lambda} \text{tr}(\sigma) I \right), \quad (2.6)$$

where $\mu > 0$ and $\lambda \geq 0$ are the Lamé coefficients. In this case, $\sigma_e(u) = 2\mu\epsilon(u) + \lambda \operatorname{div} u I$. Finally, $c_0 \geq 0$ is the mass storativity and K stands for the permeability tensor that is spatially-dependent, uniformly bounded, symmetric, and positive definite, i.e, for constants $0 < k_{\min} \leq k_{\max} < \infty$,

$$\forall \text{ a.e. } x \in \Omega, \quad k_{\min} \zeta^T \zeta \leq \zeta^T K(x) \zeta \leq k_{\max} \zeta^T \zeta, \quad \forall \zeta \in \mathbb{R}^d. \quad (2.7)$$

To close the system, we impose the boundary conditions

$$u = g_u \quad \text{on } \Gamma_D^u \times (0, T], \quad \sigma n = 0 \quad \text{on } \Gamma_N^\sigma \times (0, T], \quad (2.8)$$

$$p = g_p \quad \text{on } \Gamma_D^p \times (0, T], \quad z \cdot n = 0 \quad \text{on } \Gamma_N^z \times (0, T], \quad (2.9)$$

where $\Gamma_D^u \cup \Gamma_N^\sigma = \Gamma_D^p \cup \Gamma_N^z = \partial$ and n is the outward unit normal vector field on ∂ , along with the initial condition $p(x, 0) = p_0(x)$ in Ω . Compatible initial data for the rest of the variables can be obtained from (2.1) and (2.2) at $t = 0$. Well posedness analysis for this system can be found in [50].

We use the same mixed variational formulation for (2.1)–(2.9) as discussed in [32], which was based on the approach in [36]. Recall that we introduced a rotation Lagrange multiplier $\gamma := \frac{1}{2}(\nabla u - \nabla u^T) \in \mathbb{N}$, which was used to impose weakly the symmetry of the stress tensor σ . Following the same arguments as in [32], we obtain the following mixed variational formulation for (2.1)–(2.9), find $(\sigma, u, \gamma, z, p) : [0, T] \rightarrow \mathbb{X} \times V \times \mathbb{Q} \times Z \times W$ such that $p(0) = p_0$ and for a.e. $t \in (0, T)$,

$$(A(\sigma + \alpha p I), \tau) + (u, \operatorname{div} \tau) + (\gamma, \tau) = \langle g_u, \tau n \rangle_{\Gamma_D^u}, \quad \forall \tau \in \mathbb{X}, \quad (2.10)$$

$$(\operatorname{div} \sigma, v) = -(f, v), \quad \forall v \in V, \quad (2.11)$$

$$(\sigma, \xi) = 0, \quad \forall \xi \in \mathbb{Q}, \quad (2.12)$$

$$(K^{-1}z, q) - (p, \operatorname{div} q) = -\langle g_p, q \cdot n \rangle_{\Gamma_D^p}, \quad \forall q \in Z, \quad (2.13)$$

$$c_0(\partial_t p, w) + \alpha(\partial_t A(\sigma + \alpha p I), w I) + (\operatorname{div} z, w) = (g, w), \quad \forall w \in W, \quad (2.14)$$

where

$$\begin{aligned} \mathbb{X} &= \{ \tau \in H(\operatorname{div}; \Omega, \mathbb{M}) : \tau n = 0 \text{ on } \Gamma_N^\sigma \}, & V &= L^2(\Omega, \mathbb{R}^d), & \mathbb{Q} &= L^2(\Omega, \mathbb{N}), \\ Z &= \{ q \in H(\operatorname{div}; \Omega) : q \cdot n = 0 \text{ on } \Gamma_N^z \}, & W &= L^2(\Omega). \end{aligned}$$

It was shown in [5] that the system (2.10)–(2.14) is well posed.

In the MFE setting, the variational formulation corresponding to (2.10)–(2.14) reads as follows: find $(\sigma_h, u_h, \gamma_h, z_h, p_h) : [0, T] \rightarrow \mathbb{X}_h \times V_h \times \mathbb{Q}_h \times Z_h \times W_h$ such that for a.e. $t \in (0, T)$, $(\sigma_h, u_h, \gamma_h, z_h, p_h) : [0, T] \rightarrow \mathbb{X}_h \times V_h \times \mathbb{Q}_h \times Z_h \times W_h$ such that, for a.e. $t \in (0, T)$,

$$(A(\sigma_h + \alpha p_h I), \tau) + (u_h, \operatorname{div} \tau) + (\gamma_h, \tau) = \langle g_u, \tau n \rangle_{\Gamma_D^u}, \quad \forall \tau \in \mathbb{X}_h, \quad (2.15)$$

$$(\operatorname{div} \sigma_h, v) = -(f, v), \quad \forall v \in V_h, \quad (2.16)$$

$$(\sigma_h, \xi) = 0, \quad \forall \xi \in \mathbb{Q}_h, \quad (2.17)$$

$$(K^{-1}z_h, q) - (p_h, \operatorname{div} q) = -\langle g_p, q \cdot n \rangle_{\Gamma_D^p}, \quad \forall q \in Z_h, \quad (2.18)$$

$$c_0(\partial_t p_h, w) + \alpha(\partial_t A(\sigma_h + \alpha p_h I), w I) + (\operatorname{div} z_h, w) = (g, w), \quad \forall w \in W_h, \quad (2.19)$$

where $\mathbb{X}_h \times V_h \times \mathbb{Q}_h \times Z_h \times W_h \subset \mathbb{X} \times V \times \mathbb{Q} \times Z \times W$ can be chosen from any of the inf-sup stable MFE families and the discrete initial data, $p_{h,0}$, is obtained from the elliptic projection of the continuous initial data.

For solving the mechanics part, $\mathbb{X}_h \times V_h \times \mathbb{Q}_h$ can be chosen from any of the stable triplets suitable for solving linear elasticity problem equations with weakly imposed symmetry. Examples of such triplets include [52, 3, 8, 9, 10, 17, 28, 13, 14, 19, 4, 37], where all the listed triplets satisfy the inf-sup condition,

$$\forall v \in V_h, \xi \in \mathbb{Q}_h, \quad \|v\| + \|\xi\| \leq C \sup_{0 \neq \tau \in \mathbb{X}_h} \frac{(v, \operatorname{div} \tau) + (\xi, \tau)}{\|\tau\|_{\operatorname{div}}}. \quad (2.20)$$

For the flow part, $Z_h \times W_h$ could be chosen from any of the stable pressure-velocity pair of MFE spaces such as the Raviart-Thomas (\mathcal{RT}) or Brezzi-Douglas-Marini (\mathcal{BDM}) spaces. These families

are presented in detail in [15], where it is shown that they satisfy the following inf-sup condition,

$$\forall w \in W_h, \quad \|w\| \leq C \sup_{0 \neq q \in Z_h} \frac{(\operatorname{div} q, w)}{\|q\|_{\operatorname{div}}}. \quad (2.21)$$

We also note the following properties of A and K which will be useful in the analysis of our method, there exist constants $0 < a_{\min} \leq a_{\max} < \infty$ and $0 < k_{\min} \leq k_{\max} < \infty$ such that

$$a_{\min} \|\tau\|^2 \leq (A\tau, \tau) \leq a_{\max} \|\tau\|^2, \quad \forall \tau \in \mathbb{X}, \quad (2.22)$$

$$k_{\min} \|q\|^2 \leq (Kq, q) \leq k_{\max} \|q\|^2, \quad \forall q \in Z. \quad (2.23)$$

2.2 Multiscale mortar domain decomposition method

Let $\Omega = \cup_{i=1}^N \Omega_i$ be a union of non-overlapping shape regular polygonal subdomains, where each subdomain is a union of elements of finite element partition \mathcal{T}_h . Let $\Gamma_{i,j} = \partial\Omega_i \cap \partial\Omega_j$, $\Gamma = \cup_{i,j=1}^N \Gamma_{i,j}$, and $\Gamma_i = \partial\Omega_i \cap \Gamma = \partial\Omega_i \setminus \partial\Omega$ denote the interior subdomain interfaces. The domain discretization technique we develop in this section is the generalization of the monolithic non-overlapping domain decomposition technique developed in [32], where the sub-domains are allowed to have multiscale non-matching grids at their interfaces. Let h_i be the diameter of the maximal element in the mesh on Ω_i and define $h = \max_i h_i$. For $1 \leq i \leq N$, let $\mathbb{X}_{h,i} \times V_{h,i} \times \mathbb{Q}_{h,i} \times Z_{h,i} \times W_{h,i}$ be a family of stable mixed finite elements defined on the subdomain Ω_i . These spaces could be chosen from any of the stable family of spaces discussed in [32]. Let the finite element spaces $\mathbb{X}_{h,i}$, $V_{h,i}$, $\mathbb{Q}_{h,i}$, $Z_{h,i}$, and $W_{h,i}$ contain polynomials of degree less than or equal to $k \geq 1$, $l \geq 0$, $j \geq 0$, and $s \geq 0$, respectively. We define the global FE spaces, defined on Ω , as follows:

$$\mathbb{X}_h = \bigoplus_{1 \leq i \leq N} \mathbb{X}_{h,i}, \quad V_h = \bigoplus_{1 \leq i \leq N} V_{h,i}, \quad \mathbb{Q}_h = \bigoplus_{1 \leq i \leq N} \mathbb{Q}_{h,i}, \quad Z_h = \bigoplus_{1 \leq i \leq N} Z_{h,i}, \quad W_h = \bigoplus_{1 \leq i \leq N} W_{h,i}.$$

The spaces V_h , \mathbb{Q}_h , and W_h are equipped with L^2 -norms. The spaces \mathbb{X}_h and Z_h are equipped with the norms

$$\|\tau\|_{\mathbb{X}_h}^2 := \|\tau\|^2 + \|\operatorname{div}_h \tau\|^2 \quad \text{and} \quad \|\zeta\|_{Z_h}^2 := \|\zeta\|^2 + \|\operatorname{div}_h \zeta\|^2,$$

where for simplicity we define $\operatorname{div}_h \varphi|_{\Omega_i} := \operatorname{div}(\varphi|_{\Omega_i})$. We note that functions in \mathbb{X}_h and Z_h do not have continuity of the normal components across the subdomain interfaces. This discontinuity is addressed using Lagrange multipliers defined on suitable mortar spaces on the interface Γ . We use relatively coarser mortar finite elements satisfying certain coarseness conditions (which will be discussed in the later sections) to approximate the traces of the displacement vector and the pressure at the interfaces. Let $\mathcal{T}_{H,i,j}$ be a shape regular quasi-uniform finite element partition of $\Gamma_{i,j}$ constructed using a simplicial or quadrilateral mesh in $d-1$ dimensions with maximal element diameter H . Define the global mortar fine element spaces on the union of sub-domain interfaces, Γ , to be,

$$\Lambda_H = \bigoplus_{1 \leq i < j \leq N} \begin{pmatrix} \Lambda_{H,i,j}^u \\ \Lambda_{H,i,j}^p \end{pmatrix}, \quad \Lambda_H^u = \bigoplus_{1 \leq i < j \leq N} \Lambda_{H,i,j}^u, \quad \text{and} \quad \Lambda_H^p = \bigoplus_{1 \leq i < j \leq N} \Lambda_{H,i,j}^p,$$

where $\Lambda_{H,i,j}^u \subset (L^2(\Gamma_{i,j}))^d$ and $\Lambda_{H,i,j}^p \subset L^2(\Gamma_{i,j})$ are mortar finite element spaces on $\Gamma_{i,j}$ representing the displacement and pressure Lagrange multipliers, respectively. We assume that these mortar spaces contain either continuous or discontinuous polynomials of degree up to $m \geq 0$. Conditions on the degree and richness of the mortar spaces in order to get a well-posed and stable method will be discussed in the later sections.

The multiscale mortar domain decomposition formulation for the mixed Biot problem in a semi-discrete form reads as follows: for $1 \leq i \leq N$, find $(\sigma_{h,i}, u_{h,i}, \gamma_{h,i}, z_{h,i}, p_{h,i}, \lambda_H) : [0, T] \rightarrow \mathbb{X}_{h,i} \times$

$V_{h,i} \times \mathbb{Q}_{h,i} \times Z_{h,i} \times W_{h,i} \times \Lambda_H$ such that $p_{h,i}(0) = p_{h,0}|_{\Omega_i}$ and for a.e. $t \in (0, T)$,

$$\begin{aligned} (A(\sigma_{h,i} + \alpha p_{h,i} I), \tau)_{\Omega_i} + (u_{h,i}, \operatorname{div} \tau)_{\Omega_i} + (\gamma_{h,i}, \tau)_{\Omega_i} \\ = \langle g_u, \tau n_i \rangle_{\partial\Omega_i \cap \Gamma_D^u} + \langle \lambda_H^u, \tau n_i \rangle_{\Gamma_i}, \quad \forall \tau \in \mathbb{X}_{h,i}, \end{aligned} \quad (2.24)$$

$$(\operatorname{div} \sigma_{h,i}, v)_{\Omega_i} = -(f, v)_{\Omega_i}, \quad \forall v \in V_{h,i}, \quad (2.25)$$

$$(\sigma_{h,i}, \xi)_{\Omega_i} = 0, \quad \forall \xi \in \mathbb{Q}_{h,i}, \quad (2.26)$$

$$(K^{-1} z_{h,i}, \zeta)_{\Omega_i} - (p_{h,i}, \operatorname{div} \zeta)_{\Omega_i} = -\langle g_p, \zeta \cdot n_i \rangle_{\partial\Omega_i \cap \Gamma_D^p} - \langle \lambda_H^p, \zeta \cdot n_i \rangle_{\Gamma_i}, \quad \forall \zeta \in Z_{h,i}, \quad (2.27)$$

$$c_0 (\partial_t p_{h,i}, w)_{\Omega_i} + \alpha (\partial_t A(\sigma_{h,i} + \alpha p_{h,i} I), w I)_{\Omega_i} + (\operatorname{div} z_{h,i}, w)_{\Omega_i} = (g, w)_{\Omega_i}, \quad \forall w \in W_{h,i}, \quad (2.28)$$

$$\sum_{i=1}^N \langle \sigma_{h,i} n_i, \mu^u \rangle_{\Gamma_i} = 0, \quad \forall \mu^u \in \Lambda_H^u, \quad (2.29)$$

$$\sum_{i=1}^N \langle z_{h,i} \cdot n_i, \mu^p \rangle_{\Gamma_i} = 0, \quad \forall \mu^p \in \Lambda_H^p, \quad (2.30)$$

where n_i is the outward unit normal vector field on Ω_i . Note that equations (2.29)–(2.30) enforces a notion of weak continuity of normal components of the stress tensor and velocity vector across the interface Γ and that both the flow and the elasticity problems are of Dirichlet type.

For simplicity of the analysis, we assume that $\Gamma_D^u = \Gamma_D^p = \partial\Omega$ and $g_u = g_p = 0$, to get the following reformulation of (2.24)–(2.30): find $(\sigma_h, u_h, \gamma_h, z_h, p_h, \lambda_H) : [0, T] \rightarrow \mathbb{X}_h \times V_h \times \mathbb{Q}_h \times Z_h \times W_h \times \Lambda_H$ such that $p_{h,i}(0) = p_{h,0}|_{\Omega_i}$ and for a.e. $t \in (0, T)$,

$$(A(\sigma_h + \alpha p_h I), \tau) + \sum_{i=1}^N (u_h, \operatorname{div} \tau)_{\Omega_i} + (\gamma_h, \tau) = \sum_{i=1}^N \langle \lambda_H^u, \tau n_i \rangle_{\Gamma_i}, \quad \forall \tau \in \mathbb{X}_h, \quad (2.31)$$

$$\sum_{i=1}^N (\operatorname{div} \sigma_h, v)_{\Omega_i} = -(f, v), \quad \forall v \in V_h, \quad (2.32)$$

$$(\sigma_h, \xi) = 0, \quad \forall \xi \in \mathbb{Q}_h, \quad (2.33)$$

$$(K^{-1} z_h, \zeta) - \sum_{i=1}^N (p_h, \operatorname{div} \zeta)_{\Omega_i} = \sum_{i=1}^N -\langle \lambda_H^p, \zeta \cdot n_i \rangle_{\Gamma_i}, \quad \forall \zeta \in Z_h, \quad (2.34)$$

$$c_0 \left(\frac{\partial p_h}{\partial t}, w \right) + \alpha \left(\frac{\partial}{\partial t} A(\sigma_h + \alpha p_h I), w I \right) + \sum_{i=1}^N (\operatorname{div} z_h, w)_{\Omega_i} = (g, w), \quad \forall w \in W_h, \quad (2.35)$$

$$\sum_{i=1}^N \langle \sigma_h n_i, \mu^u \rangle_{\Gamma_i} = 0, \quad \forall \mu^u \in \Lambda_H^u, \quad (2.36)$$

$$\sum_{i=1}^N \langle z_h \cdot n_i, \mu^p \rangle_{\Gamma_i} = 0, \quad \forall \mu^p \in \Lambda_H^p. \quad (2.37)$$

2.3 Projection and interpolation operators

In this subsection, we discuss various interpolation and projection operators useful in the analysis of the method.

Let $\mathcal{Q}_{h,i}^u : (L^2(\partial\Omega_i))^d \rightarrow \mathbb{X}_{h,i} n_i$ and $\mathcal{Q}_{h,i}^p : L^2(\partial\Omega_i) \rightarrow Z_{h,i} \cdot n_i$ be projection operators onto the trace of the normal components of $\mathbb{X}_{h,i}$ and $Z_{h,i}$, respectively such that for any $\phi_u \in (L^2(\partial\Omega_i))^d$ and $\phi_p \in L^2(\partial\Omega_i)$,

$$\langle \phi_u - \mathcal{Q}_{h,i}^u \phi_u, \tau n_i \rangle_{\partial\Omega_i} = 0, \quad \forall \tau \in \mathbb{X}_{h,i}, \quad (2.38)$$

$$\langle \phi_p - \mathcal{Q}_{h,i}^p \phi_p, \zeta \cdot n_i \rangle_{\partial\Omega_i} = 0, \quad \forall \zeta \in Z_{h,i}. \quad (2.39)$$

We define $\mathcal{Q}_{h,i} : (L^2(\partial\Omega_i))^d \times L^2(\partial\Omega_i) \rightarrow \mathbb{X}_{h,i}n_i \times Z_{h,i} \cdot n_i$ as

$$\mathcal{Q}_{h,i} = \begin{pmatrix} \mathcal{Q}_{h,i}^u \\ \mathcal{Q}_{h,i}^p \end{pmatrix}. \quad (2.40)$$

For any inf-sup stable pair of finite element spaces, $\mathbb{X}_{h,i} \times V_{h,i}$, with $\operatorname{div} \mathbb{X}_{h,i} = V_{h,i}$, there exists a mixed canonical interpolant [15], $\Pi_i^\sigma : H^\epsilon(\Omega_i, \mathbb{M}) \cap \mathbb{X}_i \rightarrow \mathbb{X}_{h,i}$, for any $\epsilon > 0$, such that for any $\tau \in H^\epsilon(\Omega_i, \mathbb{M}) \cap \mathbb{X}_{h,i}$,

$$(\operatorname{div}(\Pi_i^\sigma \tau - \tau), v)_{\Omega_i} = 0, \quad \forall v \in V_{h,i}, \quad (2.41)$$

$$\langle (\Pi_i^\sigma \tau - \tau)n_i, \hat{\tau}n_i \rangle_{\Gamma_i} = 0, \quad \forall \hat{\tau} \in \mathbb{X}_{h,i}, \quad (2.42)$$

$$\|\Pi_i^\sigma \tau\|_{\Omega_i} \leq C (\|\tau\|_{L^\epsilon(\Omega_i)} + \|\operatorname{div} \tau\|_{\Omega_i}). \quad (2.43)$$

Similarly for any inf-sup stable pair, $Z_{h,i} \times W_{h,i}$, with $\operatorname{div} Z_{h,i} = W_{h,i}$, there exists a mixed canonical interpolant $\Pi_i^z : (H^\epsilon(\Omega_i))^d \cap Z_i \rightarrow Z_{h,i}$ such that for any $\zeta \in (H^\epsilon(\Omega_i))^d \cap Z_i$, the following holds

$$(\operatorname{div}(\Pi_i^z \zeta - \zeta), w)_{\Omega_i} = 0, \quad \forall w \in W_{h,i}, \quad (2.44)$$

$$\langle (\Pi_i^z \zeta - \zeta) \cdot n, \hat{\zeta} \cdot n \rangle_{\Gamma_i} = 0, \quad \forall \hat{\zeta} \in Z_{h,i}, \quad (2.45)$$

$$\|\Pi_i^z \zeta\|_{Z_i} \leq C (\|\zeta\|_{H^\epsilon(\Omega_i)} + \|\operatorname{div} \zeta\|_{\Omega_i}). \quad (2.46)$$

Let $\mathcal{P}_{h,i}^p$ denote the L^2 -orthogonal projection, $\mathcal{P}_{h,i}^p : L^2(\Omega_i) \rightarrow W_{h,i}$, such that for any $w \in L^2(\Omega_i)$,

$$\left(\mathcal{P}_{h,i}^p w - w, \hat{w} \right)_{\Omega_i} = 0, \quad \forall \hat{w} \in W_{h,i}. \quad (2.47)$$

Let $\mathcal{P}_{h,i}^u$ denote the L^2 -orthogonal projection, $\mathcal{P}_{h,i}^u : (L^2(\Omega_i))^d \rightarrow V_{h,i}$, such that for any $v \in (L^2(\Omega_i))^d$,

$$\left(\mathcal{P}_{h,i}^u v - v, \hat{v} \right)_{\Omega_i} = 0, \quad \forall \hat{v} \in V_{h,i}. \quad (2.48)$$

We also use $\mathcal{R}_{h,i}$ to denote the orthogonal projection, $\mathcal{R}_{h,i} : L^2(\Omega_i, \mathbb{N}) \rightarrow \mathbb{Q}_{h,i}$ such that for any $\xi \in L^2(\Omega_i, \mathbb{N})$,

$$\left(\mathcal{R}_{h,i} \xi - \xi, \hat{\xi} \right)_{\Omega_i} = 0, \quad \forall \hat{\xi} \in \mathbb{Q}_{h,i}. \quad (2.49)$$

For the analysis of the method, we will use an elliptic projection operator, $\hat{\Pi}_i^\sigma$ onto $\mathbb{X}_{h,i}$ as defined in [33]. Define $\hat{\Pi}_i^\sigma : H^\epsilon(\Omega_i, \mathbb{M}) \cap \mathbb{X}_i \rightarrow \mathbb{X}_{h,i}$ as the operator that takes $\sigma \in H^\epsilon(\Omega_i, \mathbb{M}) \cap \mathbb{X}_i$ to the finite element approximation, $\hat{\sigma}$, of the following Neumann problem: for any $\sigma \in H^\epsilon(\Omega_i, \mathbb{M})$, find $(\hat{\sigma}, \hat{u}, \hat{\gamma}) \in \mathbb{X}_{h,i} \times V_{h,i} \times \mathbb{Q}_{h,i}$ such that

$$(\hat{\sigma}, \tau)_{\Omega_i} + (\hat{u}, \operatorname{div} \tau)_{\Omega_i} + (\hat{\gamma}, \tau)_{\Omega_i} = (\sigma, \tau)_{\Omega_i}, \quad \forall \tau \in \mathbb{X}_{h,i}, \quad (2.50)$$

$$(\operatorname{div} \hat{\sigma}, v)_{\Omega_i} = (\operatorname{div} \sigma, v)_{\Omega_i}, \quad \forall v \in V_{h,i}, \quad (2.51)$$

$$(\hat{\sigma}, \xi)_{\Omega_i} = (\sigma, \xi)_{\Omega_i}, \quad \forall \xi \in \mathbb{Q}_{h,i}, \quad (2.52)$$

$$\hat{\sigma}n_i = (\Pi_i^\sigma \sigma)n_i \quad \text{on } \partial\Omega_i. \quad (2.53)$$

More details on the well-posedness and properties of $\hat{\Pi}_i^\sigma$ can be found in [33]. In particular, the following bounds hold

$$\|\sigma - \hat{\Pi}_i^\sigma \sigma\|_{\Omega_i} \leq C \|\sigma - \Pi_i \sigma\|_{\Omega_i}, \quad \sigma \in H^1(\Omega_i, \mathbb{M}),$$

$$\|\hat{\Pi}_i^\sigma \sigma\|_{\Omega_i} \leq C (\|\sigma\|_{H^\epsilon(\Omega_i)} + \|\operatorname{div} \sigma\|_{\Omega_i}), \quad \sigma \in H^\epsilon(\Omega_i, \mathbb{M}) \cap \mathbb{X}_i, \quad 0 < \epsilon \leq 1.$$

We also use the Scott-Zhang interpolants (see [49]) $\mathcal{I}_H^u : H^1(\Gamma) \rightarrow \Lambda_H^u \cap C(\Gamma)$ and $\mathcal{I}_H^p : H^1(\Gamma) \rightarrow \Lambda_H^p \cap C(\Gamma)$, defined to preserve the trace on $\partial\Gamma$ for functions that are zero on $\partial\Gamma$.

The operators defined above satisfy the following approximation bounds:

$$\|\psi - \mathcal{I}_H^u \psi\|_{t, \Gamma_{i,j}} \leq CH^{\hat{m}-t} \|\psi\|_{\hat{m}, \Gamma_{i,j}}, \quad 0 \leq t \leq 1, \quad t \leq \hat{m} \leq m+1, \quad (2.54)$$

$$\|\psi - \mathcal{I}_H^p \psi\|_{t, \Gamma_{i,j}} \leq CH^{\hat{m}-t} \|\psi\|_{\hat{m}, \Gamma_{i,j}}, \quad 0 \leq t \leq 1, \quad t \leq \hat{m} \leq m+1, \quad (2.55)$$

$$\|v - \mathcal{P}_{h,i}^u v\|_{\Omega_i} \leq Ch^{\hat{l}} \|v\|_{\hat{l}, \Omega_i}, \quad 0 \leq \hat{l} \leq l+1, \quad (2.56)$$

$$\|\zeta - \mathcal{P}_{h,i}^p \zeta\|_{\Omega_i} \leq Ch^{\hat{s}} \|\zeta\|_{\hat{s}, \Omega_i}, \quad 0 \leq \hat{s} \leq s+1, \quad (2.57)$$

$$\|\xi - \mathcal{R}_{h,i} \xi\|_{\Omega_i} \leq Ch^{\hat{j}} \|\xi\|_{\hat{j}, \Omega_i}, \quad 0 \leq \hat{j} \leq j+1, \quad (2.58)$$

$$\|\psi - \mathcal{Q}_{h,i}^u \psi\|_{\Gamma_{i,j}} \leq Ch^{\hat{k}+t} \|\psi\|_{\hat{k}, \Gamma_{i,j}}, \quad 0 \leq \hat{k} \leq k+1, \quad (2.59)$$

$$\|\psi - \mathcal{Q}_{h,i}^p \psi\|_{\Gamma_{i,j}} \leq Ch^{\hat{r}+t} \|\psi\|_{\hat{r}, \Gamma_{i,j}}, \quad 0 \leq \hat{r} \leq r+1, \quad (2.60)$$

$$\|\tau - \hat{\Pi}_i^\sigma \tau\|_{\Omega_i} \leq Ch^{\hat{k}} \|\tau\|_{\hat{k}, \Omega_i}, \quad 0 \leq \hat{k} \leq k+1, \quad (2.61)$$

$$\|\zeta - \Pi_i^z \zeta\|_{\Omega_i} \leq Ch^{\hat{r}} \|\zeta\|_{\hat{r}, \Omega_i}, \quad 0 \leq \hat{r} \leq r+1, \quad (2.62)$$

$$\|\operatorname{div}(\tau - \hat{\Pi}_i^\sigma \tau)\|_{\Omega_i} \leq Ch^{\hat{l}} \|\operatorname{div} \tau\|_{\hat{l}, \Omega_i}, \quad 0 \leq \hat{l} \leq l+1, \quad (2.63)$$

$$\|\operatorname{div}(\zeta - \Pi_i^z \zeta)\|_{\Omega_i} \leq Ch^{\hat{s}} \|\operatorname{div} \tau\|_{\hat{s}, \Omega_i}, \quad 0 \leq \hat{s} \leq s+1, \quad (2.64)$$

where the functions ψ , v , ζ , τ , and ξ are taken from the domains of the operators acting on them. Bound (2.54) can be found in [49], bounds (2.56)–(2.60) and (2.63)–(2.64) are standard L^2 -projection approximation bounds [16], and bounds (2.61)–(2.62) can be found in [15, 47, 33].

We will also use the trace inequalities

$$\|\psi\|_{t, \Gamma_{i,j}} \leq C \|\psi\|_{t+\frac{1}{2}, \Omega_i}, \quad t > 0, \quad (2.65)$$

$$\langle \psi, \tau n \rangle_{\partial \Omega_i} \leq C \|\psi\|_{\frac{1}{2}, \partial \Omega_i} \|\tau\|_{H(\operatorname{div}; \Omega_i)}, \quad \langle \psi, \zeta \cdot n \rangle_{\partial \Omega_i} \leq C \|\psi\|_{\frac{1}{2}, \partial \Omega_i} \|\zeta\|_{H(\operatorname{div}; \Omega_i)}, \quad (2.66)$$

which can be found in [30] and [15, 47], respectively.

Finally, define the projection operators $\hat{\Pi}^\sigma$, Π^z , \mathcal{P}_h^p , \mathcal{P}_h^u , \mathcal{R}_h on respective spaces defined in global domain, Ω , to be the piece-wise application of $\hat{\Pi}_i^\sigma$, Π_i^z , $\mathcal{P}_{h,i}^p$, $\mathcal{P}_{h,i}^u$, $\mathcal{R}_{h,i}$, respectively on subdomains Ω_i for $i = 1, \dots, N$.

2.4 Spaces of weakly continuous stress and velocity

In this section, we introduce the spaces of weakly continuous stress tensors and velocity vectors, which are defined as follows:

$$\mathbb{X}_{h,0} = \left\{ \tau \in \mathbb{X}_h : \sum_{i=1}^N \langle \tau n_i, \mu^u \rangle_{\Gamma_i} = 0, \quad \forall \mu^u \in \Lambda_H^u \right\}$$

and

$$Z_{h,0} = \left\{ \zeta \in Z_h : \sum_{i=1}^N \langle \zeta \cdot n_i, \mu^p \rangle_{\Gamma_i} = 0, \quad \forall \mu^p \in \Lambda_H^p \right\}.$$

In order to find a priori error estimates for the method (2.31)–(2.37) using techniques developed for single domain system (2.15)–(2.19) in [5], we restate (2.31)–(2.37) in terms of $\mathbb{X}_{h,0}$ and $Z_{h,0}$ as

follows: find $(\sigma_h, u_h, \gamma_h, z_h, p_h) : [0, T] \rightarrow (\mathbb{X}_{h,0}, V_h, \mathbb{Q}_h, Z_{h,0}, W_h)$ such that $p_h(0) = p_{h,0}$ and

$$(A(\sigma_h + \alpha p_h I), \tau) + \sum_{i=1}^N (u_h, \operatorname{div} \tau)_{\Omega_i} + (\gamma_h, \tau) = 0, \quad \forall \tau \in \mathbb{X}_{h,0}, \quad (2.67)$$

$$\sum_{i=1}^N (\operatorname{div} \sigma_h, v)_{\Omega_i} = -(f, v), \quad \forall v \in V_h, \quad (2.68)$$

$$(\sigma_h, \xi) = 0, \quad \forall \xi \in \mathbb{Q}_h, \quad (2.69)$$

$$(K^{-1} z_h, \zeta) - \sum_{i=1}^N (p_h, \operatorname{div} \zeta)_{\Omega_i} = 0, \quad \forall \zeta \in Z_{h,0}, \quad (2.70)$$

$$c_0 (\partial_t p_h, w) + \alpha (\partial_t A(\sigma_h + \alpha p_h I), wI) + \sum_{i=1}^N (\operatorname{div} z_h, w)_{\Omega_i} = (g, w), \quad \forall w \in W_h. \quad (2.71)$$

Note that constructing basis functions for function spaces, $\mathbb{X}_{h,0}$ and $Z_{h,0}$, is difficult and we use the above formulation only for the sake of error analysis. In the later sections, we will present a reduction to interface problem approach to design the numerical algorithm using any of the popular sub-domain spaces $\mathbb{X}_{h,i}$ and $Z_{h,i}$ discussed earlier.

3 Analysis of the MMMFE Method

In this section, we present well-posedness and error analysis of the DD formulation developed in the previous section. We start out by proving inf-sup stability bounds for weakly continuous stress, $\mathbb{X}_{h,0}$, and velocity, $Z_{h,0}$, spaces under appropriate conditions on the mortar space, Λ_H . Under the same conditions, we show that the multiscale mortar DD method is well-posed and stable. We finish the section by proving a combined a priori error bound for all the variables in the formulation.

3.1 Inf-sup stability for the weakly continuous spaces

In this subsection, we give inf-sup stability bounds for the weakly continuous stress, $\mathbb{X}_{h,0}$, and velocity, $Z_{h,0}$, spaces under appropriate conditions on the mortar space, Λ_H .

Assumption 1. *The mortar space Λ_H is chosen so that there exists a positive constant C independent of H and h such that the following inequality holds:*

$$\|\mu\|_{\Gamma_{i,j}} \leq C (\|\mathcal{Q}_{h,i}\mu\|_{\Gamma_{i,j}} + \|\mathcal{Q}_{h,j}\mu\|_{\Gamma_{i,j}}), \quad \forall \mu \in \Lambda_H, \quad 1 \leq i < j \leq n. \quad (3.1)$$

Remark 3.1. *Note that assumption (3.1) implies that the space Λ_H cannot be too rich compared to subdomain stress-velocity FE spaces (similar approach to [7]) in the sense that Λ_H^u and Λ_H^p are well controlled by their projections on to the normal traces of stress and velocity sub-domain spaces respectively. In practice, this condition can be easily obtained by taking a coarser mortar mesh satisfying $h < H \leq 1$ (see [7, 6, 42]).*

Lemma 1. *Under the assumption (3.1), there exists a constant $\beta_D > 0$, independent of h and H such that for any $\mu^p \in \Lambda_H^p$, the following holds:*

$$\|\mu^p\|_{\Gamma} \leq \beta_D \sup_{0 \neq \zeta \in Z_h} \frac{\sum_{i=1}^N \langle \zeta \cdot n_i, \mu^p \rangle_{\Gamma_i}}{\|\zeta\|_{Z_h}}. \quad (3.2)$$

Proof. We start with any $\mu^p \in \Lambda_H^p$ and extend it by zero on $\partial\Omega$. Let ϕ_i be the solution to the following auxiliary problem

$$\operatorname{div} \nabla \phi_i = \overline{\mathcal{Q}_{h,i}^p \mu^p}, \quad \text{in } \Omega_i, \quad (3.3)$$

$$\nabla \phi_i \cdot n_i = \mathcal{Q}_{h,i}^p \mu^p, \quad \text{on } \partial\Omega_i, \quad (3.4)$$

where $\overline{\mathcal{Q}_{h,i}^p \mu^p}$ denotes the mean value of $\mathcal{Q}_{h,i}^p \mu^p$ on $\partial\Omega_i$. The above problem can be reformulated in the mixed form by defining $\psi_i = \nabla\phi_i$. The aforementioned elliptic problem is well-posed and the elliptic regularity (see [30]) gives

$$\|\psi_i\|_{1/2,\Omega_i} + \|\operatorname{div}\psi\|_{\Omega_i} \leq C\|\mathcal{Q}_{h,i}^p \mu^p\|_{\partial\Omega_i}. \quad (3.5)$$

Take $\zeta_{h,i} = \Pi^z \psi_i \in Z_{h,i}$ and (2.45) combined with (3.4) implies that $\zeta_{h,i} \cdot n_i = \mathcal{Q}_{h,i}^p \mu$ on $\partial\Omega_i$. This equality along with the definition of $\mathcal{Q}_{h,i}^p$ imply

$$\begin{aligned} \sum_{i=1}^N \langle \zeta_{h,i} \cdot n_i, \mu^p \rangle_{\Gamma_i} &= \sum_{i=1}^N \langle \Pi^z \psi_i \cdot n_i, \mu^p \rangle_{\partial\Omega_i} = \sum_{i=1}^N \langle \Pi^z \psi_i \cdot n_i, \mathcal{Q}_{h,i}^p \mu^p \rangle_{\partial\Omega_i} \\ &= \sum_{i=1}^N \langle \mathcal{Q}_{h,i}^p \mu^p, \mathcal{Q}_{h,i}^p \mu^p \rangle_{\partial\Omega_i} \geq C \sum_{i=1}^N \|\mu\|_{\Gamma_i}, \end{aligned} \quad (3.6)$$

where we have used the mortar coarseness assumption (3.1).

Next, we note that

$$\|\zeta_{h,i}\|_{Z_i} \leq C \sum_{i=1}^N \|\mu\|_{\Gamma_i}, \quad (3.7)$$

which follows from the stability of the canonical projection Π_i^z , (2.46), with $\epsilon = 1/2$, (3.5) and the stability of $\mathcal{Q}_{h,i}^p$.

Finally, (3.7) combined with (3.6) and defining $\zeta := \zeta_{h,i}$ on Ω_i completes the proof. \square

Lemma 2. *Under the assumption (3.1), there exists a constant $\beta_E > 0$, independent of h and H such that for any $\mu^u \in \Lambda_H^u$, the following bound holds*

$$\|\mu^u\|_{\Gamma} \leq \beta_E \sup_{0 \neq \tau \in \mathbb{X}_h} \frac{\sum_{i=1}^N \langle \tau n_i, \mu^u \rangle_{\Gamma_i}}{\|\tau\|_{\mathbb{X}_h}}. \quad (3.8)$$

Proof. The proof follows similar arguments as in the proof of the previous lemma, starting with any $\mu^u \in \Lambda_H^u$ and using elliptic regularity of corresponding elliptic problem and stability of the projections Π_i^σ and $\mathcal{Q}_{h,i}^u$. \square

Lemma 3. *Under the assumption (3.1), there exists a linear operator $\Pi_0^\sigma : H^{\frac{1}{2}+\epsilon}(\Omega, \mathbb{M}) \cap \mathbb{X} \rightarrow \mathbb{X}_{h,0}$ for any $\epsilon > 0$, such that for any $\tau \in H^{\frac{1}{2}+\epsilon}(\Omega, \mathbb{M}) \cap \mathbb{X}$,*

$$\sum_{i=1}^N (\operatorname{div}(\Pi_0^\sigma \tau - \tau), v)_{\Omega_i} = 0, \quad \forall v \in V_h, \quad (3.9)$$

$$(\Pi_0^\sigma \tau - \tau, \xi) = 0, \quad \forall \xi \in \mathbb{Q}_h, \quad (3.10)$$

$$\|\Pi_0^\sigma \tau\| \leq C \left(\|\tau\|_{\frac{1}{2}+\epsilon} + \|\operatorname{div}\tau\| \right), \quad (3.11)$$

$$\|\Pi_0^\sigma \tau - \tau\| \leq C \left(\sum_{i=1}^N h^{\tilde{t}} \|\tau\|_{\tilde{t},\Omega_i} + h^{\tilde{k}} H^{\frac{1}{2}} \|\tau\|_{\tilde{k}+\frac{1}{2}} \right), \quad 0 < \tilde{t} \leq k+1, 0 < \tilde{k} \leq k+1, \quad (3.12)$$

$$\|\operatorname{div}(\Pi_0^\sigma \tau - \tau)\|_{\Omega_i} \leq C h^{\tilde{l}} \|\operatorname{div}\tau\|_{\tilde{l},\Omega_i}, \quad 0 \leq \tilde{l} \leq l+1. \quad (3.13)$$

Proof. The proof is based on constructing $\Pi_0^\sigma \tau|_{\partial\Omega_i} = \hat{\Pi}_i^\sigma(\tau + \delta\tau_i)$, where the correction $\delta\tau_i$ is designed to give weak continuity of the normal components. The proof of (3.9)–(3.12) is given in [33, Lemma 4.6]. Bound (3.13) follows from (3.9) and the approximation properties of the L^2 -projection [16]. \square

Lemma 4. *Under the assumption (3.1), there exists a linear operator $\Pi_0^z : \left(H^{\frac{1}{2}+\epsilon}(\Omega) \right)^d \cap Z \rightarrow Z_{h,0}$ such that for any $1 \leq i \leq N$ and $\zeta \in \left(H^{\frac{1}{2}+\epsilon}(\Omega) \right)^d \cap Z$,*

$$\sum_{i=1}^N (\operatorname{div}(\Pi_0^z \zeta - \zeta), w)_{\Omega_i} = 0, \quad \forall w \in W_h, \quad (3.14)$$

$$\|\Pi_0^z \zeta\|_{Z_h} \leq C \left(\|\zeta\|_{\frac{1}{2}+\epsilon} + \|\operatorname{div} \zeta\| \right), \quad (3.15)$$

$$\|\Pi_0^z \zeta - \zeta\| \leq C \left(\sum_{i=1}^N h^{\tilde{t}} \|\zeta\|_{\tilde{t}, \Omega_i} + h^{\tilde{r}} H^{\frac{1}{2}} \|\zeta\|_{\tilde{r}+\frac{1}{2}} \right), \quad 0 < \tilde{t} \leq r+1, 0 < \tilde{r} \leq r+1, \quad (3.16)$$

$$\|\operatorname{div}(\Pi_0^z \zeta - \zeta)\|_{\Omega_i} \leq C h^{\tilde{s}} \|\operatorname{div} \zeta\|_{\tilde{s}, \Omega_i}, \quad 0 \leq \tilde{s} \leq s+1. \quad (3.17)$$

Proof. The proof follows from the arguments given in [6, Section 3] and [7, Section 3]. \square

Lemmas 3 and 4 along with Fortin's Lemma [26, 15] imply the following inf-sup stability bounds with respect to the weakly continuous spaces of stress and velocity.

Lemma 5. *Under the assumption (3.1), there exists positive constants C_E and C_D independent of the discretization parameters h and H such that*

$$\forall v \in V_h, \xi \in \mathbb{Q}_h, \quad \|v\| + \|\xi\| \leq C_E \sup_{0 \neq \tau \in \mathbb{X}_{h,0}} \frac{\sum_{i=1}^N (v, \operatorname{div} \tau)_{\Omega_i} + (\xi, \tau)}{\|\tau\|_{\mathbb{X}_h}}, \quad (3.18)$$

$$\forall w \in W_h, \quad \|w\| \leq C_D \sup_{0 \neq \zeta \in Z_{h,0}} \frac{\sum_{i=1}^N (\operatorname{div} \zeta, w)_{\Omega_i}}{\|\zeta\|_{Z_h}}. \quad (3.19)$$

3.2 Well-posedness of the semi-discrete MMMFE formulation

In this subsection, we show the existence of a unique solution to the system of equations (2.31)–(2.37) under the assumption (3.1). We follow closely the proof for the well-posedness of the multipoint flux method for the Biot system given in [5]. We base our proof on the theory for showing the existence of solution to a degenerate parabolic system [51]. In particular, we use [51, IV, Theorem 6.1(b)] which is stated as follows:

Theorem 6. *Let the linear, symmetric, and monotone operator \mathcal{N} be given for the real vector space E to its algebraic dual E^* , and let E'_b be the Hilbert space which is the dual of E with the seminorm $|x|_b = \sqrt{\mathcal{N}x(x)}$ for $x \in E$. Let $\mathcal{M} \subset E \times E'_b$ be a relation with the domain $D = \{x \in E : \mathcal{M}(x) \neq \emptyset\}$. Assume that \mathcal{M} is monotone and $\operatorname{Range}(\mathcal{N} + \mathcal{M}) = E'_b$. Then for each $x_0 \in D$ and for each $\mathcal{F} \in W^{1,1}(0, T; E'_b)$, there is a solution x of*

$$\frac{d}{dt} (\mathcal{N}x(t) + \mathcal{M}(x(t))) \ni \mathcal{F}(t), \quad \text{a.e. } 0 < t < T,$$

with

$$\mathcal{N}x \in W^{1,\infty}(0, T; E'_b), x(t) \in D, \text{ for all } 0 \leq t \leq T, \text{ and } \mathcal{N}x(0) = \mathcal{N}x_0.$$

Using the above theorem, we now prove that the semi-discrete system (2.31)–(2.37) is well-posed.

Theorem 7. *For each $(f, g) \in W^{1,\infty}(0, T; (L^2(\Omega))^d) \times W^{1,\infty}(0, T; L^2(\Omega))$ and compatible initial data $(\sigma_{h,0}, u_{h,0}, \gamma_{h,0}, z_{h,0}, p_{h,0}, \lambda_{H,0})$, the system of equations (2.31)–(2.37) has a unique solution, provided that the assumption (3.1) holds.*

Proof. We start by reformulating (2.31)–(2.37) to fit the setting of Theorem 6. For this purpose,

we define operators

$$\begin{aligned}
(A_{\sigma\sigma}\sigma_h, \tau) &= (A\sigma_h, \tau), \quad (A_{\sigma p}\sigma_h, w) = \alpha(A\sigma_h, wI), \quad (A_{\sigma u}\sigma_h, v) = \sum_{i=1}^N (\operatorname{div} \sigma_{h,i}, v), \\
(A_{\sigma\gamma}\sigma_h, \xi) &= (\sigma_h, \xi), \quad (A_{\sigma\lambda}\sigma_h, \mu^u) = \sum_{i=1}^N \langle \sigma_h n_i, \mu^u \rangle_{\Gamma_i}, \quad (A_{zz}z_h, \zeta) = (K^{-1}z_h, \zeta), \\
(A_{zp}z_h, w) &= -\sum_{i=1}^N (\operatorname{div} z_{h,i}, w), \quad (A_{z\lambda}z_h, \mu^p) = \sum_{i=1}^N \langle z_h \cdot n_i, \mu^p \rangle_{\Gamma_i}, \\
(A_{pp}p_h, w) &= c_0(p_h, w) + \alpha^2(Ap_h I, wI).
\end{aligned}$$

Let us introduce the new variables $\dot{u}_h, \dot{\gamma}_h$, and $\dot{\lambda}_H^u$ representing $\partial_t u_h, \partial_t \gamma_h$, and $\partial_t \lambda_H^u$, respectively. We differentiate equation (2.31) in time to get

$$(\partial_t A(\sigma_h + \alpha p_h I), \tau) + \sum_{i=1}^N (\dot{u}_h, \operatorname{div} \tau)_{\Omega_i} + (\dot{\gamma}_h, \tau) = \sum_{i=1}^N (\dot{\lambda}_H^u, \tau n_i)_{\Gamma_i}, \quad \forall \tau \in \mathbb{X}_h. \quad (3.20)$$

Using the above definitions of operators and using (3.20) instead of equation (2.31), we can reformulate the problem as a system of linear equations

$$\frac{d}{dt}(\mathcal{N}\dot{x}(t) + \mathcal{M}(\dot{x}(t))) = \mathcal{F}(t) \quad 0 < t < T, \quad (3.21)$$

where

$$\dot{x} = \begin{pmatrix} \sigma_h \\ \dot{u}_h \\ \dot{\gamma}_h \\ z_h \\ p_h \\ \dot{\lambda}_H^u \\ \dot{\lambda}_H^p \end{pmatrix}, \quad N = \begin{pmatrix} A_{\sigma\sigma} & 0 & 0 & 0 & A_{\sigma p}^T & 0 & 0 \\ 0 & 0 & 0 & 0 & 0 & 0 & 0 \\ 0 & 0 & 0 & 0 & 0 & 0 & 0 \\ 0 & 0 & 0 & 0 & 0 & 0 & 0 \\ A_{\sigma p} & 0 & 0 & 0 & A_{pp} & 0 & 0 \\ 0 & 0 & 0 & 0 & 0 & 0 & 0 \\ 0 & 0 & 0 & 0 & 0 & 0 & 0 \end{pmatrix},$$

$$M = \begin{pmatrix} 0 & A_{\sigma u}^T & A_{\sigma\gamma}^T & 0 & 0 & -A_{\sigma\lambda}^T & 0 \\ -A_{\sigma u} & 0 & 0 & 0 & 0 & 0 & 0 \\ -A_{\sigma\gamma} & 0 & 0 & 0 & 0 & 0 & 0 \\ 0 & 0 & 0 & A_{zz} & A_{zp}^T & 0 & A_{z\lambda}^T \\ 0 & 0 & 0 & -A_{zp} & 0 & 0 & 0 \\ A_{\sigma\lambda} & 0 & 0 & 0 & 0 & 0 & 0 \\ 0 & 0 & 0 & A_{z\lambda} & 0 & 0 & 0 \end{pmatrix}, \quad \mathcal{F} = \begin{pmatrix} 0 \\ -f \\ 0 \\ 0 \\ g \\ 0 \\ 0 \end{pmatrix}.$$

The dual space E'_b is given by $L^2(\Omega, \mathbb{M}) \times 0 \times 0 \times 0 \times L^2(\Omega) \times 0 \times 0$ and the condition $\mathcal{F} \in W^{1,1}(0, T; E'_b)$ implies that non-zero source terms can appear only in equations with time derivatives. This means we have to take $f = 0$ in our case. We can fix this issue by considering an auxiliary problem that, for each $t \in (0, T]$, solves the system

$$\begin{pmatrix} A_{\sigma\sigma} & A_{\sigma u}^T & A_{\sigma\gamma}^T & -A_{\sigma\lambda}^T \\ -A_{\sigma u} & 0 & 0 & 0 \\ -A_{\sigma\gamma} & 0 & 0 & 0 \\ A_{\sigma\lambda} & 0 & 0 & 0 \end{pmatrix} \begin{pmatrix} \sigma_h^f \\ \partial_t u_h^f \\ \partial_t \gamma_h^f \\ \partial_t \lambda_H^{u,f} \end{pmatrix} = \begin{pmatrix} 0 \\ -f \\ 0 \\ 0 \end{pmatrix}. \quad (3.22)$$

Such an auxiliary system (3.22) is well-posed and the proof can be found in [33]. Now we can subtract the solution to (3.22) from the original system of equations (2.31)–(2.37) to obtain the modified RHS $\mathcal{F} = (A_{\sigma\sigma}(\sigma_h^f - \partial_t \sigma_h^f), 0, 0, 0, q - A_{\sigma p} \partial_t \sigma_h^f, 0, 0)^T$.

Next we show that $\text{Range}(\mathcal{N} + \mathcal{M}) = E'_b$. This can be established by showing that the following square linear homogeneous system has only the trivial solution: $(\hat{\sigma}_h, \hat{u}_h, \hat{\gamma}_h, \hat{z}_h, \hat{p}_h, \hat{\lambda}_H) \in \mathbb{X}_h \times V_h \times \mathbb{Q}_h \times Z_h \times W_h \times \Lambda_H$ such that

$$(A(\hat{\sigma}_h + \alpha \hat{p}_h I), \tau) + \sum_{i=1}^N (\hat{u}_h, \text{div } \tau)_{\Omega_i} + (\hat{\gamma}_h, \tau) - \sum_{i=1}^N \langle \hat{\lambda}_H^u, \tau n_i \rangle_{\Gamma_i} = 0, \quad \forall \tau \in \mathbb{X}_h, \quad (3.23)$$

$$\sum_{i=1}^N (\text{div } \hat{\sigma}_h, v)_{\Omega_i} = 0, \quad \forall v \in V_h,$$

$$(\hat{\sigma}_h, \xi) = 0, \quad \forall \xi \in \mathbb{Q}_h,$$

$$(K^{-1} \hat{z}_h, \zeta) - \sum_{i=1}^N (\hat{p}_h, \text{div } \zeta)_{\Omega_i} + \sum_{i=1}^N \langle \hat{\lambda}_H^p, \zeta \cdot n_i \rangle_{\Gamma_i} = 0, \quad \forall \zeta \in Z_h, \quad (3.24)$$

$$c_0 (\partial_t \hat{p}_h, w) + \alpha (A(\hat{\sigma}_h + \alpha \hat{p}_h I), wI) + \sum_{i=1}^N (\text{div } \hat{z}_h, w)_{\Omega_i} = 0, \quad \forall w \in W_h,$$

$$\sum_{i=1}^N \langle \hat{\sigma}_h n_i, \mu^u \rangle_{\Gamma_i} = 0, \quad \forall \mu^u \in \Lambda_H^u,$$

$$\sum_{i=1}^N \langle \hat{z}_h \cdot n_i, \mu^p \rangle_{\Gamma_i} = 0, \quad \forall \mu^p \in \Lambda_H^p.$$

Taking appropriate test functions $(\tau, v, \xi, \zeta, w, \mu^u, \mu^p) = (\hat{\sigma}_h, \hat{u}_h, \hat{\gamma}_h, \hat{z}_h, \hat{p}_h, \hat{\lambda}_H^u, \hat{\lambda}_H^p)$ in the above system and adding the equations together gives $\|A^{\frac{1}{2}}(\hat{\sigma}_h + \alpha \hat{p}_h I)\|^2 + c_0 \|\hat{p}_h\|^2 + \|K^{-\frac{1}{2}} \hat{z}_h\|^2 = 0$. The coercivity of A , (2.22), and K , (2.23), give $\hat{\sigma}_h + \alpha \hat{p}_h I = 0$ and $\hat{z}_h = 0$ respectively. Further, the inf-sup condition with respect to the weakly continuous space $Z_{h,0}$, (3.19), implies $\hat{p}_h = 0$ and hence we also have $\hat{\sigma}_h = 0$. Inf-sup condition with respect to the weakly continuous space $\mathbb{X}_{h,0}$, (3.18), implies $\hat{u}_h = 0$ and $\hat{\gamma}_h = 0$. Finally, (3.2) combined with (3.23) implies $\hat{\lambda}_H^u = 0$, and (3.8) combined with (3.24) implies $\hat{\lambda}_H^p = 0$. Similar arguments can be used to show that \mathcal{N} and \mathcal{M} are non-negative and therefore due to linearity, monotone.

Now to completely satisfy the hypothesis of Theorem 6, we need compatible initial data $\hat{x}_0 \in D$ which implies $\mathcal{M}\hat{x}_0 \in E'_b$. We first construct compatible initial data to the continuous system (2.10)-(2.14), $(\sigma_0, u_0, \gamma_0, z_0, p_0)^T$, from continuous initial condition, p_0 , as follows:

1. Solve equations (2.10)–(2.12) using $p = p_0$ as given initial data to get σ_0, u_0, γ_0 .
2. Set $z_0 = -K\nabla p_0$ and it is easy to show using integration by parts that this choice satisfies equation (2.13) with $p = p_0$.

Define $\tilde{x}_0 = (\sigma_0, u_0, \gamma_0, z_0, p_0, \lambda_{H,0}^u, \lambda_{H,0}^p)^T$, where $\lambda_{H,0}^u = u_0|_{\Gamma}$ and $\lambda_{H,0}^p = p_0|_{\Gamma}$. Take the initial data to the system (2.31)–(2.30), x_0 , to be the elliptic projection of \tilde{x}_0 . With the reduction of the problem to the case with $f = 0$, we have $(\mathcal{N} + \mathcal{M})\tilde{x}_0 \in E'_b$. We also have

$$(\mathcal{N} + \mathcal{M})x_0 = (\mathcal{N} + \mathcal{M})\tilde{x}_0, \quad (3.25)$$

which implies $\mathcal{M}x_0 = (\mathcal{N} + \mathcal{M})\tilde{x}_0 - \mathcal{N}x_0 \in E'_b$. Now for the modified system (3.21), we take the initial data, \hat{x}_0 to be $(\sigma_{h,0}, 0, 0, z_{h,0}, p_{h,0}, 0, 0)$, which also satisfies $\mathcal{M}\hat{x}_0 \in E'_b$. Note that initial data $u_{h,0}$, $\gamma_{h,0}$ and $\lambda_{H,0}^u$ are not needed to solve (3.21), but will be used later to recover solution to the original problem.

Now we can apply Theorem 6 to prove the existence of a unique solution

$$\hat{x} = (\sigma_h, \dot{u}_h, \dot{\gamma}_h, z_h, p_h, \lambda_H),$$

such that $\sigma_h(0) = \sigma_{h,0}$ and $p_h(0) = p_{h,0}$. It is also easy to see that $z_h(0) = z_{h,0}$ by taking $t \rightarrow 0$ in (2.70) and using the fact that $z_{h,0}$ and $p_{h,0}$ satisfy (2.70). Finally for each $t \in [0, T]$, we define u_h , γ_h , and λ_H^u as follows:

$$u_h(t) = u_{h,0} + \int_0^t \dot{u}_h(s) ds,$$

$$\gamma_h(t) = \gamma_{h,0} + \int_0^t \dot{\gamma}_h(s) ds,$$

and

$$\lambda_H^u(t) = \lambda_{H,0}^u + \int_0^t \dot{\lambda}_H^u(s) ds.$$

It is easy to show that $u_h(t)$, $\gamma_h(t)$ and $\lambda_H^u(t)$ satisfy equation (2.31). We can indeed verify this by integrating the differentiated version of this equation namely equation (3.20) with respect to time from 0 to any $t \in (0, T]$ and using the fact that $\sigma_{h,0}$, $u_{h,0}$, $\gamma_{h,0}$, and $\lambda_{H,0}^u$ satisfy equation (2.31). This completes the proof that (2.41)–(2.30) has a solution $(\sigma_h, u_h, \gamma_h, z_h, p_h, \lambda_H)$. Uniqueness of the above constructed solution follows from the stability bound for the solution variables which will be discussed in the next section. \square

3.3 Stability analysis for MMMFE formulation

In this subsection, we give a stability bound for the system (2.31)–(2.37).

Theorem 8. *Under the assumption (3.1), there exists a constant $C > 0$, independent of discretization parameters h and H , and c_0 such that the following stability bound holds for the solution of (2.31)–(2.37):*

$$\begin{aligned} & \|\sigma_h\|_{L^\infty(0,T;\mathbb{X}_h)} + \|u_h\|_{L^\infty(0,T;L^2(\Omega))} + \|\gamma_h\|_{L^\infty(0,T;L^2(\Omega))} + \|z_h\|_{L^\infty(0,T;L^2(\Omega))} + \|p_h\|_{L^\infty(0,T;L^2(\Omega))} \\ & + \|\lambda_H^u\|_{L^\infty(0,T;L^2(\Gamma))} + \|\lambda_H^p\|_{L^\infty(0,T;L^2(\Gamma))} + \|\sigma_h\|_{L^2(0,T;\mathbb{X}_h)} + \|u_h\|_{L^2(0,T;L^2(\Omega))} + \|\gamma_h\|_{L^2(0,T;L^2(\Omega))} \\ & + \|z_h\|_{L^2(0,T;Z_h)} + \|p_h\|_{L^2(0,T;L^2(\Omega))} + \|\lambda_H^u\|_{L^2(0,T;L^2(\Gamma))} + \|\lambda_H^p\|_{L^2(0,T;L^2(\Gamma))} \\ & \leq C(\|f\|_{H^1(0,T;L^2(\Omega))} + \|g\|_{H^1(0,T;L^2(\Omega))} + \|p_0\|_{H^1(\Omega)} + \|\nabla K p_0\|_{H(\text{div},\Omega)}). \end{aligned}$$

Proof. We start out by choosing the test functions

$$(\tau, v, \xi, \zeta, w, \mu^u, \mu^p) = (\sigma_h, \partial_t u_h, \partial_t \gamma_h, z_h, p_h, \partial_t \lambda_H^u, \lambda_H^p),$$

in equations (3.20) and (2.32)–(2.37) and combining them to get

$$(\partial_t A(\sigma_h + \alpha p_h I), \sigma_h + \alpha p_h I) + c_0(\partial_t p_h, p_h) + (K^{-1} z_h, z_h) = (f, \partial_t u_h) + (g, p_h).$$

The above equation can be rewritten as

$$\frac{1}{2} \partial_t \left(\|A^{\frac{1}{2}}(\sigma_h + \alpha p_h I)\|^2 + c_0 \|p_h\|^2 \right) + \|K^{-\frac{1}{2}} z_h\|^2 = \partial_t (f, u_h) - (\partial_t f, u_h) + (g, p_h). \quad (3.26)$$

For any $t \in (0, T]$, we integrate equation (3.26) with respect to time from 0 to t to get

$$\begin{aligned} & \frac{1}{2} \left(\|A^{\frac{1}{2}}(\sigma_h + \alpha p_h I)(t)\|^2 + c_0 \|p_h(t)\|^2 \right) + \int_0^t \|K^{-\frac{1}{2}} z_h\|^2 ds \\ & = \frac{1}{2} \left(\|A^{\frac{1}{2}}(\sigma_h + \alpha p_h I)(0)\|^2 + c_0 \|p_h(0)\|^2 \right) + \int_0^t ((g, p_h) - (\partial_t f, u_h)) ds + (f, u_h)(t) - (f, u_h)(0). \end{aligned}$$

On applications of the Cauchy-Schwartz and Young's inequalities, we get

$$\begin{aligned} & \|A^{\frac{1}{2}}(\sigma_h + \alpha p_h I)(t)\|^2 + c_0 \|p_h(t)\|^2 + 2 \int_0^t \|K^{-\frac{1}{2}} z_h\|^2 ds \\ & \leq \|A^{\frac{1}{2}}(\sigma_h + \alpha p_h I)(0)\|^2 + c_0 \|p_h(0)\|^2 + \epsilon \left(\int_0^t (\|p_h\|^2 + \|u_h\|^2) ds + \|u_h(t)\|^2 \right) \\ & + \frac{1}{\epsilon} \left(\int_0^t (\|g\|^2 + \|\partial_t f\|^2) ds + \|f(t)\|^2 \right) + \|f(0)\|^2 + \|u_h(0)\|^2. \end{aligned} \quad (3.27)$$

Bounds for $\|u_h\|$ and $\|\gamma_h\|$ follow from the inf-sup condition (3.18) as follows:

$$\|u_h\| + \|\gamma_h\| \leq C_E \sup_{0 \neq \tau \in \mathbb{X}_{h,0}} \frac{\sum_{i=1}^N (u_h, \text{div } \tau)_{\Omega_i} + (\gamma_h, \tau)}{\|\tau\|_{\mathbb{X}_h}}.$$

We combine the above equation along with (2.31) and the Cauchy-Schwartz inequality to obtain the bound

$$\|u_h\| + \|\gamma_h\| \leq C_E \sup_{0 \neq \tau \in \mathbb{X}_{h,0}} \frac{\left(A^{\frac{1}{2}}(\sigma_h + \alpha p_h I), A^{\frac{1}{2}}\tau \right)}{\|\tau\|_{\mathbb{X}_h}} \leq C \|A^{\frac{1}{2}}(\sigma_h + \alpha p_h I)\|. \quad (3.28)$$

Equation (3.28) also gives,

$$\int_0^t (\|u_h\|^2 + \|\gamma_h\|^2) ds \leq C \int_0^t (\|\sigma_h\|^2 + \|p_h\|^2) ds. \quad (3.29)$$

Further, choose test functions $(\tau, v, \xi, \mu^u) = (\sigma_h, u_h, \gamma_h, \lambda_H^u)$ in (2.31)–(2.33), (2.36) and combine the equations along with Cauchy-Schwartz inequality to get

$$\|\sigma_h\|^2 \leq C \left(\|p_h^2\| + \epsilon \|u_h\|^2 + \frac{1}{\epsilon} \|f\|^2 \right).$$

Combining the above inequality with inequality (3.29) yields the following bound

$$\int_0^t (\|u_h\|^2 + \|\gamma_h\|^2) ds \leq C \int_0^t \left(\|p_h^2\| + \epsilon \|u_h\|^2 + \frac{1}{\epsilon} \|f\|^2 \right) ds. \quad (3.30)$$

Bound for $\|p_h\|$ can be obtained from the inf-sup condition (3.19) and equation (2.34) as follows:

$$\|p_h\| \leq C_D \sup_{0 \neq \zeta_h \in Z_{h,0}} \frac{\sum_{i=1}^N (\operatorname{div} \zeta_h, p_h)_{\Omega_i}}{\|\zeta_h\|_{Z_h}} = C_D \sup_{0 \neq \zeta_h \in Z_{h,0}} \frac{(K^{-1}z_h, \zeta_h)}{\|\zeta_h\|_{Z_h}} \leq C \|K^{-1}z_h\|, \quad (3.31)$$

where the last inequality follows from the Cauchy-Schwartz inequality.

Further, taking test function $v = \operatorname{div}_h \sigma_h$ in (2.32) and using Cauchy-Schwartz inequality yields

$$\|\operatorname{div}_h \sigma_h\|^2 \leq \|f\|^2. \quad (3.32)$$

Finally, combining inequalities (3.27)–(3.28) and (3.30)–(3.32) and taking ϵ small enough give the following bound

$$\begin{aligned} & \|A^{\frac{1}{2}}(\sigma_h + \alpha p_h I)(t)\|^2 + \|\operatorname{div}_h \sigma_h(t)\|^2 + \|u_h(t)\|^2 + \|\gamma_h(t)\|^2 + c_0 \|p_h(t)\|^2 \\ & + \int_0^t (\|\sigma_h\|^2 + \|\operatorname{div}_h \sigma_h\|^2) ds + \int_0^t \left(\|u_h\|^2 + \|\gamma_h\|^2 + \|K^{-\frac{1}{2}}z_h\|^2 + \|p_h\|^2 \right) ds \\ & \leq C \left(\int_0^t (\|g(s)\|^2 + \|\partial_t f(s)\|^2 + \|f(s)\|^2) ds + \|f(t)\|^2 + \|\sigma_h(0)\|^2 \right. \\ & \quad \left. + \|u_h(0)\|^2 + \|p_h(0)\|^2 + \|f(0)\|^2 \right). \end{aligned} \quad (3.33)$$

Next we give bounds for $\|\operatorname{div}_h z_h\|$, $\|K^{-\frac{1}{2}}z_h(t)\|$, and $\|p_h(t)\|$ for all $t \in (0, t]$, which are independent of c_0 . We start by choosing test function $w = \operatorname{div}_h z_h$ in (2.35) and applying the Cauchy-Schwartz inequality to obtain

$$\|\operatorname{div}_h z_h\| \leq C \left(c_0 \|\partial_t p_h\| + \|\partial_t A^{\frac{1}{2}}(\sigma_h + \alpha p_h I)\| + \|q\| \right). \quad (3.34)$$

To bound the right hand side of (3.34), differentiate equations (2.31)–(2.34), and (2.36)–(2.37) with respect to time and take appropriate test functions, namely

$$(\tau, v, \xi, \zeta, w, \mu^u, \mu^p) = (\partial_t \sigma_h, \partial_t u_h, \partial_t \gamma_h, z_h, \partial_t p_h, \partial_t \lambda_H^u, \lambda_H^p),$$

in the differentiated equations and equation (2.35). Further, combining the resulting equations and integrating in time from 0 to $t \in (0, T]$ similar to what we did for equations (3.26)–(3.27) previously,

we obtain

$$\begin{aligned}
& 2 \int_0^t \left(\|\partial_t A^{\frac{1}{2}} (\sigma_h + \alpha p_h I)\|^2 + c_0 \|\partial_t p_h\|^2 \right) ds + \|K^{-\frac{1}{2}} z_h(t)\|^2 \\
& \leq \epsilon \left(\int_0^t \|\partial_t u_h\|^2 ds + \|p_h(t)\|^2 \right) + \frac{1}{\epsilon} \left(\int_0^t \|\partial_t f\|^2 ds + \|g(t)\|^2 \right) \\
& \quad + \int_0^t (\|p_h\|^2 + \|\partial_t g\|^2) ds + \|K^{-\frac{1}{2}} z_h(0)\|^2 + \|p_h(0)\|^2 + \|g(0)\|^2. \tag{3.35}
\end{aligned}$$

To bound $\|\partial_t u_h\|$ and $\|\partial_t \gamma_h\|$, we use the inf-sup condition (3.18) and equation (2.31) as before, but now in their time differentiated forms to obtain

$$\|\partial_t u_h\| + \|\partial_t \gamma_h\| \leq C \|\partial_t A^{\frac{1}{2}} (\sigma_h + \alpha p_h I)\|. \tag{3.36}$$

Combining inequalities (3.31), (3.35), and (3.36), and using small enough ϵ give

$$\begin{aligned}
& \int_0^t \left(\|\partial_t A^{\frac{1}{2}} (\sigma_h + \alpha p_h I)\|^2 + c_0 \|\partial_t p_h\|^2 + \|\partial_t u_h\|^2 + \|\partial_t \gamma_h\|^2 \right) ds + \|K^{-\frac{1}{2}} z_h(t)\|^2 + \|p_h(t)\|^2 \\
& \leq C \left(\int_0^t (\|\partial_t f\|^2 + \|p_h\|^2 + \|\partial_t g\|^2) ds + \|g(t)\|^2 + \|p_h(0)\|^2 + \|g(0)\|^2 + \|z_h(0)\|^2 \right). \tag{3.37}
\end{aligned}$$

Integrating inequality (3.34) with respect to time from 0 to $t \in (0, T]$ and combining the resulting integral inequality with inequalities (3.31) and (3.37) give

$$\begin{aligned}
& \|p_h(t)\|^2 + \|K^{-\frac{1}{2}} z_h(t)\|^2 + \int_0^t \|\operatorname{div}_h z_h\|^2 ds \leq C \left(\int_0^t (\|f(s)\|^2 + \|\partial_t f(s)\|^2 + \|g(s)\|^2 \right. \\
& \quad \left. + \|\partial_t g(s)\|^2) ds + \|f(t)\|^2 + \|g(t)\|^2 + \|\sigma_h(0)\|^2 + \|p_h(0)\|^2 + \|z_h(0)\|^2 + \|f(0)\|^2 + \|g(0)\|^2 \right).
\end{aligned}$$

Also, the coercivity of A and K given in inequalities (2.22) and (2.23), respectively gives

$$\|z_h\| \leq C \|K^{-\frac{1}{2}} z_h\|, \tag{3.38}$$

$$\|\sigma_h\| \leq C \left(\|A^{\frac{1}{2}} (\sigma_h + \alpha p_h I)(t)\| + \|p_h\| \right). \tag{3.39}$$

Next, we give a bound for $\|\lambda_H^u\|$. Combining (3.8) and (2.31) gives

$$\begin{aligned}
\|\lambda_H^u\|_{\Gamma} & \leq C \sup_{0 \neq \tau \in \mathbb{X}_h} \frac{\sum_{i=1}^N \langle \tau n_i, \lambda_H^u \rangle_{\Gamma_i}}{\|\tau\|_{\mathbb{X}_h}} \\
& = C \sup_{0 \neq \tau \in \mathbb{X}_h} \frac{1}{\|\tau\|_{\mathbb{X}_h}} \left((A(\sigma_h + \alpha p_h I), \tau) + \sum_{i=1}^N (u_h, \operatorname{div} \tau)_{\Omega_i} + (\gamma_h, \tau) \right) \\
& \leq C \left(\|A^{\frac{1}{2}} (\sigma_h + \alpha p_h I)\| + \|u_h\| + \|\gamma_h\| \right).
\end{aligned}$$

Squaring the above inequality and integrating from time 0 to t , we get the following set of inequalities

$$\|\lambda_H^u\|_{\Gamma}^2 \leq C \left(\|A^{\frac{1}{2}} (\sigma_h + \alpha p_h I)\|^2 + \|u_h\|^2 + \|\gamma_h\|^2 \right), \tag{3.40}$$

$$\int_0^t \|\lambda_H^u(s)\|_{\Gamma}^2 ds \leq C \int_0^t \left(\|A^{\frac{1}{2}} (\sigma_h + \alpha p_h I)\|^2 + \|u_h\|^2 + \|\gamma_h\|^2 \right) ds. \tag{3.41}$$

Similarly, we can bound $\|\lambda_H^p\|$ combining (3.2) and (2.34) to obtain

$$\begin{aligned}
\|\lambda_H^p\|_{\Gamma} & \leq C \sup_{0 \neq \zeta \in Z_h} \frac{\sum_{i=1}^N \langle \zeta \cdot n_i, \lambda_H^p \rangle_{\Gamma_i}}{\|\zeta\|_{Z_h}} \\
& = C \sup_{0 \neq \zeta \in Z_h} \frac{1}{\|\zeta\|_{Z_h}} \left(-(K^{-1} z_h, \zeta) + (p_h, \operatorname{div} \zeta) \right) \leq C \left(\|K^{-\frac{1}{2}} z_h\| + \|p_h\| \right),
\end{aligned}$$

and using the above inequality to obtain

$$\|\lambda_H^p\|_{\Gamma}^2 \leq C \left(\|K^{-\frac{1}{2}} z_h\|^2 + \|p_h\|^2 \right), \quad (3.42)$$

$$\int_0^t \|\lambda_H^p\|_{\Gamma}^2 ds \leq C \int_0^t \left(\|K^{-\frac{1}{2}} z_h\|^2 + \|p_h\|^2 \right) ds. \quad (3.43)$$

In order to bound the initial data, $\sigma_h(0)$, $u_h(0)$, $z_h(0)$, and $p_h(0)$, note that we obtain the discrete initial data by taking elliptic projection of the continuous initial data $(\sigma_0, u_0, \gamma_0, z_0, p_0)$ to the continuous problem (2.10)–(2.14), see (3.25). Further note that the continuous initial data is constructed using the original pressure initial data $p_0 \in H^1(\Omega)$ using the procedure mentioned in Section 2. Following the arguments used in the proof so far for the steady-state version with $t = 0$ gives

$$\begin{aligned} \|\sigma_h(0)\| + \|u_h(0)\| + \|\gamma_h(0)\| + \|z_h(0)\| + \|p_h(0)\| &\leq C (\|\sigma_0\| + \|u_0\| + \|\gamma_0\| + \|z_0\| + \|p_0\|) \\ &\leq C (\|p_0\|_{H^1(\Omega)} + \|K\nabla p_0\|_{H(\text{div};\Omega)}). \end{aligned} \quad (3.44)$$

Finally, we combine inequalities (3.33), (3.38)–(3.44) along with the fact that all the results derived so far hold for a general $t \in (0, T]$, to arrive at the stability bound in the theorem. \square

3.4 Error analysis

In this subsection, we will establish a combined a priori error estimate for all the unknowns in the formulation.

Theorem 9. *Let $(\sigma_h(t), u_h(t), \gamma_h(t), z_h(t), p_h(t), \lambda_H) \in \mathbb{X}_h \times V_h \times \mathbb{Q}_h \times Z_h \times W_h \times \Lambda_H$ be the solution to the system of equations (2.31)–(2.37) under the assumption (3.1) for $t \in [0, T]$, and suppose the solution of (2.10)–(2.14) is sufficiently smooth, then there exists a positive constant C , independent of h , H and c_0 such that the following holds:*

$$\begin{aligned} &\|\sigma - \sigma_h\|_{L^\infty(0,T;\mathbb{X}_h)} + \|u - u_h\|_{L^\infty(0,T;L^2(\Omega))} + \|\gamma - \gamma_h\|_{L^\infty(0,T;L^2(\Omega))} + \|z - z_h\|_{L^\infty(0,T;L^2(\Omega))} \\ &+ \|p - p_h\|_{L^\infty(0,T;L^2(\Omega))} + \|u - \lambda_H^u\|_{L^\infty(0,T;L^2(\Gamma))} + \|p - \lambda_H^p\|_{L^\infty(0,T;L^2(\Gamma))} + \|\sigma - \sigma_h\|_{L^2(0,T;\mathbb{X}_h)} \\ &+ \|u - u_h\|_{L^2(0,T;L^2(\Omega))} + \|\gamma - \gamma_h\|_{L^2(0,T;L^2(\Omega))} + \|z - z_h\|_{L^2(0,T;Z_h)} + \|p - p_h\|_{L^2(0,T;L^2(\Omega))} \\ &+ \|u - \lambda_H^u\|_{L^2(0,T;L^2(\Gamma))} + \|u - \lambda_H^p\|_{L^2(0,T;L^2(\Gamma))} \leq C \left(h^{k_1} \|\sigma\|_{H^1(0,T;H^{k_1}(\Omega))} \right. \\ &+ h^{k_2} H^{\frac{1}{2}} \|\sigma\|_{H^1(0,T;H^{k_2+\frac{1}{2}}(\Omega))} + h^{l_1} \|\text{div } \sigma\|_{L^\infty(0,T;H^{l_1}(\Omega))} + h^{l_2} \|\text{div } \sigma\|_{L^2(0,T;H^{l_2}(\Omega))} \\ &+ h^{l_3} \|u\|_{L^2(0,T;H^{l_3}(\Omega))} + h^{l_4} \|u\|_{L^\infty(0,T;H^{l_4}(\Omega))} + h^{j_1} \|\gamma\|_{H^1(0,T;H^{j_1}(\Omega))} \\ &+ h^{r_1} \|z\|_{H^1(0,T;H^{r_1}(\Omega))} + h^{r_2} H^{\frac{1}{2}} \|z\|_{H^1(0,T;H^{r_2+\frac{1}{2}}(\Omega))} + h^{s_1} \|\text{div } z\|_{L^2(0,T;H^{s_1}(\Omega))} \\ &\left. + h^{s_2} \|p\|_{H^1(0,T;H^{s_2}(\Omega))} + H^{m_1-\frac{1}{2}} \|u\|_{H^2(0,T;H^{m_1+\frac{1}{2}}(\Omega))} + H^{m_2-\frac{1}{2}} \|p\|_{H^1(0,T;H^{m_2+\frac{1}{2}}(\Omega))} \right), \\ &1 \leq k_1 \leq k+1, \quad 0 \leq k_2 \leq k+1, \quad 0 \leq l_1, l_2, l_3, l_4 \leq l+1, \quad 0 \leq j_1 \leq j+1, \\ &1 \leq r_1, r_2 \leq r+1, \quad 0 \leq s_1, s_2 \leq s+1, \quad 0 \leq m_1, m_2 \leq m+1. \end{aligned}$$

Proof. First, note that the solution to (2.10)–(2.14) satisfies for $1 \leq i \leq N$,

$$(A(\sigma + \alpha p I), \tau)_{\Omega_i} + (u, \text{div } \tau)_{\Omega_i} + (\gamma, \tau)_{\Omega_i} - \langle u, \tau n_i \rangle_{\Gamma_i} = 0, \quad \forall \tau \in \mathbb{X}_i, \quad (3.45)$$

$$(\text{div } \sigma, v)_{\Omega_i} = - (f, v)_{\Omega_i}, \quad \forall v \in V_i, \quad (3.46)$$

$$(\sigma, \xi)_{\Omega_i} = 0, \quad \forall \xi \in \mathbb{Q}_i, \quad (3.47)$$

$$(K^{-1}z, \zeta)_{\Omega_i} - (p, \text{div } \zeta)_{\Omega_i} + \langle p, \zeta \cdot n_i \rangle_{\Gamma_i} = 0, \quad \forall \zeta \in Z_i, \quad (3.48)$$

$$c_0 (\partial_t p, w)_{\Omega_i} + \alpha (\partial_t A(\sigma + \alpha p I), w I)_{\Omega_i} + (\text{div } z, w)_{\Omega_i} = (g, w)_{\Omega_i}, \quad \forall w \in W_i, \quad (3.49)$$

Subtracting (2.67)–(2.71) from (3.45)–(3.49) gives

$$\begin{aligned} & (A((\sigma - \sigma_h) + \alpha(p - p_h)I), \tau) + \sum_{i=1}^N ((u - u_h), \operatorname{div} \tau)_{\Omega_i} \\ & + ((\gamma - \gamma_h), \tau) = \sum_{i=1}^N \langle u, \tau n_i \rangle_{\Gamma_i}, \quad \forall \tau \in \mathbb{X}_{h,0}, \end{aligned} \quad (3.50)$$

$$\sum_{i=1}^N (\operatorname{div}(\sigma - \sigma_h), v)_{\Omega_i} = 0, \quad \forall v \in V_h, \quad (3.51)$$

$$((\sigma - \sigma_h), \xi) = 0, \quad \forall \xi \in \mathbb{Q}_h, \quad (3.52)$$

$$(K^{-1}(z - z_h), \zeta) - \sum_{i=1}^N ((p - p_h), \operatorname{div} \zeta)_{\Omega_i} = - \sum_{i=1}^N \langle p, \zeta \cdot n_i \rangle_{\Gamma_i}, \quad \forall \zeta \in Z_{h,0}, \quad (3.53)$$

$$\begin{aligned} & c_0(\partial_t(p - p_h), w) + \alpha(\partial_t A((\sigma - \sigma_h) + \alpha(p - p_h)I), wI) \\ & + \sum_{i=1}^N (\operatorname{div}(z - z_h), w)_{\Omega_i} = 0, \quad \forall w \in W_h. \end{aligned} \quad (3.54)$$

Next, rewrite the above error equations in terms of the approximation errors ψ_\star and discretization errors ϕ_\star , for $\star \in \{\sigma, u, \gamma, z, p\}$ as follows:

$$\begin{aligned} \sigma - \sigma_h &= (\sigma - \Pi_0^\sigma \sigma) + (\Pi_0^\sigma \sigma - \sigma_h) := \psi_\sigma + \phi_\sigma, \\ u - u_h &= (u - \mathcal{P}_h^u u) + (\mathcal{P}_h^u u - u_h) := \psi_u + \phi_u, \\ \gamma - \gamma_h &= (\gamma - \mathcal{R}_h \gamma) + (\mathcal{R}_h \gamma - \gamma_h) := \psi_\gamma + \phi_\gamma, \\ z - z_h &= (z - \Pi_0^z z) + (\Pi_0^z z - z_h) := \psi_z + \phi_z, \\ p - p_h &= (p - \mathcal{P}_h^p p) + (\mathcal{P}_h^p p - p_h) := \psi_p + \phi_p, \\ u - \lambda_H^u &= (u - \mathcal{Q}_h^u u) + (\mathcal{Q}_h^u u - \lambda_H^u) := \psi_{\lambda^u} + \phi_{\lambda^u}, \\ p - \lambda_H^p &= (p - \mathcal{Q}_h^p p) + (\mathcal{Q}_h^p p - \lambda_H^p) := \psi_{\lambda^p} + \phi_{\lambda^p}. \end{aligned}$$

Combining (3.51) with (3.9) gives

$$\operatorname{div}_h \phi_\sigma = 0, \quad (3.55)$$

and (3.52) combined with (3.10) gives

$$(\phi_\sigma, \xi) = 0 \text{ for } \xi \in \mathbb{Q}_h. \quad (3.56)$$

We rewrite error equation (3.50) as

$$\begin{aligned} & (A(\phi_\sigma + \alpha\phi_p I), \tau) + \sum_{i=1}^N (\phi_u, \operatorname{div} \tau)_{\Omega_i} + (\phi_\gamma, \tau) \\ & = - (A(\psi_\sigma + \alpha\psi_p I), \tau) - (\psi_\gamma, \tau) + \sum_{i=1}^N \langle u - \mathcal{I}_H^u u, \tau n_i \rangle_{\Gamma_i}, \end{aligned} \quad (3.57)$$

where we have used

$$\sum_{i=1}^N \langle \mathcal{I}_H^u u, \tau n_i \rangle_{\Gamma_i} = 0, \quad (3.58)$$

for any $\tau \in \mathbb{X}_{h,0}$. Differentiating the above equation with respect to time gives

$$\begin{aligned} & (\partial_t A(\phi_\sigma + \alpha\phi_p I), \tau) + \sum_{i=1}^N (\partial_t \phi_u, \operatorname{div} \tau)_{\Omega_i} + (\phi_\gamma, \tau) \\ & = - (\partial_t A(\psi_\sigma + \alpha\psi_p I), \tau) - (\partial_t \psi_\gamma, \tau) + \sum_{i=1}^N \langle \partial_t (u - \mathcal{I}_H^u u), \tau n_i \rangle_{\Gamma_i}. \end{aligned} \quad (3.59)$$

Taking $\tau = \phi_\sigma$ in (3.59) and using (3.55) and (3.56) gives

$$(\partial_t A(\phi_\sigma + \alpha\phi_p I), \phi_\sigma) = -(\partial_t A(\psi_\sigma + \alpha\psi_p I), \phi_\sigma) - (\partial_t \psi_\gamma, \phi_\sigma) + \sum_{i=1}^N (\partial_t (u - \mathcal{I}_H^u u), \phi_\sigma n_i)_{\Gamma_i}. \quad (3.60)$$

Error equation (3.54) can be written as

$$c_0 (\partial_t \phi_p, w) + \alpha (\partial_t A(\phi_\sigma + \alpha\phi_p I), wI) + \sum_{i=1}^N (\operatorname{div} \phi_z, w)_{\Omega_i} = -\alpha (\partial_t A(\psi_\sigma + \alpha\psi_p I), wI), \quad (3.61)$$

where we have used (2.47) and (3.14). Taking $w = \phi_p$ in (3.61) and combining the resulting equation with (3.60) give

$$\begin{aligned} & \frac{1}{2} \partial_t \left(\|A^{\frac{1}{2}}(\phi_\sigma + \alpha\phi_p I)\|^2 + c_0 \|\phi_p\|^2 \right) + \sum_{i=1}^N (\operatorname{div} \phi_z, \phi_p)_{\Omega_i} \\ &= -(\partial_t A(\psi_\sigma + \alpha\psi_p I), \phi_\sigma + \alpha\phi_p I) - (\partial_t \psi_\gamma, \phi_\sigma) + \sum_{i=1}^N \langle \partial_t (u - \mathcal{I}_H^u u), \phi_\sigma n_i \rangle_{\Gamma_i}. \end{aligned} \quad (3.62)$$

Finally error equation (3.53) can be written as

$$(K^{-1} \phi_z, \zeta) - \sum_{i=1}^N (\phi_p, \operatorname{div} \zeta)_{\Omega_i} = - (K^{-1} \psi_z, \zeta) + \sum_{i=1}^N \langle \mathcal{I}_H^p p - p, \zeta \cdot n_i \rangle_{\Gamma_i}, \quad (3.63)$$

where we have used for $\zeta \in Z_{h,0}$,

$$\sum_{i=1}^N \langle \mathcal{I}_H^p p, \zeta \cdot n_i \rangle_{\Gamma_i} = 0, \quad (3.64)$$

and the definition of the $L^2(\Omega)$ -projection, \mathcal{P}_h^p onto space W_h .

Taking test function $\zeta = \phi_z$ in equation (3.63) and combining the resulting equation with (3.62) gives

$$\begin{aligned} & \frac{1}{2} \partial_t \left(\|A^{\frac{1}{2}}(\phi_\sigma + \alpha\phi_p I)\|^2 + c_0 \|\phi_p\|^2 \right) + \|K^{-\frac{1}{2}} \phi_z\|^2 = -(\partial_t A(\psi_\sigma + \alpha\psi_p I), \phi_\sigma + \alpha\phi_p I) \\ & \quad - (\partial_t \psi_\gamma, \phi_\sigma) - (K^{-1} \psi_z, \phi_z) + (\psi_\sigma, \partial_t \phi_\gamma) - \sum_{i=1}^N \langle \partial_t (\mathcal{I}_H^u u - u), \phi_\sigma n_i \rangle_{\Gamma_i} \\ & \quad + \sum_{i=1}^N \langle \mathcal{I}_H^p p - p, \phi_z \cdot n_i \rangle_{\Gamma_i}, \end{aligned} \quad (3.65)$$

where we have used (3.56) to conclude that $(\phi_\sigma, \partial_t \phi_\gamma) = 0$.

Next, we bound the first three terms on the right hand side of (3.65).

$$\begin{aligned} & -(\partial_t A(\psi_\sigma + \alpha\psi_p I), \phi_\sigma + \alpha\phi_p I) - (\partial_t \psi_\gamma, \phi_\sigma) - (K^{-1} \psi_z, \phi_z) \\ & \leq \|\partial_t A(\psi_\sigma + \alpha\psi_p I)\| \|\phi_\sigma + \alpha\phi_p I\| + \|\partial_t \psi_\gamma\| \|\phi_\sigma\| + \|K^{-1} \psi_z\| \|\phi_z\| \\ & \leq \frac{C}{\epsilon} (\|\partial_t \psi_\sigma\|^2 + \|\partial_t \psi_p\|^2 + \|\partial_t \psi_\gamma\|^2 + \|\psi_z\|^2) + \epsilon (\|\phi_\sigma\|^2 + \|\phi_p\|^2 + \|\phi_z\|^2), \end{aligned} \quad (3.66)$$

where we have used the operator bounds (2.22) and (2.23) along with Young's inequality for a some $\epsilon > 0$.

Next, we give a bound on the last two boundary terms in the right hand side of equation (3.65). For this, we note that the following bounds hold for any $(\tau, v) \in H(\operatorname{div}; \Omega, \mathbb{M}) \times H_0^1(\Omega, \mathbb{R}^d)$ and $(\zeta, w) \in H(\operatorname{div}; \Omega) \times H_0^1(\Omega)$:

$$\begin{aligned} \langle \mathcal{I}_H^u v - v, \tau n_i \rangle_{\Gamma_i} &= \langle E_i(\mathcal{I}_H^u v - v), \tau n_i \rangle_{\partial\Omega_i} \\ &\leq C \|E_i(\mathcal{I}_H^u v - v)\|_{\frac{1}{2}, \partial\Omega_i} \|\tau\|_{H(\operatorname{div}; \Omega_i)} \leq C \|\mathcal{I}_H^u v - v\|_{\frac{1}{2}, \Gamma_i} \|\tau\|_{H(\operatorname{div}; \Omega_i)}, \end{aligned} \quad (3.67)$$

$$\begin{aligned} \langle \mathcal{I}_H^p w - w, \zeta \cdot n_i \rangle_{\Gamma_i} &= \langle E_i(\mathcal{I}_H^p \zeta - \zeta), \zeta \cdot n_i \rangle_{\partial\Omega_i} \\ &\leq C \|E_i(\mathcal{I}_H^p \zeta - \zeta)\|_{\frac{1}{2}, \partial\Omega_i} \|\zeta\|_{H(\text{div}; \Omega_i)} \leq C \|\mathcal{I}_H^p \zeta - \zeta\|_{\frac{1}{2}, \Gamma_i} \|\zeta\|_{H(\text{div}; \Omega_i)}, \end{aligned} \quad (3.68)$$

where E_i denotes the extension by zero from Γ_i to $\partial\Omega_i$, which is continuous in the $H^{\frac{1}{2}}$ -norm for functions that are zero on $\partial\Gamma$, and we have used the trace inequality (2.66). Taking $(\tau, v) = (\phi_\sigma, \partial_t u)$ and $(\zeta, w) = (\phi_z, p)$ in (3.67) and (3.68), respectively, and using Young's inequality gives

$$\langle \partial_t(\mathcal{I}_H^u u - u), \phi_\sigma n_i \rangle_{\Gamma_i} \leq \frac{C}{\epsilon} \|\partial_t(\mathcal{I}_H^u u - u)\|_{\frac{1}{2}, \Gamma_i}^2 + \epsilon \|\phi_\sigma\|_{\Omega_i}^2, \quad (3.69)$$

$$\langle \mathcal{I}_H^p p - p, \phi_z \cdot n_i \rangle_{\Gamma_i} \leq \frac{C}{\epsilon} \|\mathcal{I}_H^p p - p\|_{\frac{1}{2}, \Gamma_i}^2 + \epsilon (\|\phi_z\|_{\Omega_i}^2 + \|\text{div} \phi_z\|_{\Omega_i}^2), \quad (3.70)$$

where we also used (3.55). Combining inequalities (3.65)–(3.69) respect to time from 0 to $t \in (0, T]$ gives

$$\begin{aligned} &\|A^{\frac{1}{2}}(\phi_\sigma + \alpha\phi_p I)(t)\|^2 + c_0 \|\phi_p(t)\|^2 + \int_0^t \|K^{-1}\phi_z\|^2 \\ &\leq C \int_0^t (\|\partial_t \psi_\sigma\|^2 + \|\partial_t \psi_p\|^2 + \|\partial_t \psi_\gamma\|^2 + \|\psi_z\|^2 + \sum_{i=1}^N \|\mathcal{I}_H^u \partial_t u - \partial_t u\|_{\frac{1}{2}, \Gamma_i}^2 \\ &\quad + \sum_{i=1}^N \|\mathcal{I}_H^p p - p\|_{\frac{1}{2}, \Gamma_i}^2) ds + \epsilon \int_0^t (\|\phi_\sigma\|^2 + \|\phi_p\|^2 + \|\phi_z\|^2) ds \\ &\quad + C \int_0^t \|\text{div}_h \phi_z\|^2 ds + \int_0^t (\psi_\sigma, \partial_t \phi_\gamma) ds + \|A^{\frac{1}{2}}(\phi_\sigma + \alpha\phi_p I)(0)\|^2 + c_0 \|\phi_p(0)\|^2, \end{aligned} \quad (3.71)$$

To bound the term $\int_0^t (\psi_\sigma, \partial_t \phi_\gamma) ds$, we use integration by parts as follows:

$$\begin{aligned} \int_0^t (\psi_\sigma, \partial_t \phi_\gamma) ds &= (\psi_\sigma(t), \phi_\gamma(t)) - (\psi_\sigma(0), \phi_\gamma(0)) - \int_0^t (\partial_t \psi_\sigma, \phi_\gamma) ds \\ &\leq \frac{C}{\epsilon} \left(\int_0^t \|\partial_t \psi_\sigma\|^2 ds + \|\psi_\sigma(t)\|^2 \right) + \epsilon \left(\int_0^t \|\phi_\gamma\|^2 ds + \|\phi_\gamma(t)\|^2 \right) + C (\|\psi_\sigma(0)\|^2 + \|\phi_\gamma(0)\|^2), \end{aligned} \quad (3.72)$$

where we have used the Cauchy-Schwartz and Young's inequality.

Next, we bound the errors of the form ϕ_\star for $\star \in \{\sigma, \gamma, u, p\}$.

Using the inf-sup condition (3.18) and the error equation (3.55) gives

$$\begin{aligned} \|\phi_u\| + \|\phi_\gamma\| &\leq C \sup_{0 \neq \tau \in \mathbb{X}_{h,0}} \frac{\sum_{i=1}^N (\phi_u, \text{div} \tau)_{\Omega_i} + (\phi_\gamma, \tau)}{\|\tau\|_{\mathbb{X}_h}} \\ &\leq C \sup_{0 \neq \tau \in \mathbb{X}_{h,0}} \frac{1}{\|\tau\|_{\mathbb{X}_h}} \left| (A(\phi_\sigma + \alpha\phi_p I), \tau) + (A(\psi_\sigma + \alpha\psi_p I), \tau) + (\psi_\gamma, \tau) \right. \\ &\quad \left. - \sum_{i=1}^N ((\mathcal{I}_H^u u - u), \tau n_i)_{\Gamma_i} \right| \\ &\leq C \left(\|A^{\frac{1}{2}}(\phi_\sigma + \alpha\phi_p I)\| + \|\psi_\sigma\| + \|\psi_\gamma\| + \|\psi_p\| + \sum_{i=1}^N \|\mathcal{I}_H^u u - u\|_{\frac{1}{2}, \Gamma_i} \right), \end{aligned} \quad (3.73)$$

where we have used Cauchy-Schwartz inequality, (3.55) and (3.67) with $v = u$ to get last inequality. Integrating (3.73) with respect to time from 0 to $t \in (0, T]$ gives

$$\begin{aligned} \int_0^t (\|\phi_u\|^2 + \|\phi_\gamma\|^2) ds &\leq C \int_0^t (\|\phi_\sigma\|^2 + \alpha \|\phi_p I\|^2) ds \\ &\quad + C \int_0^t \left(\|\psi_\sigma\|^2 + \|\psi_\gamma\|^2 + \|\psi_p\|^2 + \sum_{i=1}^N \|\mathcal{I}_H^u u - u\|_{\frac{1}{2}, \Gamma_i}^2 \right) ds. \end{aligned} \quad (3.74)$$

To bound $\|\phi_p\|$, we use the inf-sup stability condition (3.19) to get

$$\begin{aligned}
\|\phi_p\| &\leq C \sup_{0 \neq \zeta \in Z_{h,0}} \frac{\sum_{i=1}^N (\operatorname{div} \zeta, \phi_p)_{\Omega_i}}{\|\zeta\|_{Z_h}} \\
&\leq C \sup_{0 \neq \zeta \in Z_{h,0}} \frac{(K^{-1} \phi_z, \zeta) + (K^{-1} \psi_z, \zeta) - \sum_{i=1}^N \langle \mathcal{I}_H^p p - p, \zeta \cdot n_i \rangle_{\Gamma_i}}{\|\zeta\|_{Z_h}} \\
&\leq C \left(\|\psi_z\| + \|K^{-\frac{1}{2}} \phi_z\| + \sum_{i=1}^N \|\mathcal{I}_H^p p - p\|_{\frac{1}{2}, \Gamma_i} \right), \tag{3.75}
\end{aligned}$$

where we have used (3.63) and (3.64) to obtain second inequality and (3.68) with $w = p$ to obtain the last one. Integrating (3.75) in time from 0 to $t \in (0, T]$ yields

$$\int_0^t \|\phi_p\|^2 ds \leq C \int_0^t \left(\|\psi_z\|^2 + \|K^{-\frac{1}{2}} \phi_z\|^2 + \sum_{i=1}^N \|\mathcal{I}_H^p p - p\|_{\frac{1}{2}, \Gamma_i}^2 \right) ds. \tag{3.76}$$

To bound the term $\int_0^t \|\phi_\sigma\|^2 ds$, we take $\tau = \phi_\sigma$ in (3.57) and $\xi = \phi_\gamma$ in (3.52), and use (3.55)–(3.56) and Young’s inequality to get

$$\begin{aligned}
\|A^{\frac{1}{2}} \phi_\sigma\|^2 &= - \left(A^{\frac{1}{2}} \alpha \phi_p I, \phi_\sigma \right) - (A(\psi_\sigma + \alpha \psi_p I), \phi_\sigma) - (\psi_\gamma, \phi_\sigma) - \sum_{i=1}^N \langle \mathcal{I}_H^u u - u, \phi_\sigma n_i \rangle_{\Gamma_i} \\
&+ (\psi_\sigma, \phi_\gamma) \leq C \left((\|\phi_p\| + \|\psi_\sigma\| + \|\psi_p\| + \|\psi_\gamma\|) \|\phi_\sigma\| + \sum_{i=1}^N \|\mathcal{I}_H^u u - u\|_{\frac{1}{2}, \Gamma_i} \|\phi_\sigma\|_{H(\operatorname{div}; \Omega_i)} \right. \\
&\quad \left. + \|\psi_\sigma\| \|\phi_\gamma\| \right) \leq \frac{C}{\epsilon} \left(\|\psi_\sigma\|^2 + \|\psi_p\|^2 + \|\psi_\gamma\|^2 + \sum_{i=1}^N \|\mathcal{I}_H^u u - u\|_{\frac{1}{2}, \Gamma_i}^2 + \|\phi_p\|^2 \right) \\
&\quad + \epsilon (\|\phi_\sigma\|^2 + \|\phi_\gamma\|^2), \tag{3.77}
\end{aligned}$$

where we have used (3.67) with $(\tau, v) = (\phi_\sigma, u)$ to arrive at the first inequality and (2.22) with Young’s inequality to justify the last inequality. Now again using (2.22), integrating (3.77) with respect to time from 0 to $t \in (0, T]$, and taking ϵ small enough, we get

$$\begin{aligned}
\int_0^t \|\phi_\sigma\|^2 ds &\leq C \left(\int_0^t (\|\psi_\sigma\|^2 + \|\psi_p\|^2 + \|\psi_\gamma\|^2 + \sum_{i=1}^N \|\mathcal{I}_H^u u - u\|_{\frac{1}{2}, \Gamma_i}^2 + \|\phi_p\|^2) ds \right) \\
&\quad + \epsilon \int_0^t \|\phi_\gamma\|^2 ds. \tag{3.78}
\end{aligned}$$

Combining (3.71)–(3.78), using (3.55), and taking ϵ small enough gives

$$\begin{aligned}
&\|A^{\frac{1}{2}} (\phi_\sigma + \alpha \phi_p I)\|^2 + \|\phi_u\|^2 + \|\phi_\gamma\|^2 + \|c_0^{\frac{1}{2}} \phi_p\|^2 + \|\operatorname{div}_h \phi_\sigma\|^2 \\
&+ \int_0^t \left(\|\phi_\sigma\|^2 + \|\phi_u\|^2 + \|\phi_\gamma\|^2 + \|K^{-\frac{1}{2}} \phi_z\|^2 + \|\phi_p\|^2 + \|\operatorname{div}_h \phi_\sigma\|^2 \right) \\
&\leq C \int_0^t \left(\|\partial_t \psi_\sigma\|^2 + \|\partial_t \psi_p\|^2 + \|\partial_t \psi_\gamma\|^2 + \|\psi_\sigma\|^2 + \|\psi_p\|^2 + \|\psi_\gamma\|^2 + \|\psi_z\|^2 \right) ds + C (\|\psi_\sigma\|^2 \\
&\quad + \|\psi_p\|^2 + \|\psi_\gamma\|^2) + C \int_0^t \|\operatorname{div}_h \phi_z\|^2 ds + C \sum_{i=1}^N \left(\|\mathcal{I}_H^u u - u(t)\|_{\frac{1}{2}, \Gamma_i}^2 + \|\mathcal{I}_H^p p - p(t)\|_{\frac{1}{2}, \Gamma_i}^2 \right) \\
&\quad + C \sum_{i=1}^N \int_0^t \left(\|\mathcal{I}_H^u \partial_t u - \partial_t u\|_{\frac{1}{2}, \Gamma_i}^2 + \|\mathcal{I}_H^u u - u\|_{\frac{1}{2}, \Gamma_i}^2 + \|\mathcal{I}_H^p p - p\|_{\frac{1}{2}, \Gamma_i}^2 \right) ds \\
&\quad + C (\|\phi_\sigma(0)\|^2 + \|\phi_p(0)\|^2 + \|\phi_\gamma(0)\|^2). \tag{3.79}
\end{aligned}$$

Bound on $\sum_{i=1}^N \|\operatorname{div} \phi_z\|_{\Omega_i}$.

Take $w = \phi_z$ in (3.54) to get, for $i = 1, 2, \dots, N$,

$$\begin{aligned} \|\operatorname{div} \phi_z\|_{\Omega_i}^2 &= -(c_0 \partial_t \phi_p, \operatorname{div} \phi_z)_{\Omega_i} - (c_0 \partial_t \phi_p, \operatorname{div} \phi_z)_{\Omega_i} - \alpha (\partial_t A (\phi_\sigma + \alpha \phi_p I), \operatorname{div} \phi_z I)_{\Omega_i} \\ &\quad - \alpha (\partial_t A (\psi_\sigma + \alpha \psi_p I), \operatorname{div} \phi_z I)_{\Omega_i} + (\psi_z, \operatorname{div} \phi_z)_{\Omega_i} = -(c_0 \partial_t \phi_p, \operatorname{div} \phi_z)_{\Omega_i} \\ &\quad - \alpha (\partial_t A (\phi_\sigma + \alpha \phi_p I), \operatorname{div} \phi_z I)_{\Omega_i} - \alpha (\partial_t A (\psi_\sigma + \alpha \psi_p I), \operatorname{div} \phi_z I)_{\Omega_i}, \end{aligned}$$

where the last equality follows from (2.47) and (3.14). Finally, summing the above equation over all the subdomain indices and using (2.22), we get, for $i = 1, 2, \dots, N$,

$$\|\operatorname{div} \phi_z\|_{\Omega_i} \leq C \left(\|c_0^{\frac{1}{2}} \partial_t \phi_p\|_{\Omega_i} + \|\partial_t A^{\frac{1}{2}} (\phi_\sigma + \alpha \phi_p I)\|_{\Omega_i} + \|\psi_p\|_{\Omega_i} + \|\psi_\sigma\|_{\Omega_i} \right). \quad (3.80)$$

Squaring the above equation and summing over all the subdomain indices give

$$\sum_{i=1}^N \|\operatorname{div} \phi_z\|_{\Omega_i}^2 \leq C \left(\|c_0^{\frac{1}{2}} \partial_t \phi_p\|^2 + \|\partial_t A^{\frac{1}{2}} (\phi_\sigma + \alpha \phi_p I)\|^2 + \|\psi_p\|^2 + \|\psi_\sigma\|^2 \right). \quad (3.81)$$

In order to bound $\|c_0^{\frac{1}{2}} \partial_t \phi_p\|^2$ and $\|\partial_t A^{\frac{1}{2}} (\phi_\sigma + \alpha \phi_p I)\|^2$, we use arguments similar to the ones used in the stability analysis for the method. Differentiate (3.55), (3.56), and (3.63) in time, combine them with (3.59), and take test functions $\tau = \partial_t \phi_\sigma$, $\xi = \partial_t \phi_\gamma$, $q = \phi_z$, and $w = \partial_t \phi_p$ to get the following time differentiated version of (3.65):

$$\begin{aligned} \|\partial_t A^{\frac{1}{2}} (\phi_\sigma + \alpha \phi_p I)\|^2 + \|c_0^{\frac{1}{2}} \partial_t \phi_p\|^2 + \frac{1}{2} \partial_t \|K^{-\frac{1}{2}} \phi_z\|^2 &= -(\partial_t A (\psi_\sigma + \alpha \psi_p I), \partial_t (\phi_\sigma + \alpha \phi_p I)) \\ &\quad - (\partial_t \psi_\gamma, \partial_t (\phi_\sigma + \alpha \phi_p I)) - (\partial_t K^{-1} \psi_z, \phi_z) + (\partial_t \psi_\sigma, \partial_t \phi_\gamma) - \sum_{i=1}^N \langle \partial_t (\mathcal{I}_H^u u - u), \partial_t \phi_\sigma n_i \rangle_{\Gamma_i} \\ &\quad + \sum_{i=1}^N \langle \mathcal{I}_H^p \partial_t p - \partial_t p, \phi_z \cdot n_i \rangle_{\Gamma_i}, \end{aligned} \quad (3.82)$$

where we have used the fact that $(\partial_t \psi_\gamma, \partial_t \alpha \phi_p I) = 0$ to write

$$(\partial_t \psi_\gamma, \partial_t \phi_\sigma) = (\partial_t \psi_\gamma, \partial_t (\phi_\sigma + \alpha \phi_p I)).$$

To bound $\sum_{i=1}^N \langle \partial_t (\mathcal{I}_H^u u - u), \partial_t \phi_\sigma n_i \rangle_{\Gamma_i}$, we use integration by parts to rewrite

$$\begin{aligned} \sum_{i=1}^N \langle \partial_t (\mathcal{I}_H^u u - u), \partial_t \phi_\sigma n_i \rangle_{\Gamma_i} &= \frac{\partial}{\partial t} \left(\sum_{i=1}^N \langle \partial_t (\mathcal{I}_H^u u - u), \phi_\sigma n_i \rangle_{\Gamma_i} \right) \\ &\quad - \sum_{i=1}^N \langle \partial_t^2 (\mathcal{I}_H^u u - u), \phi_\sigma n_i \rangle_{\Gamma_i}. \end{aligned} \quad (3.83)$$

To bound the last term on the right hand side of the above equation, we take $(\tau, v) = (\phi_\sigma, \partial_t^2 u)$ in (3.67) to get

$$\left| \sum_{i=1}^N \langle \partial_t^2 (\mathcal{I}_H^u u - u), \phi_\sigma n_i \rangle_{\Gamma_i} \right| \leq C \sum_{i=1}^N \|\mathcal{I}_H^u \partial_t^2 u - \partial_t^2 u\|_{\frac{1}{2}, \Gamma_i} \|\phi_\sigma\|_{H(\operatorname{div}; \Omega_i)}. \quad (3.84)$$

To bound $\sum_{i=1}^N \langle \mathcal{I}_H^p \partial_t p - \partial_t p, \partial_t \phi_z \cdot n_i \rangle_{\Gamma_i}$, we take $(\zeta, w) = (\phi_z, \partial_t p)$ in (3.68), to get

$$\left| \sum_{i=1}^N \langle \mathcal{I}_H^p \partial_t p - \partial_t p, \phi_z \cdot n_i \rangle_{\Gamma_i} \right| \leq C \sum_{i=1}^N \|\mathcal{I}_H^p \partial_t p - \partial_t p\|_{\frac{1}{2}, \Gamma_i} \|\phi_z\|_{H(\operatorname{div}; \Omega_i)}. \quad (3.85)$$

Combining (3.82)–(3.85), using (2.22)–(2.23) and integrating with respect to time from 0 to $t \in (0, T]$, we get

$$\begin{aligned}
& \|K^{-\frac{1}{2}}\phi_z\|^2 + \int_0^t \left(\|\partial_t A^{\frac{1}{2}}(\phi_\sigma + \alpha\phi_p I)\|^2 + \|c_0^{\frac{1}{2}}\partial_t\phi_p\|^2 \right) ds \\
& \leq C \int_0^t \left(\|\partial_t\psi_\sigma\|^2 + \|\partial_t\psi_p\|^2 + \|\partial_t\psi_\gamma\|^2 + \|\partial_t\psi_z\|^2 + \sum_{i=1}^N \|\mathcal{I}_H^u \partial_t^2 u - \partial_t^2 u\|_{\frac{1}{2}, \Gamma_i}^2 \right. \\
& \quad \left. + \sum_{i=1}^N \|\mathcal{I}_H^p \partial_t p - \partial_t p\|_{\frac{1}{2}, \Gamma_i}^2 \right) ds + C \sum_{i=1}^N \|\mathcal{I}_H^u \partial_t u - \partial_t u(t)\|_{\frac{1}{2}, \Gamma_i}^2 \\
& \quad + \epsilon \left(\int_0^t \left(\|\phi_\sigma\|^2 + \|\partial_t\phi_\gamma\|^2 + \|\phi_z\|^2 + \sum_{i=1}^N \|\operatorname{div} \phi_z\|_{\Omega_i}^2 \right) ds + \|\phi_\sigma(t)\|^2 \right) \\
& \quad + C \left(\|K^{-\frac{1}{2}}\phi_z(0)\|^2 + \|\phi_\sigma(0)\|^2 + \sum_{i=1}^N \|\mathcal{I}_H^u \partial_t u - \partial_t u(0)\|_{\frac{1}{2}, \Gamma_i}^2 \right), \tag{3.86}
\end{aligned}$$

where we have used Young's inequality for $\epsilon > 0$ and (3.67) with $(\tau, v) = (\phi_\sigma, \partial_t u)$.

Using the inf-sup condition (3.18) with $v = \partial_t\phi_u$, $\xi = \partial_t\phi_\gamma$, the time-differentiated (3.57), and following the steps similar to the ones used to arrive at (3.74), we get

$$\begin{aligned}
& \int_0^t \left(\|\partial_t\phi_u\|^2 + \|\partial_t\phi_\gamma\|^2 \right) ds \leq C \left(\int_0^t \|\partial_t A^{\frac{1}{2}}(\phi_\sigma + \alpha\phi_p I)\|^2 ds \right. \\
& \quad \left. + \int_0^t \left(\|\partial_t\psi_\sigma\|^2 + \|\partial_t\psi_\gamma\|^2 + \|\partial_t\psi_p\|^2 + \sum_{i=1}^N \|\mathcal{I}_H^u \partial_t u - \partial_t u(t)\|_{\frac{1}{2}, \Gamma_i}^2 \right) ds \right). \tag{3.87}
\end{aligned}$$

Combining (3.86)–(3.87), taking ϵ small enough, and using (3.75) implies

$$\begin{aligned}
& \|K^{-\frac{1}{2}}\phi_z(t)\|^2 + \|\phi_p(t)\|^2 + \int_0^t \left(\|\partial_t A^{\frac{1}{2}}(\phi_\sigma + \alpha\phi_p I)\|^2 + \|c_0^{\frac{1}{2}}\partial_t\phi_p\|^2 \right) ds \\
& \leq C \int_0^t \left(\|\partial_t\psi_\sigma\|^2 + \|\partial_t\psi_p\|^2 + \|\partial_t\psi_\gamma\|^2 + \|\partial_t\psi_z\|^2 + \sum_{i=1}^N \|\mathcal{I}_H^u \partial_t^2 u - \partial_t^2 u\|_{\frac{1}{2}, \Gamma_i}^2 \right. \\
& \quad \left. + \sum_{i=1}^N \|\mathcal{I}_H^p \partial_t p - \partial_t p\|_{\frac{1}{2}, \Omega_i}^2 \right) ds + C \sum_{i=1}^N \|\mathcal{I}_H^u \partial_t u - \partial_t u(t)\|_{\frac{1}{2}, \Gamma_i}^2 \\
& \quad + \|\mathcal{I}_H^p p - p(t)\|_{\frac{1}{2}, \Gamma_i}^2 + \epsilon \left(\int_0^t \left(\|\phi_\sigma\|^2 + \|\phi_z\|^2 + \sum_{i=1}^N \|\operatorname{div} \phi_z\|_{\Omega_i}^2 \right) ds \right) \\
& \quad + \epsilon \left(\|\phi_\sigma(t)\|^2 \right) + C \left(\|\psi_z(t)\|^2 + \|K^{-\frac{1}{2}}\phi_z(0)\|^2 + \|\phi_\sigma(0)\|^2 \right) \\
& \quad + C \left(\sum_{i=1}^N \|\mathcal{I}_H^u \partial_t u - \partial_t u(0)\|_{\frac{1}{2}, \Gamma_i}^2 \right). \tag{3.88}
\end{aligned}$$

Combining (3.81) and (3.88) gives

$$\begin{aligned}
& \|K^{-\frac{1}{2}}\phi_z(t)\|^2 + \|\phi_p(t)\|^2 + \int_0^t \|\operatorname{div}_h \phi_z\|^2 ds \\
& \leq C \int_0^t (\|\partial_t \psi_\sigma\|^2 + \|\partial_t \psi_p\|^2 + \|\partial_t \psi_\gamma\|^2 + \|\partial_t \psi_z\|^2 + \sum_{i=1}^N \|\mathcal{I}_H^u \partial_t^2 u - \partial_t^2 u\|_{\frac{1}{2}, \Gamma_i}^2 \\
& \quad + \sum_{i=1}^N \|\mathcal{I}_H^p \partial_t p - \partial_t p\|_{\frac{1}{2}, \Gamma_i}^2) ds + C \sum_{i=1}^N \left(\|\mathcal{I}_H^u \partial_t u - \partial_t u\|_{\frac{1}{2}, \Gamma_i}^2 \right. \\
& \quad \left. + \|\mathcal{I}_H^p p - p(t)\|_{\frac{1}{2}, \Gamma_i}^2 \right) + \epsilon \left(\int_0^t (\|\phi_\sigma\|^2 + \|\phi_z\|^2 + \sum_{i=1}^N \|\operatorname{div} \phi_z\|_{\Omega_i}^2) ds + \|\phi_\sigma(t)\|^2 \right) \\
& \quad + C \left(\|\psi_z(t)\|^2 + \|K^{-\frac{1}{2}}\phi_z(0)\|^2 + \|\phi_\sigma(0)\|^2 + \sum_{i=1}^N \|\mathcal{I}_H^u \partial_t u - \partial_t u(0)\|_{\frac{1}{2}, \Gamma_i}^2 \right). \tag{3.89}
\end{aligned}$$

Coercivity of A , (2.22), also implies

$$\|\phi_\sigma\| \leq C \left(\|A^{\frac{1}{2}}(\phi_\sigma + \alpha\phi_p I)\| + \|\phi_p\| \right). \tag{3.90}$$

Bound on $\|\lambda_H^u\|_\Gamma$ and $\|\lambda_H^p\|_\Gamma$.

In order to bound $\|\lambda_H^u\|_\Gamma$, we take the difference between equations (2.10) and (2.31) to get

$$\begin{aligned}
& (A((\sigma - \sigma_h) + \alpha(p - p_h)I), \tau) + \sum_{i=1}^N ((u - u_h), \operatorname{div} \tau)_{\Omega_i} + ((\gamma - \gamma_h), \tau) \\
& \quad - \sum_{i=1}^N (u, \tau n_i)_{\Gamma_i} = \sum_{i=1}^N (u - \lambda_H^u, \tau n_i)_{\Gamma_i}, \quad \forall \tau \in \mathbb{X}_h.
\end{aligned}$$

We can split the error terms in the above equation and use (2.38) to rewrite the above equation as

$$\begin{aligned}
& \sum_{i=1}^N \langle \phi \lambda_H^u, \tau n_i \rangle_{\Gamma_i} = (A(\phi_\sigma + \alpha\phi_p), \tau) + (A(\psi_\sigma + \alpha\psi_p), \tau) + \sum_{i=1}^N (\phi_u, \operatorname{div} \tau)_{\Omega_i} \\
& \quad + \sum_{i=1}^N (\psi_u, \operatorname{div} \tau)_{\Omega_i} + (\phi_\gamma, \tau) + (\psi_\gamma, \tau) + \sum_{i=1}^N \langle \mathcal{I}_H^u u - u, \tau n_i \rangle_{\Gamma_i}, \quad \forall \tau \in \mathbb{X}_h. \tag{3.91}
\end{aligned}$$

Inf-sup stability bound (3.8) combined with (3.91) implies

$$\begin{aligned}
\|\phi \lambda_H^u\|_\Gamma & \leq C \sup_{0 \neq \tau \in \mathbb{X}_h} \frac{\sum_{i=1}^N \langle \tau n_i, \phi \lambda_H^u \rangle_{\Gamma_i}}{\|\tau\|_{\mathbb{X}_h}} = C \sup_{0 \neq \tau \in \mathbb{X}_h} \left(\frac{(A(\phi_\sigma + \alpha\phi_p), \tau) + (A(\psi_\sigma + \alpha\psi_p), \tau)}{\|\tau\|_{\mathbb{X}_h}} \right. \\
& \quad \left. + \frac{\sum_{i=1}^N (\phi_u, \operatorname{div} \tau)_{\Omega_i} + \sum_{i=1}^N (\psi_u, \operatorname{div} \tau)_{\Omega_i} + (\phi_\gamma, \tau) + (\psi_\gamma, \tau) + \sum_{i=1}^N \langle \mathcal{I}_H^u u - u, \tau n_i \rangle_{\Gamma_i}}{\|\tau\|_{\mathbb{X}_h}} \right) \\
& \leq C \left(\|A^{\frac{1}{2}}(\phi_\sigma + \alpha\phi_p I)\| + \|\phi_u\| + \|\phi_\gamma\| \right) + C \left(\|\psi_\sigma\| + \|\psi_p\| + \|\psi_u\| + \|\psi_\gamma\| \right. \\
& \quad \left. + \sum_{i=1}^N \|\mathcal{I}_H^u u - u\|_{\frac{1}{2}, \Gamma_i} \right),
\end{aligned}$$

where in the last inequality, we have used (2.22) and (3.67) with $v = u$. Squaring the above inequality

and then integrating with respect to time from 0 to t yields the following two bounds

$$\begin{aligned} \|\phi_{\lambda_H^u}\|_{\Gamma}^2 &\leq C \left(\|A^{\frac{1}{2}}(\phi_{\sigma} + \alpha\phi_p I)\|^2 + \|\phi_u\|^2 + \|\phi_{\gamma}\|^2 \right) \\ &\quad + C \left(\|\psi_{\sigma}\|^2 + \|\psi_p\|^2 + \|\psi_u\|^2 + \|\psi_{\gamma}\|^2 + \sum_{i=1}^N \|\mathcal{I}_H^u u - u\|_{\frac{1}{2}, \Gamma_i}^2 \right), \end{aligned} \quad (3.92)$$

$$\begin{aligned} \int_0^t \|\phi_{\lambda_H^u}\|_{\Gamma}^2 ds &\leq C \int_0^t \left(\|A^{\frac{1}{2}}(\phi_{\sigma} + \alpha\phi_p I)\|^2 + \|\phi_u\|^2 + \|\phi_{\gamma}\|^2 \right) ds \\ &\quad + C \int_0^t \left(\|\psi_{\sigma}\|^2 + \|\psi_p\|^2 + \|\psi_u\|^2 + \|\psi_{\gamma}\|^2 + \sum_{i=1}^N \|\mathcal{I}_H^u u - u\|_{\frac{1}{2}, \Gamma_i}^2 \right) ds. \end{aligned} \quad (3.93)$$

Following similar arguments, we can bound $\|\lambda_H^p\|_{\Gamma}$ as well. To achieve this, take the difference between equations (3.48) and (2.34) to get the following error equation

$$\begin{aligned} (K^{-1}\phi_z, \zeta) + (K^{-1}\psi_z, \zeta) - \sum_{i=1}^N (\phi_p, \operatorname{div} \zeta)_{\Omega_i} - \sum_{i=1}^N (\psi_p, \operatorname{div} \zeta)_{\Omega_i} \\ - \sum_{i=1}^N \langle \mathcal{I}_H^p p - p, \zeta \cdot n_i \rangle_{\Gamma_i} = \sum_{i=1}^N -\langle \lambda_H^p, \zeta \cdot n_i \rangle_{\Gamma_i} = \sum_{i=1}^N -\langle \phi_{\lambda_H^p}, \zeta \cdot n_i \rangle_{\Gamma_i}, \quad \forall \zeta \in Z_h, \end{aligned} \quad (3.94)$$

where the last equality follows from (2.39). Inf-sup stability bound (3.2) combined with (3.94) implies

$$\begin{aligned} \|\phi_{\lambda_H^p}\|_{\Gamma} &\leq C \sup_{0 \neq \zeta \in Z_h} \frac{\sum_{i=1}^N \langle \zeta \cdot n_i, \phi_{\lambda_H^p} \rangle_{\Gamma_i}}{\|\zeta\|_{Z_h}} \\ &= C \sup_{0 \neq \zeta \in Z_h} \frac{(K^{-1}\phi_z, \zeta) + (K^{-1}\psi_z, \zeta) - \sum_{i=1}^N (\phi_p, \operatorname{div} \zeta)_{\Omega_i} - \sum_{i=1}^N (\psi_p, \operatorname{div} \zeta)_{\Omega_i} \\ &\quad + \frac{-\sum_{i=1}^N \langle \mathcal{I}_H^p p - p, \zeta \cdot n_i \rangle_{\Gamma_i}}{\|\zeta\|_{Z_h}}}{\|\zeta\|_{Z_h}} \leq C \left(\|K^{-\frac{1}{2}}\phi_z\| + \|\phi_p\| + \|\psi_z\| + \|\psi_p\| \right. \\ &\quad \left. + \sum_{i=1}^N \|\mathcal{I}_H^p p - p\|_{\frac{1}{2}, \Gamma_i} \right), \end{aligned} \quad (3.95)$$

where we have used (2.23) and (3.68) with $w = p$. Squaring the above bound and then integrating with respect to time from 0 to t give the following

$$\|\phi_{\lambda_H^p}\|_{\Gamma}^2 \leq C \left(\|K^{-\frac{1}{2}}\phi_z\|^2 + \|\phi_p\|^2 \right) + C \left(\|\psi_z\|^2 + \|\psi_p\|^2 + \sum_{i=1}^N \|\mathcal{I}_H^p p - p\|_{\frac{1}{2}, \Gamma_i}^2 \right), \quad (3.96)$$

$$\begin{aligned} \int_0^t \|\phi_{\lambda_H^p}\|_{\Gamma}^2 ds &\leq C \int_0^t \left(\|K^{-\frac{1}{2}}\phi_z\|^2 + \|\phi_p\|^2 \right) ds \\ &\quad + C \int_0^t \left(\|\psi_z\|^2 + \|\psi_p\|^2 + \sum_{i=1}^N \|\mathcal{I}_H^p p - p\|_{\frac{1}{2}, \Gamma_i}^2 \right) ds. \end{aligned} \quad (3.97)$$

Combining (3.79), (3.89)–(3.90), (3.92)–(3.93) and (3.96)–(3.97), and taking ϵ small enough,

we obtain

$$\begin{aligned}
& \|\phi_\sigma(t)\|_{\mathbb{X}_h}^2 + \|\phi_u(t)\|^2 + \|\phi_\gamma(t)\|^2 + \|\phi_z(t)\|^2 + \|\phi_p(t)\|^2 + \|\phi_{\lambda_H^u}(t)\|_\Gamma^2 + \|\phi_{\lambda_H^p}(t)\|_\Gamma^2 \\
& + \int_0^t (\|\phi_\sigma\|_{\mathbb{X}_h}^2 + \|\phi_u\|^2 + \|\phi_\gamma\|^2 + \|\phi_z\|_{\mathbb{Z}_h}^2 + \|\phi_p\|^2 + \|\phi_{\lambda_H^u}\|_\Gamma^2 + \|\phi_{\lambda_H^p}\|_\Gamma^2) ds \\
& \leq C \left(\int_0^t (\|\partial_t \psi_\sigma\|^2 + \|\partial_t \psi_p\|^2 + \|\partial_t \psi_\gamma\|^2 + \|\partial_t \psi_z\|^2 + \|\psi_\sigma\|^2 + \|\psi_p\|^2 + \|\psi_\gamma\|^2 + \|\psi_z\|^2) ds \right. \\
& + \int_0^t (\|\mathcal{I}_H^p u - u\|_{\frac{1}{2}, \Gamma}^2 + \|\partial_t(\mathcal{I}_H^u u - u)\|_{\frac{1}{2}, \Gamma}^2 + \|\partial_t^2(\mathcal{I}_H^u u - u)\|_{\frac{1}{2}, \Gamma}^2 \\
& + \|\mathcal{I}_H^p p - p\|_{\frac{1}{2}, \Gamma}^2 + \|\partial_t(\mathcal{I}_H^p p - p)\|_{\frac{1}{2}, \Gamma}^2) ds + \|\psi_\sigma(t)\|^2 + \|\psi_p(t)\|^2 + \|\psi_\gamma(t)\|^2 + \|\psi_z(t)\|^2 \\
& + \|(\mathcal{I}_H^u u - u)(t)\|_{\frac{1}{2}, \Gamma}^2 + \|\partial_t(\mathcal{I}_H^u u - u)(t)\|_{\frac{1}{2}, \Gamma}^2 + \|(\mathcal{I}_H^p p - p)(t)\|_{\frac{1}{2}, \Gamma}^2 \\
& \left. + \|\phi_\sigma(0)\|^2 + \|\phi_p(0)\|^2 + \|\phi_\gamma(0)\|^2 + \|\phi_z(0)\|^2 + \|\partial_t(\mathcal{I}_H^u u - u)(0)\|_{\frac{1}{2}, \Gamma}^2 \right). \tag{3.98}
\end{aligned}$$

To bound terms of the form $\|\mathcal{I}_H^u v - v\|_{\frac{1}{2}, \Gamma}$ and $\|\mathcal{I}_H^p w - w\|_{\frac{1}{2}, \Gamma}$, we use (2.54)–(2.55) and (2.65) to obtain

$$\|\mathcal{I}_H^u v - v\|_{\frac{1}{2}, \Gamma} \leq CH^{\hat{m}-\frac{1}{2}} \|v\|_{\hat{m}+\frac{1}{2}, \Omega}, \quad \frac{1}{2} \leq \hat{m} \leq m+1, \tag{3.99}$$

$$\|\mathcal{I}_H^p w - w\|_{\frac{1}{2}, \Gamma} \leq CH^{\hat{m}-\frac{1}{2}} \|w\|_{\hat{m}+\frac{1}{2}, \Omega}, \quad \frac{1}{2} \leq \hat{m} \leq m+1. \tag{3.100}$$

In order to bound the initial errors, $\|\phi_\sigma(0)\|$, $\|\phi_p(0)\|$, $\|\phi_\gamma(0)\|$, and $\|\phi_z(0)\|$, we recall that we obtain the discrete initial data from the elliptic projection of the continuous initial data (see (3.25)). Following the arguments similar to the ones used to arrive at (3.44), we get

$$\|\phi_\sigma(0)\| + \|\phi_p(0)\| + \|\phi_\gamma(0)\| + \|\phi_z(0)\| \leq C (\|\psi_\sigma(0)\| + \|\psi_p(0)\| + \|\psi_\gamma(0)\| + \|\psi_z(0)\| + \|\psi_u(0)\|). \tag{3.101}$$

Finally, combining bounds (3.98)–(3.101) with the approximation results (2.56)–(2.60), (3.12)–(3.13) and (3.16)–(3.17) completes the proof. \square

Remark 3.2. *The above theorem implies that for sufficiently smooth solution variables, the error in using our method is of $\mathcal{O}(h^{k+1} + h^{l+1} + h^{j+1} + h^{r+1} + h^{s+1} + H^{m+\frac{1}{2}})$. Assuming we use inf-sup stable pairs of FE spaces containing polynomials of degree $l = j = s$, and $k = r$, and $l \leq k$, we could choose $H = \mathcal{O}(h^{\frac{l+1}{m+1/2}})$ to get a total error bound of order $\mathcal{O}(h^{l+1})$. For example, for the choice of $l = 0$ and $m = 1$, we could choose $H = \mathcal{O}(h^{\frac{2}{3}})$ and for $l = 0$ and $m = 2$, we could choose $H = \mathcal{O}(h^{\frac{2}{5}})$ to obtain a total convergence rate of $\mathcal{O}(h)$. We will demonstrate the results for different choices of $H(h)$ in the numerical results section.*

4 Implementation

In this section, we discuss the implementation of the multiscale mortar domain decomposition technique discussed in this paper. First, we provide a fully discrete version of the system (2.31)–(2.37) using backward Euler time discretization. We use a related formulation where a time differentiated elasticity equation (2.10) is used. The reason for such a reformulation was discussed in the previous paper. The fully discrete formulation of the technique is then reduced to an interface problem which can then be solved using an iterative solver like GMRES. Finally, we discuss the possibility of computing and storing a multiscale basis which will help in increasing the efficiency of the method.

4.1 Time discretization

For time discretization, we use the backward Euler method. Let $\{t_n\}_{n=0}^{N_T}$, $t_n = n\Delta t$, $\Delta t = T/N_T$, be a uniform partition of $(0, T)$. With these choices, the fully discrete problem corresponding to

(2.31)–(2.37) reads as follows: for $0 \leq n \leq N_T - 1$ and $1 \leq i \leq N$, find $(\sigma_{h,i}^{n+1}, u_{h,i}^{n+1}, \gamma_{h,i}^{n+1}, z_{h,i}^{n+1}, p_{h,i}^{n+1}, \lambda_H^{n+1}) \in \mathbb{X}_{h,i} \times V_{h,i} \times \mathbb{Q}_{h,i} \times Z_{h,i} \times W_{h,i} \times \Lambda_H$ such that:

$$\begin{aligned} & \left(A \left(\sigma_{h,i}^{n+1} + \alpha p_{h,i}^{n+1} I \right), \tau \right)_{\Omega_i} + \left(u_{h,i}^{n+1}, \operatorname{div} \tau \right)_{\Omega_i} + \left(\gamma_{h,i}^{n+1}, \tau \right)_{\Omega_i} \\ & = \langle g_u^{n+1}, \tau n_i \rangle_{\partial \Omega_i \cap \Gamma_D^u} + \langle \lambda_H^{u,n+1}, \tau n_i \rangle_{\Gamma_i}, \quad \forall \tau \in \mathbb{X}_{h,i}, \end{aligned} \quad (4.1)$$

$$\left(\operatorname{div} \sigma_{h,i}^{n+1}, v \right)_{\Omega_i} = - \left(f^{n+1}, v \right)_{\Omega_i}, \quad \forall v \in V_{h,i}, \quad (4.2)$$

$$\left(\sigma_{h,i}^{n+1}, \xi \right)_{\Omega_i} = 0, \quad \forall \xi \in \mathbb{Q}_{h,i}, \quad (4.3)$$

$$\left(K^{-1} z_{h,i}^{n+1}, \zeta \right)_{\Omega_i} - \left(p_{h,i}^{n+1}, \operatorname{div} \zeta \right)_{\Omega_i} = - \langle g_p^{n+1}, \zeta \cdot n_i \rangle_{\partial \Omega_i \cap \Gamma_D^p} - \langle \lambda_H^{p,n+1}, \zeta \cdot n_i \rangle_{\Gamma_i}, \quad \forall \zeta \in Z_{h,i}, \quad (4.4)$$

$$\begin{aligned} c_0 \left(\frac{p_{h,i}^{n+1} - p_{h,i}^n}{\Delta t}, w \right)_{\Omega_i} + \alpha \left(\frac{A \left(\sigma_{h,i}^{n+1} - \sigma_{h,i}^n \right)}{\Delta t}, w I \right)_{\Omega_i} \\ + \alpha \left(A \alpha \frac{p_{h,i}^{n+1} - p_{h,i}^n}{\Delta t} I, w I \right)_{\Omega_i} + \left(\operatorname{div} z_{h,i}^{n+1}, w \right)_{\Omega_i} = \left(g^{n+1}, w \right)_{\Omega_i}, \quad \forall w \in W_{h,i}, \end{aligned} \quad (4.5)$$

$$\sum_{i=1}^N \langle \sigma_{h,i}^{n+1} n_i, \mu^u \rangle_{\Gamma_i} = 0, \quad \forall \mu^u \in \Lambda_H^u, \quad (4.6)$$

$$\sum_{i=1}^N \langle z_{h,i}^{n+1} \cdot n_i, \mu^p \rangle_{\Gamma_i} = 0, \quad \forall \mu^p \in \Lambda_H^p. \quad (4.7)$$

Note that similarly to the matching grid case in [32], the non-matching multiscale grid method also requires initial data $p_{h,i}^0$ and $\sigma_{h,i}^0$. Such data can be obtained by taking $p_{h,i}^0$ to be the L^2 -projection of p_0 onto $W_{h,i}$ and solving a mixed elasticity non-matching grid non-overlapping domain decomposition problem obtained from (4.1)–(4.3) and (4.6) with $n = -1$ (see [33]). Also, following the case of the matching grid domain decomposition method, we will utilize a related formulation in which the elasticity equation, (2.10), is differentiated in time. The reason for this was discussed in the analysis of the resulting interface problem in [32]. We introduce new variables $\dot{u} = \partial_t u$, $\dot{\gamma} = \partial_t \gamma$, and $\dot{\lambda}_H^u = \partial_t \lambda_H^u$ representing the time derivatives of the displacement, rotation, and displacement-Lagrange multiplier function, respectively. Using time-differentiated equation (2.10) and backward Euler (see [32] for details), we get

$$\begin{aligned} & \left(A \left(\sigma_{h,i}^{n+1} + \alpha p_{h,i}^{n+1} I \right), \tau \right)_{\Omega_i} + \Delta t \left(\dot{u}_{h,i}^{n+1}, \operatorname{div} \tau \right)_{\Omega_i} + \Delta t \left(\dot{\gamma}_{h,i}^{n+1}, \tau \right)_{\Omega_i} \\ & = \Delta t \langle \partial_t g_u^{n+1}, \tau n_i \rangle_{\partial \Omega_i \cap \Gamma_D^u} + \Delta t \langle \dot{\lambda}_H^{u,n+1}, \tau n_i \rangle_{\Gamma_i} + \left(A \left(\sigma_{h,i}^n + \alpha p_{h,i}^n I \right), \tau \right)_{\Omega_i}, \quad \forall \tau \in \mathbb{X}_{h,i}. \end{aligned} \quad (4.8)$$

The original variables can be recovered using

$$u_h^n = u_h^0 + \Delta t \sum_{k=1}^n \dot{u}_h^k, \quad \gamma_h^n = \gamma_h^0 + \Delta t \sum_{k=1}^n \dot{\gamma}_h^k, \quad \lambda_H^{u,n} = \lambda_H^{u,0} + \sum_{k=1}^n \dot{\lambda}_H^{u,k}. \quad (4.9)$$

4.2 Reduction to an interface problem

Similar to the non-overlapping matching grid domain decomposition algorithm discussed in [32], we solve the system resulting from (4.8), (4.2)–(4.7) at each time step by reducing it to an interface

problem for the Lagrange multiplier function λ_H . Following similar arguments as in [32], we introduce two sets of complementary subdomain problems.

The first set of problems reads as follows: for $1 \leq i \leq N$, find $(\bar{\sigma}_{h,i}^{n+1}, \bar{u}_{h,i}^{n+1}, \bar{\gamma}_{h,i}^{n+1}, \bar{z}_{h,i}^{n+1}, \bar{p}_{h,i}^{n+1}) \in \mathbb{X}_{h,i} \times V_{h,i} \times \mathbb{Q}_{h,i} \times Z_{h,i} \times W_{h,i}$ such that

$$\begin{aligned} & \left(A(\bar{\sigma}_{h,i}^{n+1} + \alpha \bar{p}_{h,i}^{n+1} I), \tau \right)_{\Omega_i} + \Delta t \left(\bar{u}_{h,i}^{n+1}, \operatorname{div} \tau \right)_{\Omega_i} + \Delta t \left(\bar{\gamma}_{h,i}^{n+1}, \tau \right)_{\Omega_i} \\ & = \Delta t \langle g_u^{n+1}, \tau n_i \rangle_{\partial \Omega_i \cap \Gamma_D^u} + (A(\sigma_{h,i}^n + \alpha p_{h,i}^n I), \tau)_{\Omega_i}, \quad \forall \tau \in \mathbb{X}_{h,i}, \end{aligned} \quad (4.10)$$

$$\left(\operatorname{div} \bar{\sigma}_{h,i}^{n+1}, v \right)_{\Omega_i} = - (f^{n+1}, v)_{\Omega_i}, \quad \forall v \in V_{h,i}, \quad (4.11)$$

$$\left(\bar{\sigma}_{h,i}^{n+1}, \xi \right)_{\Omega_i} = 0, \quad \forall \xi \in \mathbb{Q}_{h,i}, \quad (4.12)$$

$$\left(K^{-1} \bar{z}_{h,i}^{n+1}, \zeta \right)_{\Omega_i} - \left(\bar{p}_{h,i}^{n+1}, \operatorname{div} \zeta \right)_{\Omega_i} = - \langle g_p^{n+1}, \zeta \cdot n_i \rangle_{\partial \Omega_i \cap \Gamma_D^p}, \quad \forall \zeta \in Z_{h,i}, \quad (4.13)$$

$$\begin{aligned} & c_0 \left(\bar{p}_{h,i}^{n+1}, w \right)_{\Omega_i} + \alpha \left(A(\bar{\sigma}_{h,i}^{n+1} + \alpha \bar{p}_{h,i}^{n+1} I), wI \right)_{\Omega_i} + \Delta t \left(\operatorname{div} \bar{z}_{h,i}^{n+1}, w \right)_{\Omega_i} \\ & = \Delta t \left(g^{n+1}, w \right)_{\Omega_i} + c_0 \left(p_{h,i}^n, w \right)_{\Omega_i} + \alpha \left(A(\sigma_{h,i}^n + \alpha p_{h,i}^n I), wI \right)_{\Omega_i}, \quad \forall w \in W_{h,i}. \end{aligned} \quad (4.14)$$

Note that these subdomain problems have zero Dirichlet data at the subdomain interface, the true source terms f and g , outside boundary conditions g_u and g_p , and initial data $\sigma_{h,i}^n$ and $p_{h,i}^n$.

The second set of equations reads as follows: given $\lambda_H \in \Lambda_H$, for $1 \leq i \leq N$, find $(\sigma_{h,i}^{*,n+1}(\lambda_H), \dot{u}_{h,i}^{*,n+1}(\lambda_H), \dot{\gamma}_{h,i}^{*,n+1}(\lambda_H), z_{h,i}^{*,n+1}(\lambda_H), p_{h,i}^{*,n+1}(\lambda_H)) \in \mathbb{X}_{h,i} \times V_{h,i} \times \mathbb{Q}_{h,i} \times Z_{h,i} \times W_{h,i}$ such that:

$$\begin{aligned} & \left(A(\sigma_{h,i}^{*,n+1}(\lambda_H) + \alpha p_{h,i}^{*,n+1}(\lambda_H) I), \tau \right)_{\Omega_i} + \Delta t \left(\dot{u}_{h,i}^{*,n+1}(\lambda_H), \operatorname{div} \tau \right)_{\Omega_i} \\ & + \Delta t \left(\dot{\gamma}_{h,i}^{*,n+1}(\lambda_H), \tau \right)_{\Omega_i} = \Delta t \langle \lambda_H \dot{u}, \tau n_i \rangle_{\Gamma_i}, \quad \forall \tau \in \mathbb{X}_{h,i}, \end{aligned} \quad (4.15)$$

$$\left(\operatorname{div} \sigma_{h,i}^{*,n+1}(\lambda_H), v \right)_{\Omega_i} = 0, \quad \forall v \in V_{h,i}, \quad (4.16)$$

$$\left(\sigma_{h,i}^{*,n+1}(\lambda_H), \xi \right)_{\Omega_i} = 0, \quad \forall \xi \in \mathbb{Q}_{h,i}, \quad (4.17)$$

$$\left(K^{-1} z_{h,i}^{*,n+1}(\lambda_H), \zeta \right)_{\Omega_i} - \left(p_{h,i}^{*,n+1}(\lambda_H), \operatorname{div} \zeta \right)_{\Omega_i} = - \langle \lambda_H^p, \zeta \cdot n_i \rangle_{\Gamma_i}, \quad \forall \zeta \in Z_{h,i}, \quad (4.18)$$

$$\begin{aligned} & c_0 \left(p_{h,i}^{*,n+1}(\lambda_H), w \right)_{\Omega_i} + \alpha \left(A(\sigma_{h,i}^{*,n+1}(\lambda_H) + \alpha p_{h,i}^{*,n+1}(\lambda_H) I), wI \right)_{\Omega_i} \\ & + \Delta t \left(\operatorname{div} z_{h,i}^{*,n+1}(\lambda_H), w \right)_{\Omega_i} = 0, \quad \forall w \in W_{h,i}. \end{aligned} \quad (4.19)$$

Note that this set of problems has λ_H as the Dirichlet boundary data on the interface Γ , compared to λ_h in the matching grid case. This system also has zero source terms, zero boundary data on part of the outside boundary $\partial \Omega$, and zero data from the previous time step.

Define the bilinear form $a_{H,i}^{n+1} : \lambda_H \times \lambda_H \rightarrow \mathbb{R}$, $1 \leq i \leq N$, $a_H^{n+1} : \lambda_H \times \lambda_H \rightarrow \mathbb{R}$, and the linear functional $g_H^{n+1} : \lambda_H \rightarrow \mathbb{R}$ for all $0 \leq n \leq N_T - 1$ by

$$a_{H,i}^{n+1}(\lambda_H, \mu) = \langle \sigma_{h,i}^{*,n+1}(\lambda_H) n_i, \mu^u \rangle_{\Gamma_i} - \langle z_{h,i}^{*,n+1}(\lambda_H) \cdot n_i, \mu^p \rangle_{\Gamma_i}, \quad a_H^{n+1}(\lambda_H, \mu) = \sum_{i=1}^N a_{H,i}^{n+1}(\lambda_H, \mu), \quad (4.20)$$

$$g_H^{n+1}(\mu) = \sum_{i=1}^N \left(- \langle \bar{\sigma}_{h,i}^{n+1} n_i, \mu^u \rangle_{\Gamma_i} + \langle \bar{z}_{h,i}^{n+1} \cdot n_i, \mu^p \rangle_{\Gamma_i} \right). \quad (4.21)$$

It follows from (4.6)–(4.7) that for each $0 \leq n \leq N_T - 1$, the solution to the global problem (4.8), (4.2)–(4.7) is equivalent to solving the interface problem for $\lambda_H^{n+1} \in \Lambda_H$:

$$a_H^{n+1}(\lambda_H^{n+1}, \mu) = g_H^{n+1}(\mu), \quad \forall \mu \in \Lambda_H, \quad (4.22)$$

and setting

$$\begin{aligned}\sigma_{h,i}^{n+1} &= \sigma_{h,i}^{*,n+1}(\lambda_H^{n+1}) + \bar{\sigma}_{h,i}^{n+1}, & \dot{u}_{h,i}^{n+1} &= \dot{u}_{h,i}^{*,n+1}(\lambda_H^{n+1}) + \bar{u}_{h,i}^{n+1}, & \dot{\gamma}_{h,i}^{n+1} &= \dot{\gamma}_{h,i}^{*,n+1}(\lambda_H^{n+1}) + \bar{\gamma}_{h,i}^{n+1}, \\ z_{h,i}^{n+1} &= z_{h,i}^{*,n+1}(\lambda_H^{n+1}) + \bar{z}_{h,i}^{n+1}, & p_{h,i}^{n+1} &= p_{h,i}^{*,n+1}(\lambda_H^{n+1}) + \bar{p}_{h,i}^{n+1}.\end{aligned}$$

4.3 Solving the interface problem

In order to solve the interface problem (4.22), we introduce linear operators $\mathcal{A}_{H,i}^{n+1} : \Lambda_{H,i} \rightarrow \Lambda_{H,i}$, for $1 \leq i \leq N$ and $\mathcal{A}_H^{n+1} : \Lambda_H \rightarrow \Lambda_H$ such that for any $\lambda_H \in \Lambda_H$,

$$\langle \mathcal{A}_{H,i}^{n+1} \lambda_{H,i}, \mu \rangle_{\Gamma_i} = \langle \sigma_{h,i}^{*,n+1}(\lambda_H) n_i, \mu^u \rangle_{\Gamma_i} - \langle z_{h,i}^{*,n+1}(\lambda_H) \cdot n_i, \mu^p \rangle_{\Gamma_i}, \quad \forall \mu \in \Lambda_{H,i}, \quad (4.23)$$

$$\mathcal{A}_H^{n+1} \lambda_H = \sum_{i=1}^N \mathcal{A}_{H,i}^{n+1} \lambda_{H,i}, \quad (4.24)$$

where $\lambda_{H,i}$ and $\Lambda_{H,i}$ denote the restrictions of λ_H and Λ_H to Γ_i , respectively. We also define the vector $G_H^{n+1} \in \Lambda_H$ as

$$\langle G_H^{n+1}, \mu \rangle_{\Gamma} = \sum_{i=1}^N \left(-\langle \bar{\sigma}_{h,i}^{n+1} n_i, \mu^u \rangle_{\Gamma_i} + \langle \bar{z}_{h,i}^{n+1} \cdot n_i, \mu^p \rangle_{\Gamma_i} \right), \quad \forall \mu \in \Lambda_{H,i}. \quad (4.25)$$

Interface problem (4.22) can now be reformulated as finding $\lambda_H \in \Lambda_H$ such that

$$\mathcal{A}_H^{n+1} \lambda_H = G_H^{n+1}. \quad (4.26)$$

Consider the L^2 orthogonal projections, $\mathcal{Q}_{h,i}^{u,T} : \mathbb{X}_{h,i} n_i \rightarrow \Lambda_H^u$ and $\mathcal{Q}_{h,i}^{p,T} : Z_{h,i} \cdot n_i \rightarrow \Lambda_H^p$ such that for any $\tau \in \mathbb{X}_{h,i}$ and $\zeta \in Z_{h,i}$,

$$\begin{aligned}\langle \mathcal{Q}_{h,i}^{u,T}(\tau n_i) - \tau n_i, \mu^u \rangle_{\Gamma_i} &= 0, & \forall \mu^u \in \Lambda_H^u, \\ \langle \mathcal{Q}_{h,i}^{p,T}(\zeta \cdot n_i) - \zeta \cdot n_i, \mu^p \rangle_{\Gamma_i} &= 0, & \forall \mu^p \in \Lambda_H^p.\end{aligned}$$

where n_i is the unit outward normal to $\partial\Omega_i$. Define $\mathcal{Q}_{h,i}^T : \mathbb{X}_{h,i} n_i \times Z_{h,i} \cdot n_i \rightarrow \Lambda_H^u \times \Lambda_H^p$ such that for any $\tau \in \mathbb{X}_{h,i}$ and $\zeta \in Z_{h,i}$

$$\mathcal{Q}_{h,i}^T \begin{pmatrix} \tau n_i \\ \zeta \cdot n_i \end{pmatrix} = \begin{pmatrix} \mathcal{Q}_{h,i}^{u,T} \tau n_i \\ \mathcal{Q}_{h,i}^{p,T} \zeta \cdot n_i \end{pmatrix}. \quad (4.27)$$

Using the above notations, we note that

$$\mathcal{A}_{H,i}^{n+1} \lambda_{H,i} = \mathcal{Q}_{h,i}^T \begin{pmatrix} \sigma_{h,i}^{*,n+1}(\lambda_H) n_i \\ -z_{h,i}^{*,n+1}(\lambda_H) \cdot n_i \end{pmatrix}, \quad G_H^{n+1} = \begin{pmatrix} \sum_{i=1}^N -\mathcal{Q}_{h,i}^{u,T} \bar{\sigma}_{h,i}^{n+1} n_i \\ \sum_{i=1}^N \mathcal{Q}_{h,i}^{p,T} \bar{z}_{h,i}^{n+1} \cdot n_i \end{pmatrix}, \quad (4.28)$$

for $i = 1, 2, \dots, N$.

To solve the interface problem (4.26), we use an iterative method like GMRES with an initial guess $\lambda_{H,0} \in \Lambda_H$ at each time step, $t_n = n\Delta t$. A detailed description is given in Algorithm 1 (also see [23]).

This method has the performance advantage over the similar method for matching grids discussed in [32] that a coarse mortar mesh could be used to obtain a smaller interface problem due to the reduction in the mortar degrees of freedom. We implement this algorithm and study various test cases in the numerical results section.

Algorithm 1 Solving interface problem using GMRES algorithm.

1. Solve the first set of complementary equations, (4.10)–(4.14), and compute G_H^{n+1} using (4.28).
 2. Pick an initial guess $\lambda_{H,0} \in \Lambda_H$.
 3. Project the mortar function onto the subdomain boundaries, $\lambda_{H,0,i} \rightarrow \mathcal{Q}_{h,i}(\lambda_{H,0,i})$.
 4. Solve the second set of complementary equations, (4.15)–(4.19), using the projected function $\mathcal{Q}_{h,i}(\lambda_{H,0,i})$ as Dirichlet boundary data to obtain $\sigma_{h,i}^{*,n+1}(\lambda_{H,0})$ and $z_{h,i}^{*,n+1}(\lambda_{H,0})$.
 5. Project the solution variables to the mortar space, $\sigma_{h,i}^{*,n+1}(\lambda_{H,0}) n_i \rightarrow \mathcal{Q}_{h,i}^{u,T} \sigma_{h,i}^{*,n+1}(\lambda_{H,0}) n_i$ and $z_{h,i}^{*,n+1}(\lambda_{H,0}) \cdot n_i \rightarrow \mathcal{Q}_{h,i}^{p,T} z_{h,i}^{*,n+1}(\lambda_{H,0}) \cdot n_i$.
 6. Compute the action $\mathcal{A}_H^{n+1} \lambda_{H,0}$ using (4.28).
 7. Update λ_H using $\mathcal{A}_H^{n+1} \lambda_{H,0}$ in the GMRES algorithm.
 8. Repeat steps 3 – 7, with updated values of λ_H , until the residual for the GMRES algorithm goes below a predetermined tolerance.
-

4.4 Implementation with multiscale stress-flux basis (MSB)

A coarser mortar mesh can lead to a smaller interface problem, but even in that case, the number of subdomain solves of the type (4.15)–(4.19) is directly proportional to both the number of mortar space degrees of freedom and the number of time steps used. We propose the construction and use of a multiscale stress-flux basis (MSB) which makes the number of subdomain solves independent of the number of iterations required for the interface problem and the number of time steps used.

Let $\{\beta_{H,i}^k\}_{k=0}^{N_H}$ be a basis for $\Lambda_{H,i}$, where N_H denotes the number of degrees of freedom associated with the finite element space $\Lambda_{H,i}$. We calculate and store the action of the interface operator of the form

$$\mathcal{A}_{H,i} \beta_{H,i}^k = \mathcal{Q}_{h,i}^T \begin{pmatrix} \sigma_{h,i}^*(\beta_{H,i}^k) n_i \\ -z_{h,i}^*(\beta_{H,i}^k) \cdot n_i \end{pmatrix}, \quad (4.29)$$

for $k = 1, 2, \dots, N_H$, where we obtain $\sigma_{h,i}^*(\beta_{H,i}^k)$ and $z_{h,i}^*(\beta_{H,i}^k)$ by solving (4.15)–(4.19) with $\beta_{H,i}^k$ as the Dirichlet boundary data. A detailed description of the construction of the multiscale basis elements $\{\phi_{H,i}^k\}_{k=0}^{N_H}$, where $\phi_{H,i}^k = \mathcal{A}_{H,i} \beta_{H,i}^k$ is given in Algorithm 2, (also see [23, 33] for similar constructions).

Algorithm 2 Construction of multiscale stress-flux basis

for $k = 1, \dots, N_H$:

1. Project $\beta_{H,i}^k$ onto the subdomain boundary, $\beta_{H,i}^k \rightarrow \mathcal{Q}_{h,i}(\beta_{H,i}^k)$.
2. Solve the system (4.15)–(4.19) using the projected function $\mathcal{Q}_{h,i}(\beta_{H,i}^k)$ as the Dirichlet boundary data, to obtain $\sigma_{h,i}^*(\beta_{H,i}^k)$ and $z_{h,i}^*(\beta_{H,i}^k)$.
3. Project the solution variables to the mortar space to obtain $\phi_{H,i}^k = \begin{pmatrix} \mathcal{Q}_{h,i}^{u,T} \sigma_{h,i}^*(\beta_{H,i}^k) n_i \\ -\mathcal{Q}_{h,i}^{p,T} z_{h,i}^*(\beta_{H,i}^k) \cdot n_i \end{pmatrix}$.

end for

For any $\mu \in \Lambda_{H,i}$, consider the mortar basis decomposition, $\mu = \sum_{k=0}^{N_H} \mu_i \beta_{H,i}^k$. We can calculate the action of the interface operator on μ as follows:

$$\mathcal{A}_{H,i} \mu = \sum_{k=0}^{N_H} \mu_i \phi_{H,i}^k. \quad (4.30)$$

We can use the multiscale basis to replace steps 3–6 in Algorithm 1, by taking linear combinations of the form (4.30). Note that the multiscale stress-flux basis is computed and saved once and can be reused over all time steps, which gains a significant performance advantage in the case of time-dependent parabolic problems like the one we are studying.

We further discuss and compare the efficiency of using the multiscale stress-flux basis with other methods in Example 2 in the numerical section of this paper.

5 Numerical Results

In this section, we report the results of various numerical tests designed to verify and compare the well-posedness, stability, and convergence of the multiscale mortar non-overlapping domain decomposition method for the Biot system of poroelasticity that we have developed in this paper. We compare the computational efficiency in different cases, including the matching and non-matching grids on the subdomains, and also discuss the advantages of using a multiscale basis. The numerical schemes are implemented using deal.II finite element package [2, 11].

In all the examples, we have used the FE triplet $\mathbb{X}_h \times V_h \times \mathbb{Q}_h = \mathcal{BDM}_1^2 \times Q_0^2 \times Q_0$ ([8]) for elasticity and the FE pair $Z_h \times W_h = \mathcal{BDM}_1 \times Q_0$ ([15]) for Darcy on quadrilateral meshes. Here Q_k denotes polynomials of degree k in each variable. For the mortar spaces, λ_H^u is taken to be DQ_m^2 , and λ_H^p is taken to be DQ_m with $m = 1$ or 2 , where DQ_k represents the discontinuous finite element spaces containing polynomials of degree k , which lives on the subdomain interface. The degrees of FEM spaces used in this section is given in Table 1. For solving the interface problem, we use non-restarted unpreconditioned GMRES with a tolerance on the relative residual $\frac{\tau_k}{r_0}$ as the stopping criteria. For all the examples, this tolerance is taken to be 10^{-6} .

Table 1: Degree of polynomials associated with FEM spaces used for numerical experiments.

$\Lambda_H : m$	$\mathbb{X}_h : k$	$V_h : l$	$\mathbb{Q}_h : j$	$Z_h : r$	$W_h : s$
1 (linear)	1	0	0	1	0
2 (quadratic)	1	0	0	1	0

In Example 1, we test and compare the convergence, stability, and efficiency of the multiscale mortar DD method using linear ($m = 1$) and quadratic ($m = 2$) mortar spaces. We do this by solving a system of equations with a known solution on successively refined meshes.

In Example 2, we apply the multiscale DD method to solve a more practical problem, using a highly heterogeneous medium. We compare the efficiency of the multiscale versus fine scale methods and study the computational advantage of constructing a multiscale stress-flux basis (MSB) discussed in Section 4.4 of this paper.

In Example 1, we solve the system of PDEs on a checkerboard global mesh, which consists of non-matching grids on all subdomain interfaces. In particular, the coarsest multiscale mesh in all examples follows a subdomain mesh size ratio $\frac{1}{4} : \frac{1}{6} : \frac{1}{6} : \frac{1}{4}$ as shown in Figure 5.4. The corresponding coarsest mortar-interface mesh consists of two elements with mesh size $\frac{1}{2}$.

5.1 Example 1: testing convergence rates

In this example, we test the well-posedness, convergence, and stability of the multiscale mortar DD method using linear ($m = 1$) and quadratic ($m = 2$) mortar spaces. The global computational domain Ω is taken to be the unit square $(0, 1)^2$. We consider the following analytical solution

$$p = \exp(t)(\sin(\pi x) \cos(\pi y) + 10), \quad u = \exp(t) \begin{pmatrix} x^3 y^4 + x^2 + \sin((1-x)(1-y)) \cos(1-y) \\ (1-x)^4 (1-y)^3 + (1-y)^2 + \cos(xy) \sin(x) \end{pmatrix}.$$

The physical and numerical parameters are given in Table 2. Using this information, we derive the right hand side and initial conditions essential to solve the system (2.1)–(2.9). We partition Ω into four square subdomains with non-matching grids as shown in Figure 5.4.

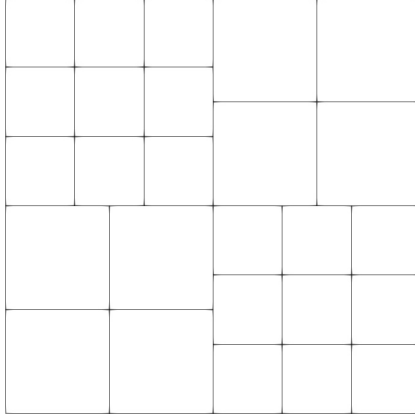


Figure 5.4: Example 1, coarsest non matching subdomain grid on $(0,1)^2$.

We consider two different cases, with linear and quadratic mortar spaces, where the former contains polynomials of degree 1 and the latter contains polynomials of degree 2. To test the convergence and verify the theoretical a priori error estimates, we successively refine the subdomain and mortar meshes. In the linear mortar case, we maintain a subdomain to mortar mesh ratio such that $H = Ch$, and in the quadratic mortar case, we maintain the ratio such that $H = C\sqrt{h}$.

The convergence tables for the cases with linear and quadratic mortar spaces with $\Delta t = 10^{-4}$ and $c_0 = 1.0$ are given in Tables 3 and 4, respectively. Tables 5–6 present the convergence table in the case of linear mortar and quadratic mortar spaces, respectively with $\Delta t = 10^{-4}$, and $c_0 = 10^{-3}$. We present the number of interface iterations, relative errors, and their convergence rates in these tables. Solution plots in the case of linear mortar with an intermediate level of refinement, $h = 1/32$, $\Delta t = 10^{-3}$ and $c_0 = 1.0$ is given in Figure 5.5 in order to compare with the plots obtained in [32] using monolithic domain decomposition technique using matching grids on subdomain interfaces. Note that plots in the case of quadratic mortar space look similar.

Table 2: Example 1, physical and numerical parameters.

Parameter	Value
Permeability tensor (K)	I
Lame coefficient (μ)	100.0
Lame coefficient (λ)	100.0
Mass storativity (c_0)	$1.0, 10^{-3}$
Biot-Willis constant (α)	1.0
Time step (Δt)	$10^{-3}, 10^{-4}$
Number of time steps	100

The numerical results that we observe are consistent with the theoretical results from the previous sections. In particular, we demonstrate the stability of the method over a 100 time steps, and Tables 3 and 4 confirm convergence rates that follow from Theorem 9 and Table 1. With linear mortar $m = 1$ and $H = Ch$, the interface error is $\mathcal{O}\left(h^{\frac{3}{2}}\right)$. With quadratic mortar $m = 2$ and $H = \sqrt{h}$, the interface error is $\mathcal{O}\left(h^{\frac{5}{4}}\right)$. In both the cases, it is dominated by the subdomain error, which is $\mathcal{O}(h)$. As a result, we expect at least $\mathcal{O}(h)$ convergence in both cases, which is what we observe. Comparison of the number of interface iterations required in the case of linear and quadratic mortars in Tables 3 and 4, respectively shows that both mortar degrees result in similar accuracy for the same level of subdomain mesh refinement. This is despite the fact that the quadratic mortar case requires smaller number of interface iterations compared to the linear mortar case with the same

Table 3: Example 1, convergence table using linear mortar ($m = 1$) with $H = Ch$, $\Delta t = 10^{-4}$ and $c_0 = 1.0$.

h	# GMRES		$\ \sigma - \sigma_h\ _{L^\infty(L^2)}$		$\ \operatorname{div}(\sigma - \sigma_h)\ _{L^\infty(L^2)}$		$\ \gamma - \gamma_h\ _{L^\infty(L^2)}$		$\ u - u_h\ _{L^\infty(L^2)}$	
1/4	16	rate	1.23e-01	rate	6.09e-01	rate	1.39e+00	rate	5.78e-01	rate
1/8	28	-0.81	3.24e-02	1.92	3.11e-01	0.97	7.07e-01	0.97	2.92e-01	0.99
1/16	46	-0.72	8.20e-03	1.98	1.56e-01	0.99	3.55e-01	0.99	1.46e-01	1.00
1/32	73	-0.67	2.08e-03	1.98	7.82e-02	1.00	1.78e-01	1.00	7.31e-02	1.00
1/64	122	-0.74	5.39e-04	1.94	3.91e-02	1.00	8.89e-02	1.00	3.65e-02	1.00

h	$\ z - z_h\ _{L^\infty(L^2)}$		$\ \operatorname{div}(z - z_h)\ _{L^2(L^2)}$		$\ p - p_h\ _{L^\infty(L^2)}$		$\ u - \lambda^u_H\ _{L^\infty(L^2)}$		$\ p - \lambda^p_H\ _{L^\infty(L^2)}$	
1/4	1.04e+00	rate	4.15e-01	rate	5.91e-02	rate	7.50e-01	rate	2.06e-01	rate
1/8	3.72e-01	1.48	1.89e-01	1.14	2.96e-02	1.00	1.90e-01	1.98	5.30e-02	1.96
1/16	1.19e-01	1.64	8.50e-02	1.15	1.48e-02	1.00	4.76e-02	1.99	1.33e-02	2.00
1/32	3.56e-02	1.74	3.97e-02	1.10	7.39e-03	1.00	1.19e-02	2.00	3.33e-03	2.00
1/64	1.08e-02	1.72	1.92e-02	1.05	3.70e-03	1.00	3.04e-03	1.97	8.37e-04	1.99

Table 4: Example 1, convergence table using quadratic mortar ($m = 2$) with $H = C\sqrt{h}$, $\Delta t = 10^{-4}$ and $c_0 = 1.0$.

h	# GMRES		$\ \sigma - \sigma_h\ _{L^\infty(L^2)}$		$\ \operatorname{div}(\sigma - \sigma_h)\ _{L^\infty(L^2)}$		$\ \gamma - \gamma_h\ _{L^\infty(L^2)}$		$\ u - u_h\ _{L^\infty(L^2)}$	
1/4	22	rate	1.26e-01	rate	6.09e-01	rate	1.39e+00	rate	5.79e-01	rate
1/16	40	-0.43	8.25e-03	1.97	1.56e-01	0.98	3.55e-01	0.99	1.46e-01	0.99
1/64	65	-0.35	5.62e-04	1.93	3.91e-02	1.00	8.89e-02	1.00	3.65e-02	1.00

h	$\ z - z_h\ _{L^\infty(L^2)}$		$\ \operatorname{div}(z - z_h)\ _{L^2(L^2)}$		$\ p - p_h\ _{L^\infty(L^2)}$		$\ u - \lambda^u_H\ _{L^\infty(L^2)}$		$\ p - \lambda^p_H\ _{L^\infty(L^2)}$	
1/4	6.72e-01	rate	3.92e-01	rate	5.92e-02	rate	7.55e-01	rate	9.70e-02	rate
1/16	8.20e-02	1.52	8.36e-02	1.11	1.48e-02	1.00	4.82e-02	1.99	6.83e-03	1.91
1/64	7.03e-03	1.77	1.92e-02	1.06	3.70e-03	1.00	3.31e-03	1.93	5.91e-04	1.77

level of subdomain mesh refinement. This is due to the choice of a coarser mortar mesh in the case of quadratic mortar case. This points towards a way to decrease the number of interface iterations by using a coarser mesh and higher mortar space degree, without any loss in accuracy. Tables 5–6 confirm that the stability and error bounds proved in previous sections are not affected by smaller values of c_0 . Further, Figure 5.5 demonstrates the efficacy of the method in enforcing continuity of solution variables across subdomain interfaces, weakly using coarse mortar spaces. In fact, the solution looks almost identical to the ones obtained using matching-subdomain grids in [32], with a smaller number of interface iterations for same level of finest subdomain mesh refinement. This demonstrates the advantage of using the multiscale technique we have developed over the completely matching case that was discussed in [32].

5.2 Example 2: heterogeneous medium

In this example, we demonstrate the performance of our method in a practical application with highly heterogeneous medium. First, we compare the efficiency of our multiscale mortar method, where $H > h$, with a fine scale method, where $H = h$. We expect the former to be more efficient than the latter because of weaker enforcement of continuity across subdomain interfaces using a coarser mortar space in the case of the multiscale method. We then study the computational advantage of using a multiscale stress-flux basis (MSB) over not using an MSB. In the case of no-MSB, the number of subdomain solves is total #GMRES iterations across all time steps + $2 \times$ number of time steps, where the last term comes from two extra solves required to solve the system (4.10)–(4.19) initially and recovering the final solution once the GMRES converges. Similarly, in the case of using MSB, total number of subdomain solves equals the $\dim(\Lambda_H) + 2 \times$ number of time steps. Note that

Table 5: Example 1, convergence table for linear mortar with $H = Ch$, $\Delta t = 10^{-4}$ and $c_0 = 10^{-3}$.

h	# GMRES		$\ \sigma - \sigma_h\ _{L^\infty(L^2)}$		$\ \operatorname{div}(\sigma - \sigma_h)\ _{L^\infty(L^2)}$		$\ \gamma - \gamma_h\ _{L^\infty(L^2)}$		$\ u - u_h\ _{L^\infty(L^2)}$	
	rate		rate		rate		rate		rate	
1/4	16		1.25e-01		6.09e-01		1.39e+00		5.78e-01	
1/8	29	-0.86	3.30e-02	1.92	3.11e-01	0.97	7.07e-01	0.97	2.92e-01	0.99
1/16	50	-0.79	8.34e-03	1.98	1.56e-01	0.99	3.55e-01	0.99	1.46e-01	1.00
1/32	87	-0.80	2.09e-03	1.99	7.82e-02	1.00	1.78e-01	1.00	7.31e-02	1.00
1/64	157	-0.85	5.38e-04	1.96	3.91e-02	1.00	8.89e-02	1.00	3.65e-02	1.00

h	$\ z - z_h\ _{L^\infty(L^2)}$		$\ \operatorname{div}(z - z_h)\ _{L^2(L^2)}$		$\ p - p_h\ _{L^\infty(L^2)}$		$\ u - \lambda^u_H\ _{L^\infty(L^2)}$		$\ p - \lambda^p_H\ _{L^\infty(L^2)}$	
	rate		rate		rate		rate		rate	
1/4	4.18e+01		2.31e+00		8.81e-01		7.52e-01		8.48e+00	
1/8	9.68e+00	2.11	7.14e-01	1.69	2.33e-01	1.92	1.90e-01	1.98	2.11e+00	2.00
1/16	2.31e+00	2.07	2.00e-01	1.84	5.93e-02	1.98	4.77e-02	1.99	5.08e-01	2.06
1/32	5.68e-01	2.02	6.02e-02	1.73	1.62e-02	1.87	1.19e-02	2.00	1.25e-01	2.02
1/64	1.42e-01	2.00	2.22e-02	1.44	5.22e-03	1.64	2.98e-03	2.00	3.12e-02	2.00

Table 6: Example 1, convergence table for quadratic mortar with $H = C\sqrt{h}$, $\Delta t = 10^{-4}$ and $c_0 = 10^{-3}$.

h	# GMRES		$\ \sigma - \sigma_h\ _{L^\infty(L^2)}$		$\ \operatorname{div}(\sigma - \sigma_h)\ _{L^\infty(L^2)}$		$\ \gamma - \gamma_h\ _{L^\infty(L^2)}$		$\ u - u_h\ _{L^\infty(L^2)}$	
	rate		rate		rate		rate		rate	
1/4	23		1.28e-01		6.09e-01		1.39e+00		5.79e-01	
1/16	41	-0.41	8.39e-03	1.97	1.56e-01	0.98	3.55e-01	0.96	1.46e-01	0.99
1/64	72	-0.41	5.61e-04	1.95	3.91e-02	1.00	8.89e-02	1.00	3.65e-02	1.00

h	$\ z - z_h\ _{L^\infty(L^2)}$		$\ \operatorname{div}(z - z_h)\ _{L^2(L^2)}$		$\ p - p_h\ _{L^\infty(L^2)}$		$\ u - \lambda^u_H\ _{L^\infty(L^2)}$		$\ p - \lambda^p_H\ _{L^\infty(L^2)}$	
	rate		rate		rate		rate		rate	
1/4	4.24e+01		2.42e+00		9.97e-01		7.57e-01		1.07e+01	
1/16	2.33e+00	2.01	2.01e-01	1.79	6.01e-02	2.06	4.83e-02	1.98	5.17e-01	2.19
1/64	1.50e-01	1.97	2.25e-02	1.58	5.40e-03	1.74	3.26e-03	1.95	3.38e-02	1.97

the first term in the number of solves in the case of no-MSB is directly proportional to the number of time steps used in time discretization, while the same in the case of MSB method is independent of the number of time steps used. This leads to MSB method being far more efficient than the no-MSB method with any choice of mortar, as long as enough number of time steps are used.

To obtain the desired level of heterogeneity in the medium, we use the porosity and the permeability data from the Society of Petroleum Engineers 10th Comparative Solution Project (SPE10)¹. The porosity and permeability fields are given on a 60×220 grid and we use the rectangular region $(0, 60) \times (0, 220)$ as the computational domain. We decompose the global domain into 3×5 subdomains consisting of identical rectangular blocks. The Young's modulus is obtained from the porosity field data using the relation $E = 10^2 \left(1 - \frac{\phi}{c}\right)^{2.1}$, where $c = 0.5$, refers to the porosity at which the Young's modulus vanishes, see [35] for details. These input fields are presented in Figure 5.6. We use parameters and boundary conditions as mentioned in Table 7, along with zero source terms. These conditions describe a flow from left to right, driven by the gradient in the pressure. We use a compatible initial condition for pressure, $p_0 = 1 - x$. To obtain the essential discrete initial data, we take the elliptic projection of the continuous initial data, see (3.25). In particular, we set p_h^0 to be the L^2 -projection of p_0 onto W_h and solve a mixed elasticity domain decomposition problem at $t = 0$ to obtain σ_h^0 . We also obtain u_h^0 , γ_h^0 , and $\lambda_H^{u,0}$ from this solve.

We use a global 60×220 grid and solve the problem using both fine scale ($H = h$) and coarse ($H > h$) mortar spaces. For the coarse mortar case, we use both linear ($m = 1$) and quadratic mortars ($m = 2$) with one and two mortars per subdomain interface. The comparison of the computed solution using different choices of mortars is given in Figures 5.7–5.12. Comparison of the number of solves required for different choices of mortar, both in the no-MSB and MSB cases are given in Table 8. We report the number of subdomain solves which dominates the computational

¹<https://www.spe.org/web/csp/datasets/set02.htm>

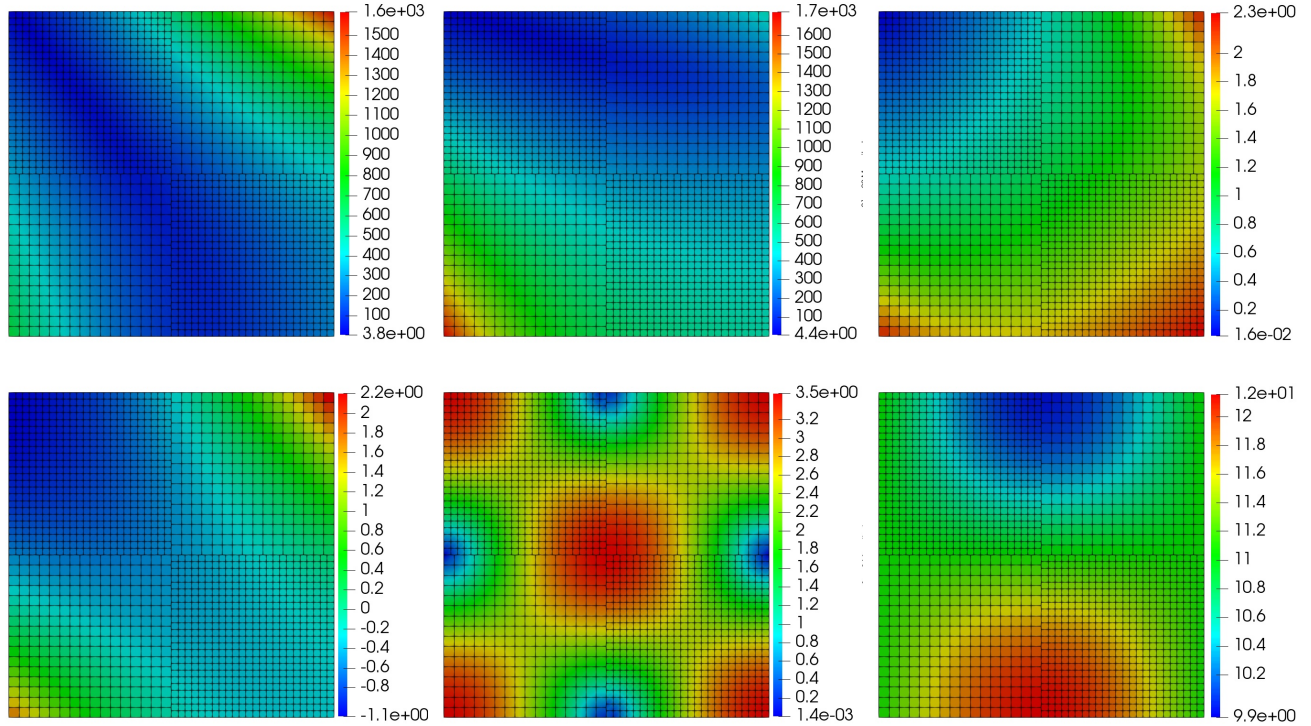


Figure 5.5: Example 1, computed solution at final time step using a linear mortar on non-matching subdomain grids, top: stress x (left), stress y (middle), displacement (right), bottom: rotation (left), velocity (middle), pressure (right). Mesh size, $h = 1/32$, $\Delta t = 10^{-3}$ and $c_0 = 1.0$.

complexity of the method.

Table 8 clearly shows that using the multiscale mortar method requires fewer number of solves compared to fine scale method and hence the former is computationally less expensive than the latter. Comparison of the computed solution for various choices of mortars in Figures 5.7–5.12 shows that we retain good amount of accuracy even in the case of the coarsest mortar case with one linear mortar per interface. We also note that using a single quadratic mortar per interface yields almost identical results as the fine scale solution which emphasizes our observation from the previous example that a coarse mortar can be compensated by choosing a higher degree for mortar space Λ_H . Table 8 also demonstrates the superiority of using MSB for a time-dependent multiscale problem like the one in our case. The number of solves in the case of no MSB is at least an order of magnitude bigger than the MSB case which implies that the construction of MSB is an excellent tool to make our multiscale mortar method even more efficient than it already is compared to the fine scale methods discussed in [32].

6 Conclusions

In this paper we presented a multiscale mortar mixed finite element technique (MMMFE) for the Biot system of poroelasticity in a five-field fully mixed formulation. This method is the generalization of the monolithic domain decomposition technique discussed in the previous paper, with the extra capability to use non-matching subdomain grids at the interface. This capability is obtained by using composite multiscale mortar Lagrange multiplier spaces that approximates displacement and pressure on a coarse mortar grid at the interface. The global problem can be reduced into a series of parallel Dirichlet type problems and an interface problem for the composite displacement-pressure Lagrange multiplier spaces which requires subdomain solves at each iteration. We showed the well-posedness and stability of the method under proper assumptions. We have also carried out an

Table 7: Example 2, parameters (top) and boundary conditions (bottom).

Parameter		Value		
Mass storativity (c_0)		1.0		
Biot-Willis constant (α)		1.0		
Time step (Δt)		10^{-3}		
Total time (T)		0.1		
Boundary	σ	u	p	z
Left	$\sigma n = -\alpha p n$	-	1	-
Bottom	$\sigma n = 0$	-	-	$z \cdot n = 0$
Right	-	0	0	-
Top	$\sigma n = 0$	-	-	$z \cdot n = 0$

Table 8: Example 2, #GMRES iterations and maximum number of subdomain solves.

mortar	Average #GMRES	Total #GMRES	Total #Solves	
			No MSB	MSB
linear fine scale	343	34375	34575	968
1 linear per interface	41	4149	4349	224
1 quadratic per interface	61	6184	6384	236
2 linear per interface	80	8010	8210	248
2 quadratic per interface	123	12302	12502	272

extensive error analysis of the method to get a combined a priori error estimate for all the unknowns in the formulation. To complete the analysis, we have done a series of numerical experiments to put the theory into test. We observed stability and convergence results as predicted by the theory and also demonstrated the application of the method to a highly heterogeneous medium. We noted that in practice, a coarser mesh with higher mortar space degree can be used to get a smaller interface problem and hence faster convergence without compromising the accuracy of the method. We conclude the paper by recalling the effectiveness of the construction and use of a pre-computed multiscale stress-flux basis (MSB), which makes the MMMFE method far more superior than the fine scale monolithic methods, especially when a coarse mortar mesh is used.

References

- [1] E. Ahmed, F. A. Radu, and J. M. Nordbotten. Adaptive poromechanics computations based on a posteriori error estimates for fully mixed formulations of Biot’s consolidation model. *Comput. Methods Appl. Mech. Engrg.*, 347:264–294, 2019.
- [2] G. Alzetta, D. Arndt, W. Bangerth, V. Boddu, B. Brands, D. Davydov, R. Gassmoeller, T. Heister, L. Heltai, K. Kormann, M. Kronbichler, M. Maier, J.-P. Pelteret, B. Turcksin, and D. Wells. The `deal.II` library, version 9.0. *Journal of Numerical Mathematics*, 26(4):173–183, 2018.
- [3] M. Amara and J. M. Thomas. Equilibrium finite elements for the linear elastic problem. *Numer. Math.*, 33(4):367–383, 1979.
- [4] I. Ambartsumyan, E. Khattatov, J. M. Nordbotten, and I. Yotov. A multipoint stress mixed finite element method for elasticity on quadrilateral grids. *Numer. Methods Partial Differential Equations*, <https://doi.org/10.1002/num.22624>, 2020.
- [5] I. Ambartsumyan, E. Khattatov, and I. Yotov. A coupled multipoint stress - multipoint flux mixed finite element method for the Biot system of poroelasticity. *Comput. Methods Appl. Mech. Engrg.*, 372:113407, 2020.
- [6] T. Arbogast, L. C. Cowsar, M. F. Wheeler, and I. Yotov. Mixed finite element methods on nonmatching multiblock grids. *SIAM J. Numer. Anal.*, 37(4):1295–1315, 2000.

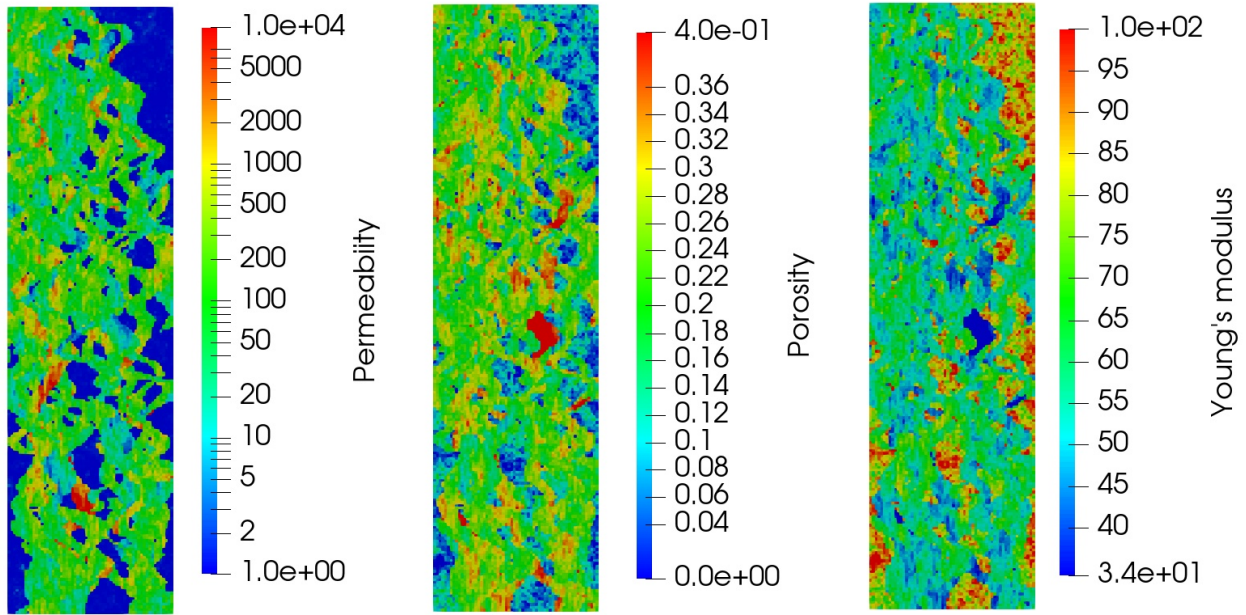


Figure 5.6: Example 2, permeability, porosity, Young's modulus.

- [7] T. Arbogast, G. Pencheva, M. F. Wheeler, and I. Yotov. A multiscale mortar mixed finite element method. *Multiscale Model. Simul.*, 6(1):319–346, 2007.
- [8] D. N. Arnold, G. Awanou, and W. Qiu. Mixed finite elements for elasticity on quadrilateral meshes. *Adv. Comput. Math.*, 41(3):553–572, 2015.
- [9] D. N. Arnold, R. S. Falk, and R. Winther. Mixed finite element methods for linear elasticity with weakly imposed symmetry. *Math. Comp.*, 76(260):1699–1723, 2007.
- [10] G. Awanou. Rectangular mixed elements for elasticity with weakly imposed symmetry condition. *Adv. Comput. Math.*, 38(2):351–367, 2013.
- [11] W. Bangerth, R. Hartmann, and G. Kanschat. deal.II – a general purpose object oriented finite element library. *ACM Trans. Math. Softw.*, 33(4):24/1–24/27, 2007.
- [12] M. A. Biot. General theory of three-dimensional consolidation. *J. Appl. Phys.*, 12(2):155–164, 1941.
- [13] D. Boffi, F. Brezzi, L. F. Demkowicz, R. G. Durán, R. S. Falk, and M. Fortin. *Mixed finite elements, compatibility conditions, and applications*, volume 1939 of *Lecture Notes in Mathematics*. Springer-Verlag, Berlin; Fondazione C.I.M.E., Florence, 2008.
- [14] D. Boffi, F. Brezzi, and M. Fortin. Reduced symmetry elements in linear elasticity. *Commun. Pure Appl. Anal.*, 8(1):95–121, 2009.
- [15] F. Brezzi and M. Fortin. *Mixed and hybrid finite element methods*, volume 15 of *Springer Series in Computational Mathematics*. Springer-Verlag, New York, 1991.
- [16] P. G. Ciarlet. *The finite element method for elliptic problems*, volume 40 of *Classics in Applied Mathematics*. Society for Industrial and Applied Mathematics, Philadelphia, PA, 2002.
- [17] B. Cockburn, J. Gopalakrishnan, and J. Guzmán. A new elasticity element made for enforcing weak stress symmetry. *Math. Comp.*, 79(271):1331–1349, 2010.
- [18] L. C. Cowsar, J. Mandel, and M. F. Wheeler. Balancing domain decomposition for mixed finite elements. *Math. Comp.*, 64(211):989–1015, 1995.
- [19] M. Farhloul and M. Fortin. Dual hybrid methods for the elasticity and the Stokes problems: a unified approach. *Numer. Math.*, 76(4):419–440, 1997.
- [20] H. Florez. About revisiting domain decomposition methods for poroelasticity. *Mathematics*, 6(10):187, 08 2018.

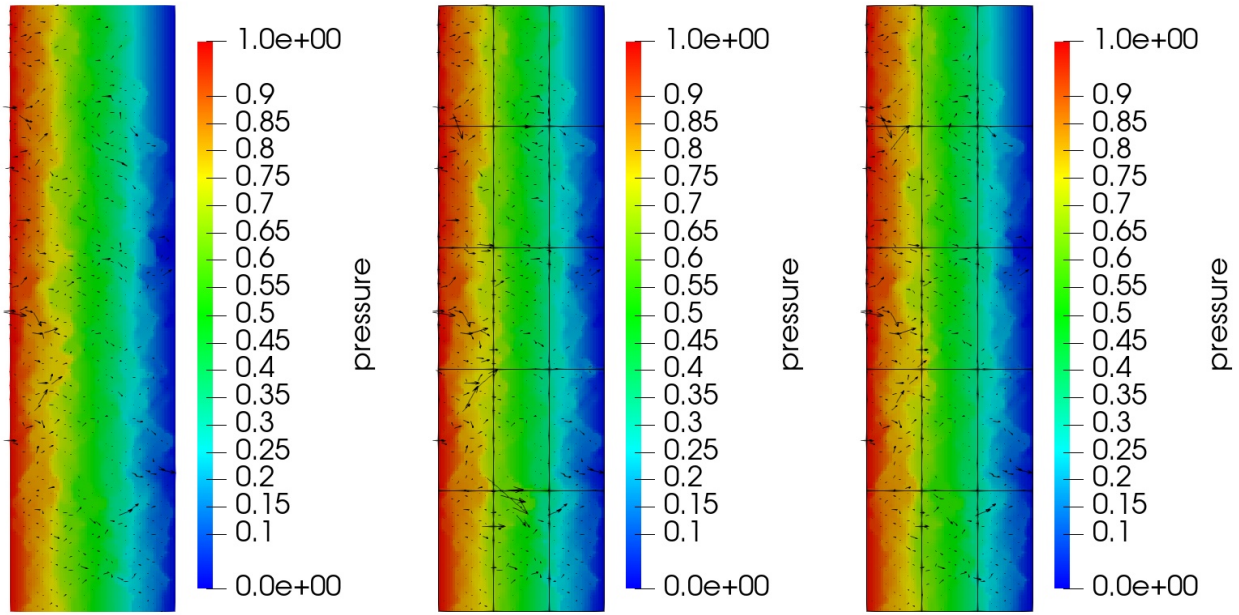


Figure 5.7: Example 2, pressure (color) and velocity (arrows): fine scale (left), single linear mortar per interface (middle), and two linear mortars per interface (right).

- [21] H. Florez and M. Wheeler. A mortar method based on nurbs for curved interfaces. *Computer Methods in Applied Mechanics and Engineering*, 310, 07 2016.
- [22] A. Fritz, S. Hübner, and B. I. Wohlmuth. A comparison of mortar and Nitsche techniques for linear elasticity. *Calcolo*, 41(3):115–137, 2004.
- [23] B. Ganis and I. Yotov. Implementation of a mortar mixed finite element method using a multiscale flux basis. *Comput. Methods Appl. Mech. Engrg.*, 198(49-52):3989–3998, 2009.
- [24] F. J. Gaspar, F. J. Lisbona, and P. N. Vabishchevich. A finite difference analysis of Biot’s consolidation model. *Appl. Numer. Math.*, 44(4):487–506, 2003.
- [25] V. Girault, G. Pencheva, M. F. Wheeler, and T. Wildey. Domain decomposition for poroelasticity and elasticity with dg jumps and mortars. *Math. Mod. Meth. Appl. S.*, 21(01):169–213, 2011.
- [26] V. Girault and P.-A. Raviart. *Finite element methods for Navier-Stokes equations*, volume 5 of *Springer Series in Computational Mathematics*. Springer-Verlag, Berlin, 1986. Theory and algorithms.
- [27] R. Glowinski and M. F. Wheeler. Domain decomposition and mixed finite element methods for elliptic problems. In *First international symposium on domain decomposition methods for partial differential equations*, pages 144–172, 1988.
- [28] J. Gopalakrishnan and J. Guzmán. A second elasticity element using the matrix bubble. *IMA J. Numer. Anal.*, 32(1):352–372, 2012.
- [29] P. Gosselet, V. Chiaruttini, C. Rey, and F. Feyel. A monolithic strategy based on an hybrid domain decomposition method for multiphysic problems. application to poroelasticity. *Revue Européenne des Elements Finis*, 13, 04 2012.
- [30] P. Grisvard. *Elliptic problems in nonsmooth domains*, volume 69 of *Classics in Applied Mathematics*. Society for Industrial and Applied Mathematics (SIAM), Philadelphia, PA, 2011.
- [31] X. Hu, C. Rodrigo, F. J. Gaspar, and L. T. Zikatanov. A nonconforming finite element method for the Biot’s consolidation model in poroelasticity. *J. Comput. Appl. Math.*, 310:143–154, 2017.
- [32] M. Jayadharan, E. Khattatov, and I. Yotov. Domain decomposition and partitioning methods for mixed finite element discretizations of the Biot system of poroelasticity. *Comput. Geosci.*, 25(6):1919–1938, 2021.

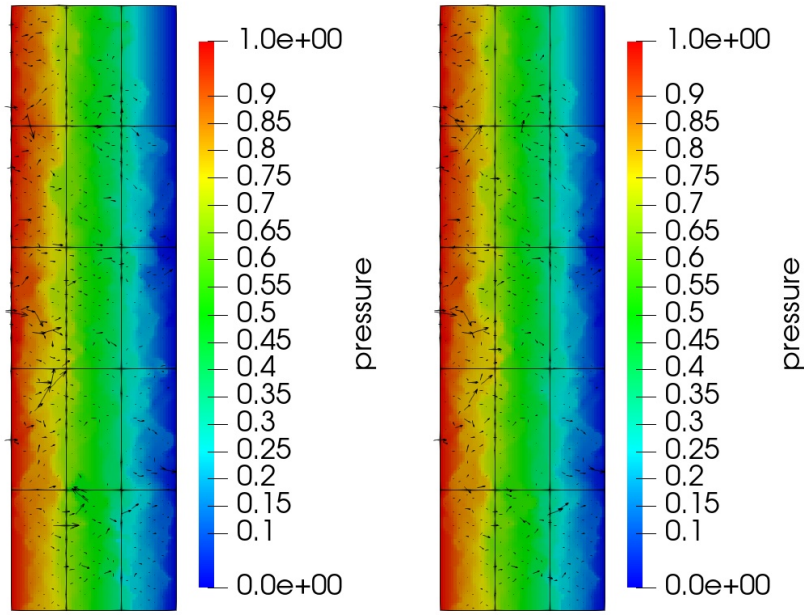


Figure 5.8: Example 2, pressure (color) and velocity (arrows): single quadratic mortar per interface (left), and two quadratic mortars per interface (right).

- [33] E. Khattatov and I. Yotov. Domain decomposition and multiscale mortar mixed finite element methods for linear elasticity with weak stress symmetry. *ESAIM Math. Model. Numer. Anal.*, 53(6):2081–2108, 2019.
- [34] H. H. Kim. A BDDC algorithm for mortar discretization of elasticity problems. *SIAM J. Numer. Anal.*, 46(4):2090–2111, 2008.
- [35] J. Kovacic. Correlation between young’s modulus and porosity in porous materials. *J. Mater. Sci. Lett.*, 18(13):1007–1010, 1999.
- [36] J. J. Lee. Robust error analysis of coupled mixed methods for Biot’s consolidation model. *J. Sci. Comput.*, 69(2):610–632, 2016.
- [37] J. J. Lee. Towards a unified analysis of mixed methods for elasticity with weakly symmetric stress. *Adv. Comput. Math.*, 42(2):361–376, 2016.
- [38] J. J. Lee. Robust three-field finite element methods for Biot’s consolidation model in poroelasticity. *BIT*, 58(2):347–372, 2018.
- [39] J. J. Lee, K.-A. Mardal, and R. Winther. Parameter-robust discretization and preconditioning of Biot’s consolidation model. *SIAM J. Sci. Comput.*, 39(1):A1–A24, 2017.
- [40] J. M. Nordbotten. Stable cell-centered finite volume discretization for Biot equations. *SIAM J. Numer. Anal.*, 54(2):942–968, 2016.
- [41] R. Oyarzúa and R. Ruiz-Baier. Locking-free finite element methods for poroelasticity. *SIAM J. Numer. Anal.*, 54(5):2951–2973, 2016.
- [42] G. Pencheva and I. Yotov. Balancing domain decomposition for mortar mixed finite element methods. *Numer. Linear Algebra Appl.*, 10(1-2):159–180, 2003.
- [43] M. Peszyńska, M. F. Wheeler, and I. Yotov. Mortar upscaling for multiphase flow in porous media. *Comput. Geosci.*, 6(1):73–100, 2002.
- [44] P. J. Phillips and M. F. Wheeler. A coupling of mixed and continuous Galerkin finite element methods for poroelasticity. I. The continuous in time case. *Comput. Geosci.*, 11(2):131–144, 2007.
- [45] P. J. Phillips and M. F. Wheeler. A coupling of mixed and discontinuous Galerkin finite-element methods for poroelasticity. *Comput. Geosci.*, 12(4):417–435, 2008.

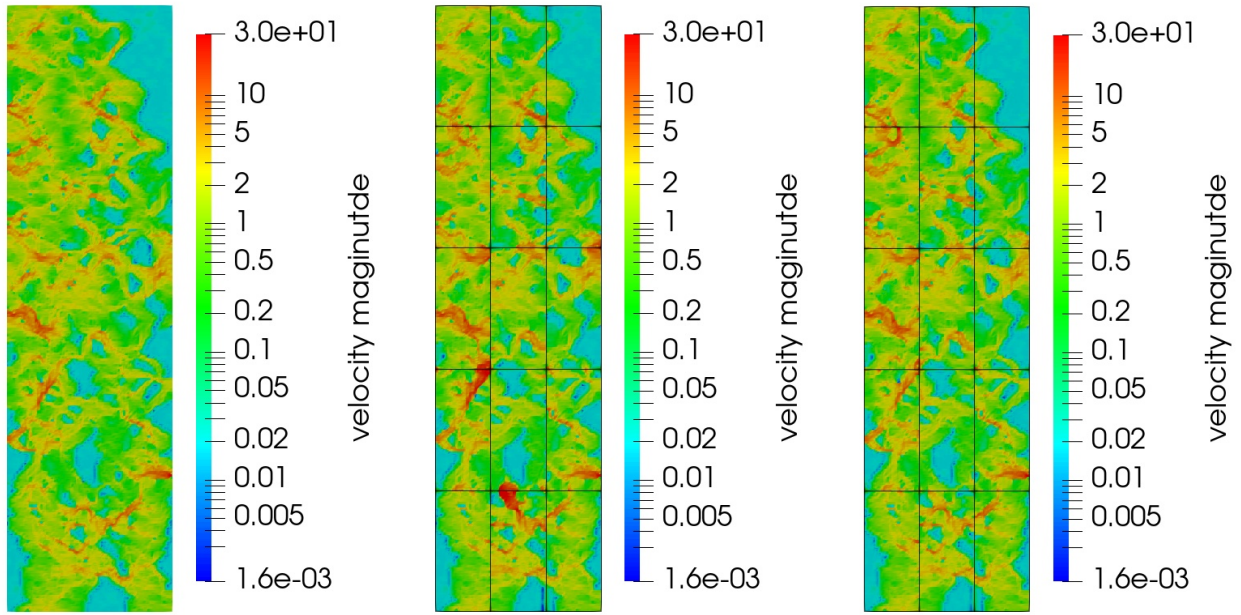


Figure 5.9: Example 2, velocity magnitude: fine scale (left), single linear mortar per interface (middle), and two linear mortars per interface (right).

- [46] A. Quarteroni and A. Valli. *Domain Decomposition Methods for Partial Differential equations*. Clarendon Press, Oxford, 1999.
- [47] J. E. Roberts and J.-M. Thomas. Mixed and hybrid methods. In *Handbook of numerical analysis, Vol. II*, Handb. Numer. Anal., II, pages 523–639. North-Holland, Amsterdam, 1991.
- [48] C. Rodrigo, F. J. Gaspar, X. Hu, and L. T. Zikatanov. Stability and monotonicity for some discretizations of the Biot’s consolidation model. *Comput. Methods Appl. Mech. Engrg.*, 298:183–204, 2016.
- [49] L. R. Scott and S. Zhang. Finite element interpolation of nonsmooth functions satisfying boundary conditions. *Math. Comput.*, 54(190):483–493, 1990.
- [50] R. Showalter. Diffusion in poro-elastic media. *Journal of Mathematical Analysis and Applications*, 251(1):310 – 340, 2000.
- [51] R. E. Showalter. *Monotone Operators in Banach Space and Nonlinear Partial Differential Equations*. Mathematical Surveys and Monographs, 49. American Mathematical Society, Providence, RI, 1997.
- [52] R. Stenberg. A family of mixed finite elements for the elasticity problem. *Numer. Math.*, 53(5):513–538, 1988.
- [53] A. Toselli and O. Widlund. *Domain decomposition methods—algorithms and theory*, volume 34 of *Springer Series in Computational Mathematics*. Springer-Verlag, Berlin, 2005.
- [54] M. F. Wheeler, G. Xue, and I. Yotov. Coupling multipoint flux mixed finite element methods with continuous Galerkin methods for poroelasticity. *Comput. Geosci.*, 18(1):57–75, 2014.
- [55] S.-Y. Yi. Convergence analysis of a new mixed finite element method for Biot’s consolidation model. *Numer. Meth. Partial. Differ. Equ.*, 30(4):1189–1210, 2014.
- [56] S.-Y. Yi. A study of two modes of locking in poroelasticity. *SIAM J. Numer. Anal.*, 55(4):1915–1936, 2017.

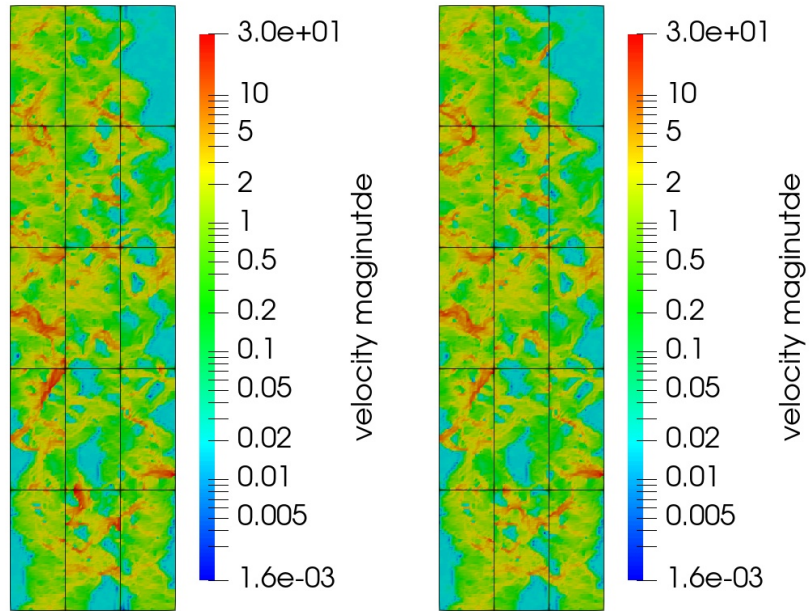


Figure 5.10: Example 2, velocity magnitude: single quadratic mortar per interface (left), and two quadratic mortars per interface (right).

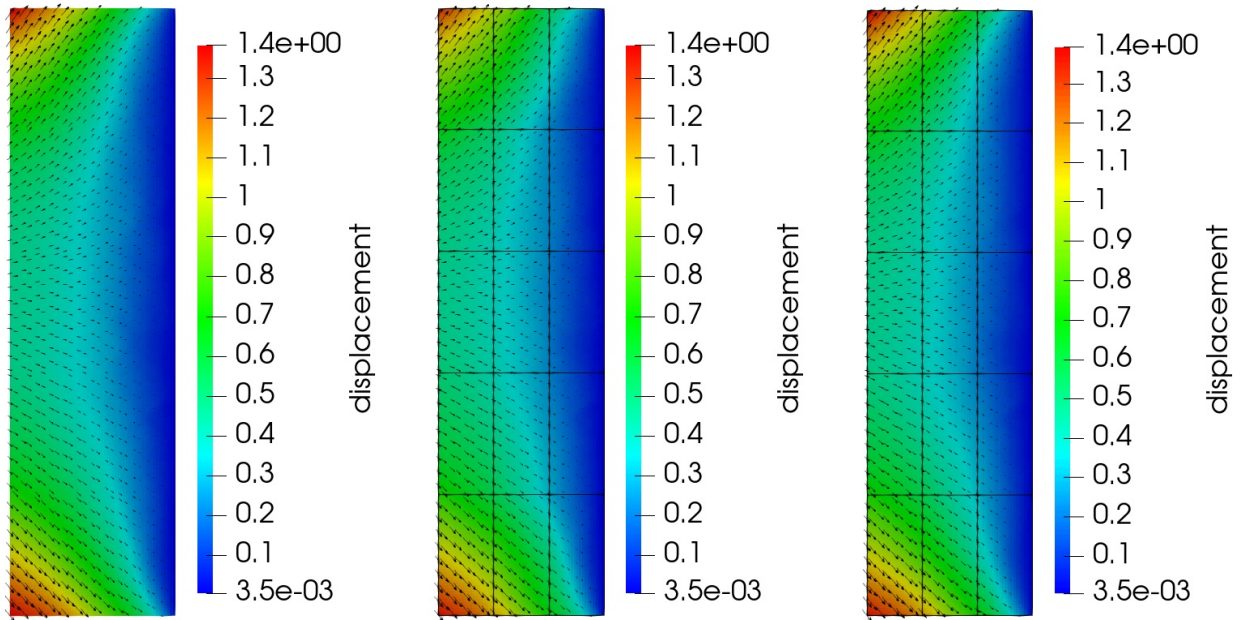


Figure 5.11: Example 2, displacement vector (arrows) and its magnitude: fine scale (left), single linear mortar per interface (middle), and two linear mortars per interface (right).

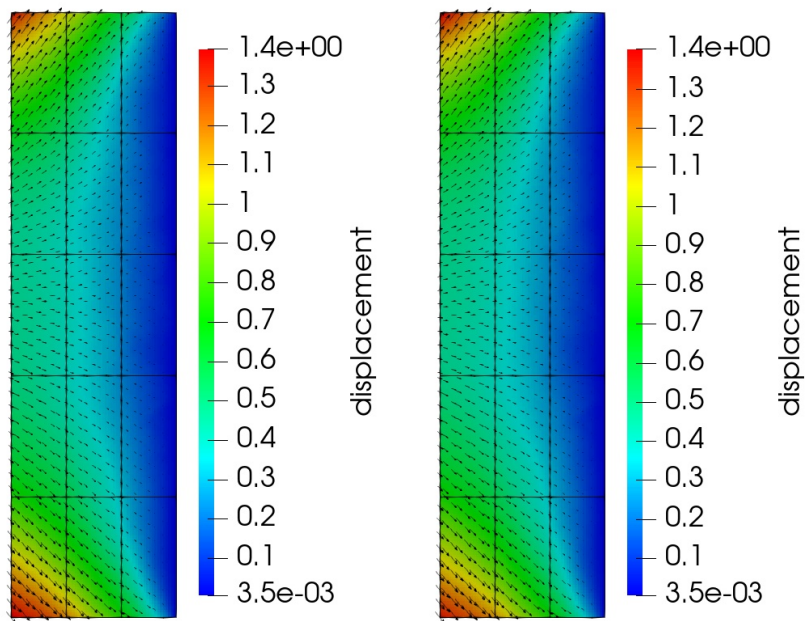


Figure 5.12: Example 2, displacement vector (arrows) and its magnitude: single quadratic mortar per interface (left), and two quadratic mortars per interface (right).